Andreia Sofia Batista Rocha

Molecular switch behind adult stem cell quiescence in mouse stomach epithelium

Department of Biomedical Sciences and Medicine

2019/2020

Andreia Sofia Batista Rocha

Molecular switch behind adult stem cell quiescence in mouse stomach epithelium

Master in Oncobiology – Molecular Mechanisms of Cancer

Work under the supervision of:

Dr. Bon-Kyoung Koo, PhD

Prof. Dr. Ana-Teresa Maia, PhD

Department of Biomedical Sciences and Medicine

2019/2020

Molecular switch behind adult stem cell quiescence in mouse stomach epithelium

Authorship Statement

I hereby declare to be the author of this work, which is original and unpublished. Authors and papers consulted are duly cited in the text and are listed in the included references.

_____

(Andreia Rocha)

“Visions are worth fighting for. Why spend your life making someone else's dreams?”

- Tim Burton

Acknowledgments

I couldn't be more grateful to my boss and supervisor Dr. Bon-Kyoung Koo for giving me this opportunity to work in a wonderful place, such as IMBA, and a lab with so many caring and brilliant people, together with many other new challenges and career options. I strongly believe that I could have not gotten a more supportive and enthusiastic person guiding me. I am enormously thankful for all the knowledge and welcoming that I have been given during this entire time in Vienna. And I strongly hope to stay in touch and continue to work with you in the future!

I would also like to express my immense gratitude to Dr. Ji-Hyun Lee who closely supervised my work during these past 10 months and taught me most of what I have learned in the institute so far! Also, I would like to say that I am extremely grateful to have had her at my side and to have had her support even outside of the lab. I got to know a lot of nice places to hang out, learn new things about different cultures and try a lot of new and tasty foods!

이박사님, 정말 감사합니다!

I am also very grateful to my co-supervisor Dr. Ana Teresa Maia, who always took a bit of her time to help me organize, correct and overall assist with my dissertation. Thank you very much! Even though far away, you managed to help me a great deal!

A big thanks to all the Koo lab members for the patience, willingness to teach and fun times spend in Vienna! I am more than happy to have join the team and met all of you! I would have been a whole lot harder without you! Thank you! A special thanks to Sam Wu for taking your time to teach me so many things and take me to football matches and Miss Isaree, my food buddy, for all the fun times!

An enormous special thanks to Aileen-Diane Bamford! I could have never got through all of this without you! Thank you so much for sharing the works and knowledge with me as well as adventures in and outside of the lab! Thank you for being so strong minded and dedicated that you even manage to get us a book in a book hunt through Vienna! Thank you for always being so supportive with me and for the incredible adventures you have put me through! Also, thank you so much for correcting my entire dissertation! I owe you a big deal!

I would also like to thank the Eilling and Urban labs for the weekly lab meetings, knowledge shared, and input given to all of us! Thank you!
Special thanks to Joonsun, Esther, Agathe, Rut, Kathe, Tatjana, Viki, Gintas, Anika, Chad and Yvonne for always being supportive and for the fun times!
I want to thank Bernardo Almeida for helping and advising me for the interview. Thank you to both you and Catarina Costa for always give me a bit of Portuguese in Vienna and at IMBA!

Thank you to all my friends back in Portugal who always supported me and cared for me even being so far away!! Special thanks to Ana Patricia who bothered to go and visit me in Vienna for my birthday and pushed me into start writing the dissertation! Thank you for all the fun times, support and for always being there for me!

An enormous thank you to my boyfriend Luis Queimado to always chat with me, appease me and help me to go through every step of my days! Thank you for spending almost 5 months in quarantine with me in Vienna, for your patience and specially for editing and proofreading my entire dissertation! I could have not been more thankful to have you always by my side! Love you.

Most importantly, a big thank you to my mom, Renata Batista and my grandparents, Antónia Batista and Luis Batista for all the financial and emotional support, for visiting me so often and for being there for me at all times! I couldn't have done this without you, and I know it was also hard for you to have me so far away, so, thank you once more for all the support! A big thanks, also, to my dad, Paulo Rocha, and brother, Miguel Rocha, to call me as often as possible and always make me laugh.

"Ideas are cheap and abundant; what is of value is the effective placement of those ideas into situations that develop into action."

- Peter Drucker

Abstract

Ulcers are sores in the stomach lining that cause pain and discomfort that tend to lead to chronic inflammation of the stomach and consequently cancer. Stomach cancer is the second leading cause of death by cancer and the fifth most common malignancy in the world. Despite its frequency, early diagnose, premalignant state characterization and discovery of new treatments remain a challenge. Understanding how the stomach tissues behave in homeostasis is key to gain knowledge and overcome many of these roadblocks.

Previous studies demonstrated that upon injury, base stem cells would exit quiescence and replenish the damaged tissue. It was then proposed that these were under the control of a reversible switch. Based on extensive injury-response data the CKI p57Kip2 appeared to be a promising candidate.

During this study, organoids and mouse models were used. With the inducible Tet-On system, p57 was knocked into gastric organoids to allow for studies of its effects and reverse them in vitro. Through these organoids, niche requirement alterations, quiescence induction ability and pathway interactors were studied. In vivo knock out and knock in effects were assessed and compared to the in vitro tests. Other Cip/Kip family members were considered and finally p57 was overexpressed in an ectopic tissue in a similar way.

Results showed that p57 can set stem cells into a quiescent state both in vitro and in vivo and has an impact on niche requirements. Pathway candidate IGF1R had a visible effect when inhibited on p57 overexpressing organoids. Short-term overexpression of Cip/Kip family members resulted in a mild phenotype of quiescence induction that needs to be confirmed in more extensive studies. Finally, although p57 was able to bring small intestinal cells into short-term quiescence, some challenges were faced. A new construct was designed to suppress these challenges, but further studies must be conducted to assure its success.

Keywords: Stomach cancer; Ulcers; p57; Quiescence; Stem cells

Resumo

Vários fatores, externos e internos, podem levar ao aparecimento de lesões no revestimento do estômago, estas lesões são designadas de úlceras e causam nos pacientes desconforto e dor. Quando presentes de forma recorrente, podem ainda levar a inflamações crónicas no tecido e em casos extremos levar também ao aumento da probabilidade de desenvolvimento de cancro gástrico.

O cancro do estômago é a segunda causa de morte por cancro mais prevalente e a quinta doença maligna mais comum no mundo. 90% dos cancros diagnosticados são do tipo adenocarcinoma, podendo este tipo de cancro ser ainda dividido em vários subgrupos. De acordo com a classificação mais comum, de Laurén, os cancros podem ser agrupados em intestinais, difusos ou mistos. Esta classificação aponta para os cancros de tipo intestinal como os que exibem uma progressão mais lenta e, por consequência, um prognóstico mais favorável, atribuindo o prognóstico mais desfavorável ao de tipo difuso.

Apesar do extenso leque de estudos referentes ao cancro do estômago, o prognóstico desta doença continua desfavorável em grande parte dos casos e as suas características pré-malignas difíceis de definir. De forma a encontrar novas formas de evitar inflamações recorrentes causadoras de cancro e novas vias de sinalização celular que levem á descoberta de novos tratamentos, será essencial entender os comportamentos destes tecidos quando se encontram em homeostasia.

No estômago estão presentes duas populações distintas de células estaminais. Uma dessas populações pode ser encontrada na região do istmo, central na glândula, e as suas células são denominadas de células-tronco estaminais e a segunda população, armazenada na base da glândula, é composta por células designadas de células principais. As células do istmo, em homeostasia, apresentam um estado proliferativo constante e estão encarregues da manutenção do tecido através da substituição de células senescentes. No caso das células estaminais da base, estas mantêm-se num estado de espera apresentando um baixo nivel de proliferaçao, estado esse denominado por quiescência.

Em estudos anteriores, foi descoberto que após danificação do epitélio do estômago, as células estaminais principais da base alteram o seu comportamento e transitam para um estado proliferativo de forma a repopular o epitélio do estômago. Foi então proposto, com base em dados obtidos através de testes conduzidos no âmbito de identificar mecanismos de resposta a danos no tecido, que estas células estaminais estariam sob a influência de um determinado estímulo e que o candidato mais promissor para iniciar esse estímulo seria a proteína inibidora de quinase 1C dependente de ciclina, também conhecida por p57Kip2.

De forma a realizar este estudo, modelos animais de rato e organoides derivados de rato em cultura foram utilizados. A proteína candidata, p57, colocada num vetor induzível, foi electroporada em organoides de forma a criar um modelo onde fosse possível estudar os seus efeitos em cultura de uma forma controlada, estando ou não a ser expressa. Com o modelo estabelecido, foram estudadas as alterações nos requerimentos e fatores de crescimento necessários no nicho das células estaminais, assim como a capacidade de a proteína induzir nas células um estado de quiescência quando estas estariam normalmente em estado proliferativo em cultura e candidatos à via de sinalização envolvente na proteína em questão. Efeitos da falta ou sobreexpressão da proteína em modelo animal foram igualmente estudados e comparados aos obtidos pela cultura de células.

Outros membros da família da proteína p57, denominada de Cip/Kip, foram igualmente testados de forma a identificar possíveis resultados que indicassem uma capacidade de atuação idêntica à mesma. Por último, foi colocada a hipótese de a proteína em questão ter a capacidade de atuar de igual forma num tecido ectópico, ou seja, onde esta não está presente em condições normais.

Os resultados demonstraram que a proteína p57 tem de facto a capacidade de colocar as células estaminais num estado de quiescência, tanto a curto prazo, 7 dias, ou a longo prazo, 3 meses, em cultura de células assim como nos modelos animais utilizados. Foi também observada na proteína uma capacidade de influenciar as células fazendo com estas alterem os seus requerimentos em relação aos fatores de crescimento necessários à manutenção do estado estaminal das células do nicho.

Tendo em conta os candidatos à via de sinalização envolvendo o p57, o recetor IGF1 foi selecionado. Foram administrados aos organoides o ligando e o inibidor deste recetor. No caso do ligando não foi observado qualquer efeito com as condições utilizadas, no entanto, o inibidor apresentou um efeito de paragem da proliferação mais imediato quando administrado a organoides que sobreexpressavam a proteína p57.

Outras proteínas da família Cip/Kip apresentaram alguma capacidade de manter os organoides num estado de quiescência, mas os resultados dos testes efetuados não foram inteiramente conclusivos. Mais estudos terão de ser feitos tendo em consideração o ajuste das doses ou a escolha de diferentes clones e condições para a realização dos mesmos.

Finalmente, a proteína em questão quando inserida em células de intestino delgado demonstrou capacidade de colocar as mesmas em quiescência a curto termo, ou seja, com 7 dias de indução. No entanto, os organoides apresentaram um silenciamento no promotor CMV onde se encontrava a proteína, o que causou uma paragem de expressão da mesma e como consequência iniciou-se a proliferação das células e assim crescimento dos organoides, não sendo por isso possível terminar com sucesso o teste a longo termo, ficando este teste sem resultados conclusivos.

De forma a contornar este silenciamento, um novo vetor foi proposto e desenvolvido, contendo uma resistência adicional a blasticidina numa tentativa de levar a que apenas os organoides que expressam o promotor sobrevivam em cultura.

Estudos considerando os efeitos desta proteína a longo termo em células do intestino delgado, tanto em cultura celular como em modelos animais, assim como possíveis efeitos do inibidor do recetor IGF1 em organoides de estômago não alterados deverão ser levados a cabo no futuro. Seria também de grande interesse estudar os efeitos da proteína p57 em organoides derivados de pacientes com cancro do estômago, e se alterações na concentração desta proteína poderão conferir algum tipo de resistência a drogas administradas regularmente neste tipo de paciente oncológico.

Palavras chave: Cancro gastrico; Úlceras; p57; Quiescencia; Células estaminais

Table of contents

List of Figures

Introduction

Materials and Methods

Results

List of Tables

Materials and Methods

Results

Abbreviations

A

Amp: Ampicillin

AmpR: Ampicillin resistance

Anxa10: Annexin A10

APC: Anaphase-promoting complex

ATP: Adenosine triphosphate

B

Bla: Blasticidin

bGH: Bovine growth hormone

BMP4: Bone Morphogenetic Protein

C

CAFs: Cancer associated fibroblasts

Cas9: CRISPR associated protein 9

CDH1: Cadherin-1

CDK: Cyclin dependent kinase

cDNA: Complementary deoxyribonucleic acid

CIN: Chromosomal instability

Cip: CDK interacting protein

CKI: Cyclin-dependent kinase inhibitor

cKO: Conditional knockout

CM: Complete media

CMV: cytomegalovirus

c-Myc: MYC proto-oncogene, bHLH transcription factor

CreER: Cre recombinase estrogen receptor

CRISPR: Clustered regularly interspaced short palindromic repeats

D

Dapi: 4’,6’-diamidino-2-phenylindole

DMSO: Dimethyl sulfoxide

DNA: Deoxyribonucleic acid

Dox: Doxycycline

DSB: Double strand break

E

EBV: Epstein–Barr Virus

EGF: Epidermal growth factor

Eppi: *Eppendorf*

ES: Embryonic stem cells

F

FGF10: Fibroblast growth factor 10

FZD: Frizzled

G

GFP: Green fluorescent protein

Gif: Gastric intrinsic factor

gRNA: Guide RNA

GS: Genomically stable

GSTM1: Glutathione S-Transferase Mu 1

H

HER2: Human epidermal growth factor receptor-type 2

Het: Heterozygous

HDR: Homology-direct repair

Hom: Homozygous

Hyg: Hygromycin

I

IGF1: Insulin-like growth factor 1

IGF1R: Insulin-like growth factor 1 receptor

IMBA: Institute of Molecular Biotechnology - Austria

iPSCs: Induced pluripotent stem cells

IRES: Internal ribosome entry site

ITR: Inverted terminal repeat

K

Kip: Kinase inhibitory protein

Klf4: Kruppel-like factor 4

L

LoxP: locus of X-over P1

LRP: Low-density lipoprotein receptor-related protein

M

MEK: Methyl ethyl ketone

miRNA: Micro ribonucleic acid

mRNA: Messanger ribonucleic acid

MSI: Microsatellite instability

mTORC: Mammalian target of rapamycin

N

Nac: N-Acetyl-L-cysteine

NDS: Normal donkey serum

NHEJ: Non-homologous end joining

Not1: *Nocardia otitidis* 1

O

Oct3/4: Octamer-binding transcription factor 3/4

OE: Over expression

P

PAM: Protospacer adjacent motif

PBS: Phosphate Buffered Saline

PCR: Polymerase chain reaction

PD03: PD0325901

PPP: Picropodophyllin

R

RNA: Ribonucleic acid

RNAi: RNA interference

ROCK: Rho-associated, coiled containing protein kinase

RSPO: Rspondin

RT: Room temperature

rtTA: Reverse tetracycline trans activator

S

sgRNA: Single guide ribonucleic acid

Shh: Sonic hedgehog

Sox2: Sex determining region Y-box 2

T

TCGA: The Cancer Genome Atlas

TGF-β: Transforming growth factor β

X

Xba1: *Xanthomonas badrii* 1

W

WHO: World health organization

WT: Wild type

1 Introduction

1.1 Stomach cancer

Stomach or gastric cancer is the second leading cause of cancer-related deaths, the fifth most common malignancy in the world and the seventh most prevalent, with over one million cases being diagnosed each year.[35;36] This type of cancer shows a higher incidence in men (1.87%) than in women (0,79%). Gastric cancer has an incidence rate that is highly variable by region and culture, being higher in Eastern and Central Asia and Latin America and lower in North and East Africa.[35] (**Figure 1**)

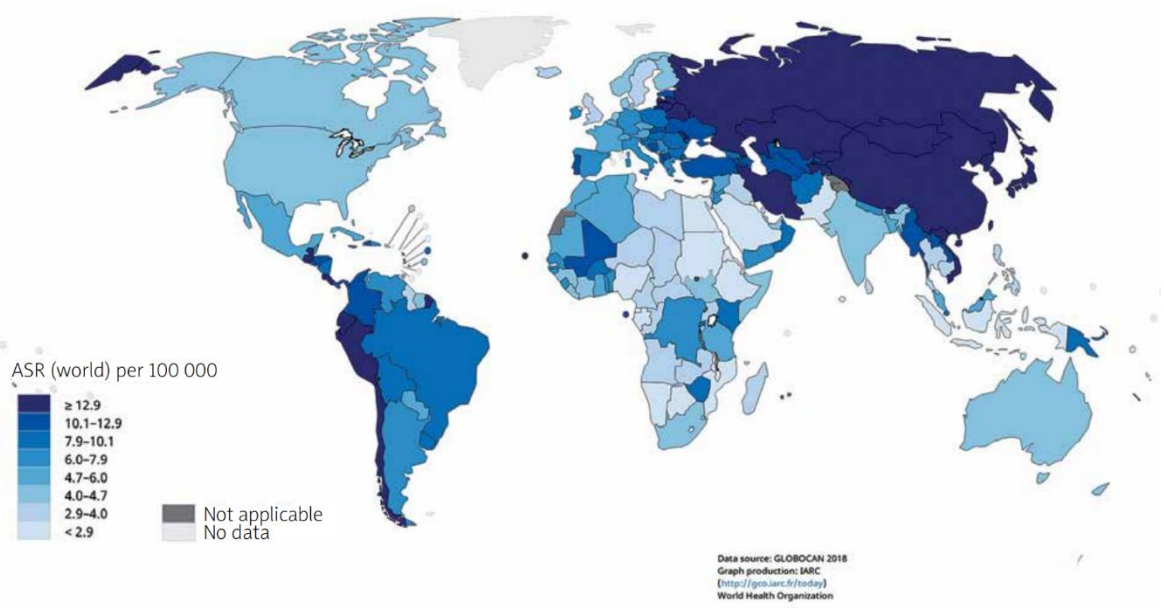

Figure 1 – **World rate for stomach cancer in 2018.** Map figure that shows the estimated world incidence rates for stomach cancer in 2018 for both sexes and all ages with a blue gradient. Light blue represents lower incidence and dark blue represents higher incidence rates. Adapted from Rawla, Prashanth et al., (2019).

Gastric cancer can be divided into different subtypes where 90% of them are adenocarcinomas. There are different classification systems. They can be either based on the WHO where the types are divided into 4 major categories, such as papillary adenocarcinoma, tubular adenocarcinoma and mucinous adenocarcinoma; the Lauren's criteria, which is the most widely used, and divides them into 3 main subtypes, intestinal, diffuse and mixed type[55]; or the Cancer

Genome Atlas (TCGA) that divided gastric adenocarcinoma into four molecular subgroups, EBV positive, MSI high, GS and CIN, based on either specific mutations or virus-related classifications.[36]

The risk factors of gastric cancer are often genetic. Certain inherited mutations cause a predisposition for the disease, such as the GSTM1-null phenotype, CDH1 gene or HER2 mutations. *Helicobacter pylori*, which is considered one of the main risk factors which may lead to two other complications that can also contribute to the disease, such as gastroesophageal reflux disease and gastric ulcers. Then there is also risk associated with smoking habits, alcoholism, chemical exposures, Epstein-Barr virus (EBV) and diet.[37]

In any case, the prognosis of gastric cancer continues to be poor. Most of the times, the lack of early diagnose possibilities leads to three out of four patients presenting non-curable advanced disease. Surgery is the main strategy held for this type of cancer, especially in Asian countries, but neoadjuvant and adjuvant chemotherapy have led to improved survival rates. Still, more efforts are needed to further succeed. [35;36] Studies in new pathways and proteins involved mainly in the specific epithelia and tissue of interest with new technologies might help with discovery of novel targets or therapies to help these patients.

1.1.1 Gastric ulcers

Ulcers are sores in the stomach lining that cause pain and discomfort. These appear due to depletion of mucous secreting cells of the tissue and consequently lack of protection against the strong acids present in the stomach. [67]

Stomach ulcers have a wide and variable range of incidence and prevalence worldwide with a high influence on wellbeing, a considerable mortality rate and are one of the risks associated with gastric cancer, as stated above. The understanding of this disease changed immensely with the finding of the infamous and already above-mentioned *Helicobacter pylori*. As said before, this disease can take away quality of life from the carrier and can be extremely painful and can later lead to chronic inflammation which might lead to further complications. Even though there have been considerable advances, ulcers remain an important problem especially because the usage of drugs that can eradicate the *Helicobacter pylori* have been associated with adverse gastrointestinal

events. Considering this and other possible pathologies associated with the stomach, understanding how the stomach responds to injury can give more insights to the tissue behaviour and help develop better treatments to these diseases that affect so many people all over the world.[38]

To find treatments and have earlier diagnosis of these pathologies it is important to understand how the tissue works in homeostatic conditions.

1.2 Homeostasis

Homeostasis is a state of balance / equilibrium. We can extract the meaning from the word itself, deriving from ancient Greek, parting "*hómoios*" meaning similar or same and "*statis*" meaning standing or state.

In biology, living organisms maintain this balance in a physical and chemical way.[1] This implies the existence of mechanisms tasked with maintaining the overall conditions when the normal state of the organism is disrupted.[2] When these fail, it can lead to chronic injuries or diseases, such as cancer.[3]

In the case of the stomach epithelium, homeostasis is maintained with an overall balance between senescence or shedding of old cells with rapid differentiation of new cells coming from the isthmus region towards the upper and middle part of the gland and a slow dividing population of stem cells that works as a reserved pool.[5;6]

1.3 Stomach

1.3.1 Structure

The human stomach epithelium can be mainly divided into three parts: the fundus or cardiac region, the corpus and the pyloric (antrum) region; While the human fundus region presents no edge limitation, in mice the stomach is divided into non-glandular or fore-stomach region and glandular stomach, where the two parts are separated by a limiting edge, and an antrum region.[4] (**Figure 2**)

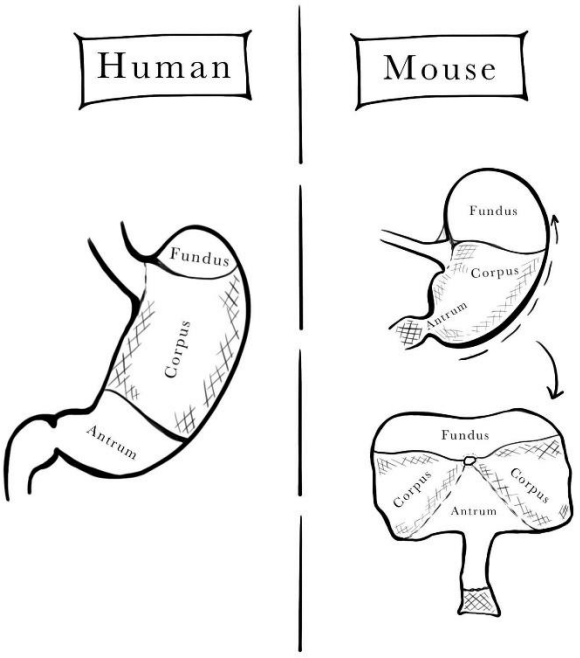

Figure 2 – **Mouse and human stomach.** Schematic figure of mouse (right side) and human (left side) stomach regions. The black lines are only representative of the different regions.

The human stomach is fully covered in a glandular structure that secretes the gastric acids needed for digestion. On the other hand, the mouse stomach has both glandular and non-glandular regions that each contribute to different functions; the glandular area of the stomach is responsible for secreting the gastric acid and the non-glandular area serves a temporary site function, providing a place for food storage and digestion.[4]

1.3.1.1 Epithelium / glands

As mentioned before, the stomach contains glandular structures that are formed from invaginations from the inner epithelium. (**Figure 3**) These structures are designated as gastric units or gastric glands. The glands protrude towards the stomach mucosa and are formed by cells of different types. Certain regions, like the corpus region, may even be characterized or subdivided by looking at the present cell types.[6]

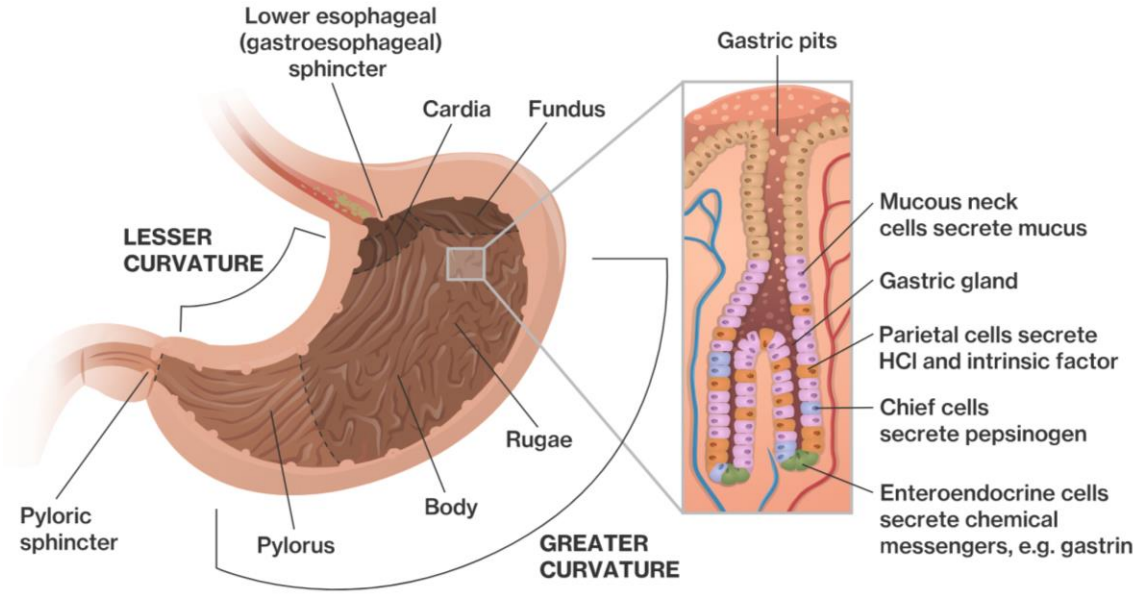

Figure 3 – **Stomach glandular structure.** Schematic figure of the stomach epithelium regions, glandular structure, cells composing the gastric units and their respective secretory functions. Adapted from https://www.coursehero.com/sg/anatomy-and-physiology/stomach/

The types of cells that comprise the stomach glands are stem cells, such as Chief (Troy^{+}) and isthmus stem cells. The Chief cells are located at the base, are usually slow dividing cells and are also capable of producing digestive enzymes, on the other hand, isthmus stem cells can be found at the isthmus region of the gland and are usually rapidly dividing cells with the ability of constantly repopulate the tissue, as stated before. Endocrine cells, which are hormonal based, have the ability to send distal signals and help coordinate hunger/satiety as well as Calcium homeostasis; these appear low in number. Mucous (neck) cells, parietal cells, which are acid producing cells, appear scattered throughout the tissue. Both Parietal cells and Chief cells are long-lived and have an estimate turnover rate of months; [5;6]**(Figure 4)**

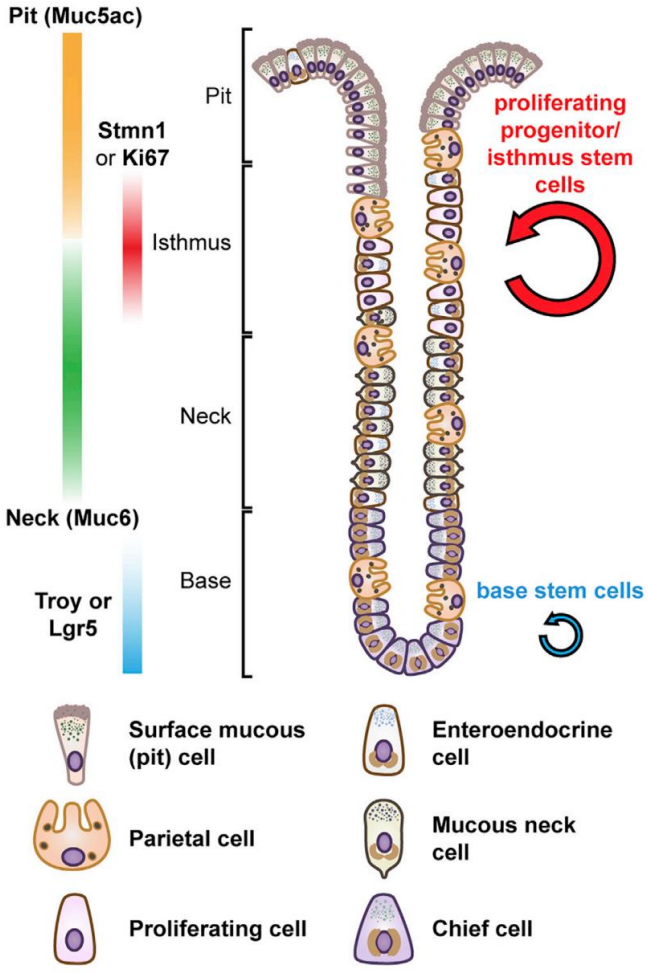

Figure 4 – **Gastric corpus gland composition**. Schematic figure of gastric corpus gland regions, cell types and their genetic markers. Adapted from Han *et al*., (2019).

Different cells will be present in different ratios throughout the various regions or even absent from it. For example, the antrum regions contain glands composed mainly by pit and mucus neck cells while glands in the corpus regions have a wider variety of cells and more stratified regions[39;46]. (**Figure 5**)

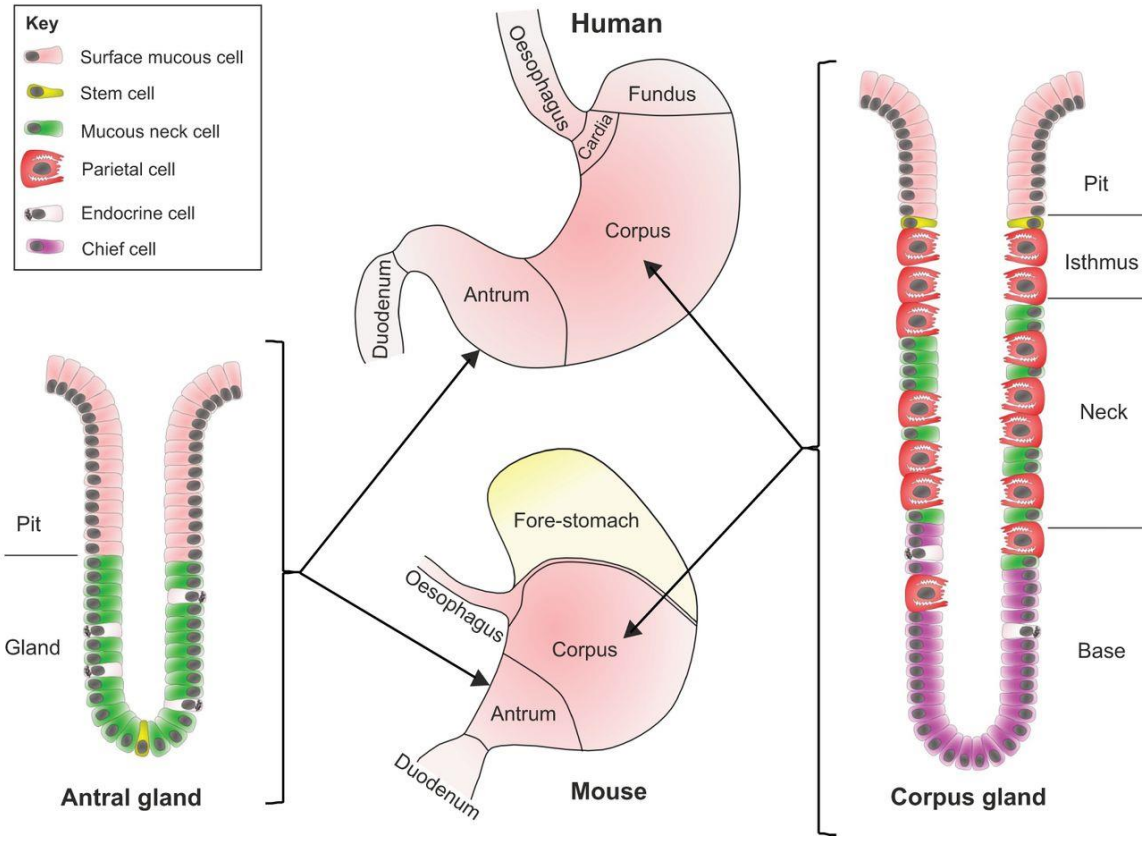

Figure 5 – **Antral vs gastric corpus glands**. Schematic figure representing the anatomy of antrum and corpus glands as well as different cell types and cell regions of human and mouse stomach. Adapted from Burkitt, Michael D., *et al*. (2017).

1.4 Stem cells

Stem cells are defined as self-renewing, which means that they can use cell division to produce copies of themselves and are also able to go through differentiation in order to evolve into a more mature or specialized cell.[8] They can be found in both adult and embryonic organisms or even induced from mature cells like fibroblasts.[15]

The adult stem cells are present in niches within certain tissues. These tissues are known to have a stem cell pool reserved for regeneration upon injury and, more importantly for the normal homeostatic turnover as maintenance for the tissue.[76] Stomach, small intestine, skin and prostate are examples of such tissues with well-known stem cell pools.[20] Some stem cell pools are still unknown or poorly understood like those found on the brain or heart.

Every type of stem cell has a determined level of potency.[13;14] They can be totipotent, pluripotent, multipotent or unipotent. Totipotent cells have the capacity to generate any cell type that constitutes an organism including extraembryonic tissues. The pluripotent cells can give rise to differentiated cell types that represent all three germ layers such as embryonic stem cells, but these exclude any extraembryonic tissues.[10] Multipotent stem cells are able to make progenitor and more specialized and mature cell types. Finally, unipotent cells are progenitors that can only differentiate to one and only one cell type. Adult stem cells can be found among the multipotency range. [11]

Stem cells are also known to have a specific epigenetic landscape. Most stem cells display a broader existence of euchromatin, which means that their genome is usually more hypomethylated and the DNA structure more open for expression.[9] That open expression tends to decrease with the

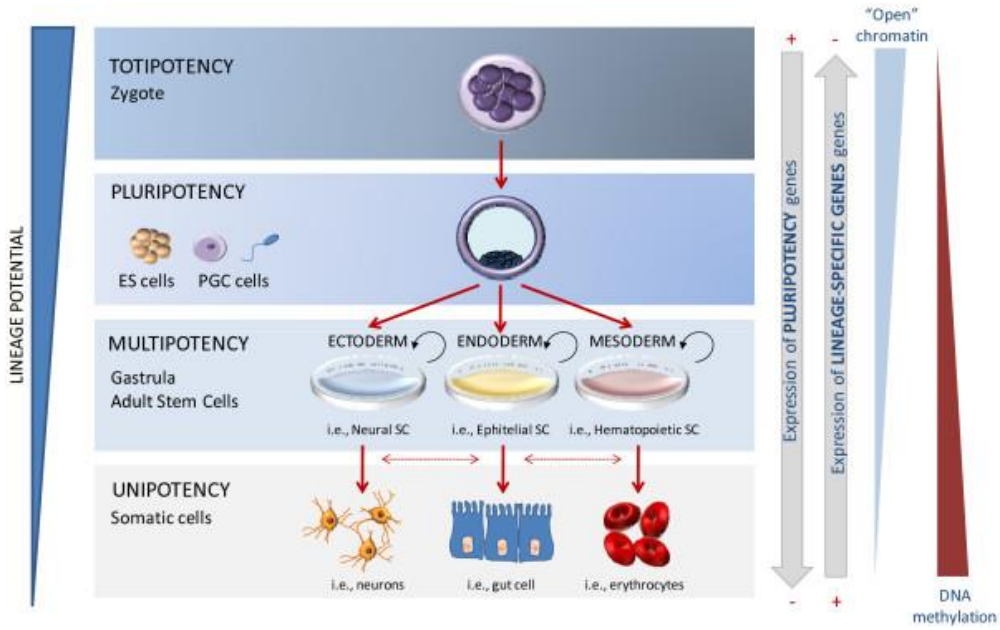

Figure 6 - **The different levels of stem cell potency.** Schematic representation of the different levels of stem cell's potency, as well as pluripotency and lineage specific gene expressions and epigenetics. Adapted from Berdasco, María. et al., (2011).

maturation process. The more differentiated the stem cell is the more methylation is present and less open chromatin is available.[12] (**Figure 6**)

As held, not only these cells have a specific epigenome but consequently, a specific set of genes being expressed that characterize them into the several categories and define their level of 'stemness'. Yamanaka**,** in 2006, tested several genes to assess which ones were crucial to set cells back to pluripotency. The genes discovered and validated were Oct3/4, Sox2, c-Myc and Klf4. Two of these transcription factors, Oct3/4 and Sox2 with the addition of Nanog were already known to function in the maintenance of pluripotency in both early embryos and ES cells. But for the induction of pluripotency, surprisingly, Nanog was dispensable. [15]

With this line of thought, induced pluripotent stem cells are then cells originated simply from differentiated somatic cells that have been reprogrammed *in vivo* to restart expression of certain distinct genes that can make a cell enter an undifferentiated state that will allow them to give rise to certain cell types once more. [15]

These cells are thought to help in regenerative medicine and are being used for translational medicine. Nonetheless, they still need a great deal of research to be safely used in regenerative medicines with human beings, since implantation of these cells often lead to teratomas and other types of tumours or cancers.[75]

However, these have the possibility to be used for translational medicine. They can be manipulated into having certain phenotypes, or even derived from a specific patient in order to conduct personalized drug testing in vitro. This could in turn have a seriously significant impact in the medical field.[16]

If the tissue of interest already has a known pool of stem cells then, depending on the availability of the pool, adult stem cells can be used for these translational studies.[72]

As previously stated, there are two populations of adult stem cells present in each of the stomach glands. One in the isthmus region, which keeps a proliferative state in homeostasis and the second at the base of the gland usually with a non-proliferative state and that can become active upon injury. Having a second population of stem cells in the same gland is a unique feature of the stomach.[7]

1.4.1 Organoids

Organoids are one of the recently developed tools that would allow the usage of stem cells in translational medicine.

Organoids are cells self-assembled into a three-dimensional shape that functions as a mirror of the derived tissue in terms of function and architecture. These are still seen as one of the most noteworthy advances in stem cell research.[17]

Having such a model aims to address some of the drawbacks of using either animal models or 2D cell cultures. Even though animal models make use of a fully working organism with many compatible components for studies, ultimately, they still derive from a different origin and also involve high costs, laborious and time-consuming work and raise big ethical concerns. 2D cell cultures are well studied and broadly used but lack the cell complexity of an organism and are also time-consuming, hard to maintain and need to be kept in stable conditions.[22]

Organoids provide us with organized cell structures that maintain a certain degree of tissue complexity and interaction. Some cultures even have multiple types of cell lineages and, more importantly, some types can be derived from human tissues. [40]

Organoids can be grown from induced pluripotent stem cells (iPSCs), human embryonic stem cells (hESCs) or adult stem cells and form an extensive panel of organs including gut, kidney, pancreas, liver, brain, and retina, among others, some being exclusively formed from each specific type of stem cell. [41]

Cerebral organoids for example, cannot be formed by adult stem cells since no particular pool is known at this stage. These are usually assembled from iPSCs, most commonly fibroblasts.[15;74]

Gut and stomach on the other hand, the models used in this study, have a characterized pool of adult stem cells that can be reached and easily used to generate the so-called mini guts or stomachs. Most of the cerebral studies using organoids are being carried out to understand brain development and diseases such as Alzheimer's and schizophrenia[41] whilst the mini-gut and stomach are mostly being used for drug tests concerning cystic fibrosis or even cancer.[42] These mini models can be even infected with pathogens to study their influence or damage on the host tissues[43] (**Figure 8**) or even co-culture with several other cell types in other to have a more close to *in vivo* approach.[40] (**Figure 7**)

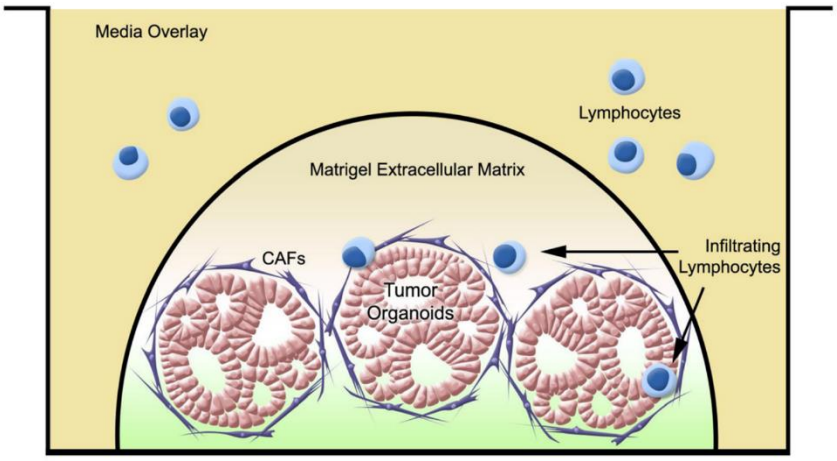

Figure 7 - **Organoids co-culture.** Schematic figure of an organoid co-culture containing lymphocytes, CAFs and tumour organoids. Adapted from Tsai. *et al*., (2018)

Nonetheless, these mini organs are still not fully approved and carry with them a series of ethical issues. Stem cells in general raise a lot of debate regarding the destruction of embryos, but since, in this case the usage of adult stem cells or iPSCs doesn't involve the embryo phase, other matters like consent, ownership, commercialization, intellectual property rights, and safety have caused controversial discussions.[17]

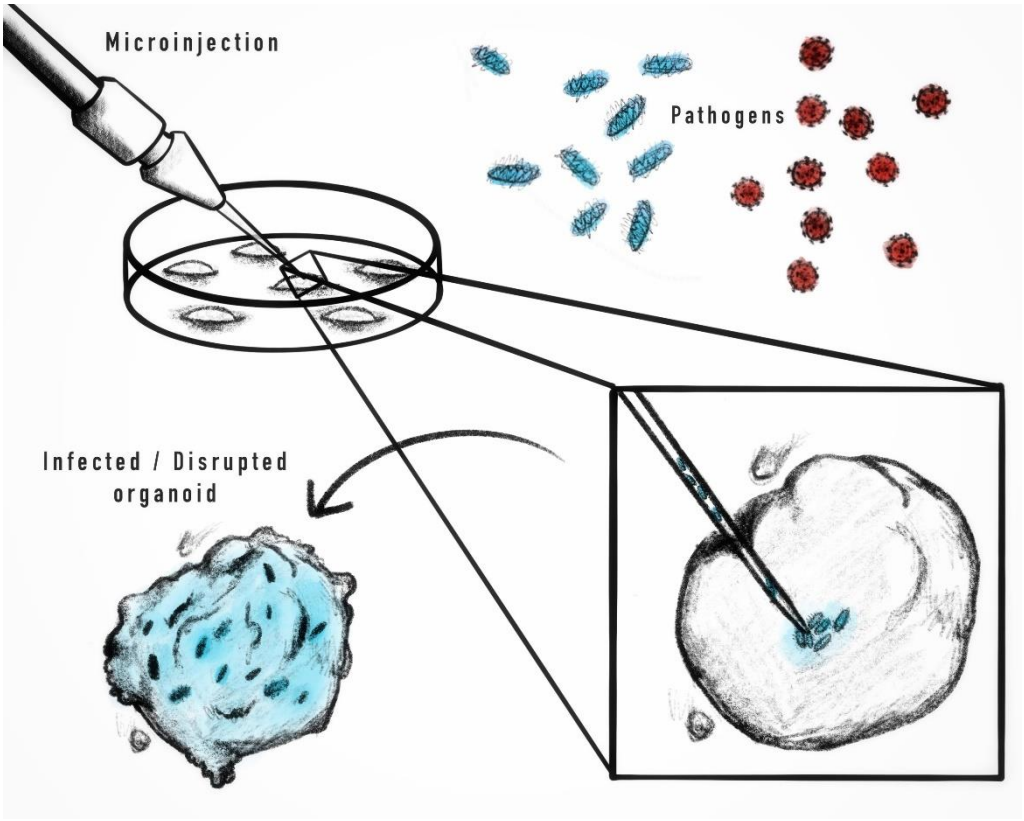

Figure 8 - **Pathogens infection on organoids.** Schematic figure of an organoid microinjection with pathogens. Adapted from https://horizon.kias.re.kr/14275/

Even considering the aforementioned ethical concerns, organoids are one of the most favorable *in vitro* models to conduct certain studies and are gain more potential with each new development.[72]

1.4.1.1 Organoids for oncology

Many methods have been used throughout the years to help with studies regarding cancer. Nevertheless, most of them still show a fair number of limitations. Xenografts are tissues, organs or living cells from species that are transplanted into a different species. In the field, immunodeficient mice are commonly used. This method is one of the most well regarded, since the tumour cells maintain more characteristics of the original site. Still, this method can experience inefficiency of the engraftments and likely changes of the cells or tissue due to the fact that the mouse system can respond to them differently or just by simple manipulation of the cells. Adding to that, as mentioned before, mouse models are costly and require a cumbersome amount of work.[18]

Primary patient-derived 2D cancer cell lines, for example, are widely used but these cells are hard to establish and lose many of the tumour heterogeneity features and microenvironment dynamics.[19]

Patient-derived cancer organoids have the ability to mimic the histology, intratumor heterogeneity and some of the cell interactions. These organoids have also been shown to remain genetically stable over time having no major chromosomal changes. Tumour derived organoids have already been established from colon, oesophagus, pancreas, stomach, liver, endometrium, prostate, breast, bladder[20] and, most recently, from ovarian cancer patients.[21] These advantages are starting to make organoids stand out as one of the most desirable models to work with for drug testing as stated above, or to study pathways involved in tumorigenic processes.[72]

1.4.1.2 Genetic engineering in organoids

As previously mentioned, organoids have been vastly used for disease modelling and therapy development. For this, techniques to generate, repair or introduce specific genetic mutations or sequences were needed.

Some of the now extensively used systems ranges from interference RNA (RNAi) to transposons and CRISPR/Cas9 systems. RNAi's don't make any changes onto the genome of the cells; these only use the cell's machinery. On the other hand, transposons like the PiggyBac and Sleeping Beauty system, can introduce the gene of interest randomly into the cell's genome for a long-term expression or can inactivate by chance an active gene and influence the cell machinery. Both systems cut the genetic sequence flanked by a specific terminal inverted repeat from one locus and place it into an alternative one.[44]

The well-known CRISPR system, first discovered in bacteria, was further built to work with an attached Cas9 endonuclease that binds to a specific 3 nucleotide sequence named PAM and a single-guide RNA (sgRNA or gRNA) that binds to a complementary sequence of DNA to guide the enzyme to the gene of interest and create a double stranded cut. This cut then leads to the activation of repair mechanisms: Non-homologous end joining (NHEJ) or homologous-direct repair (HDR). The activation of these mechanisms enables scientists to either insert a wanted sequence by HDR or to cause a gene to lose its function by NHEJ, since this leads to indel formation.[22] (**Figure 9**)

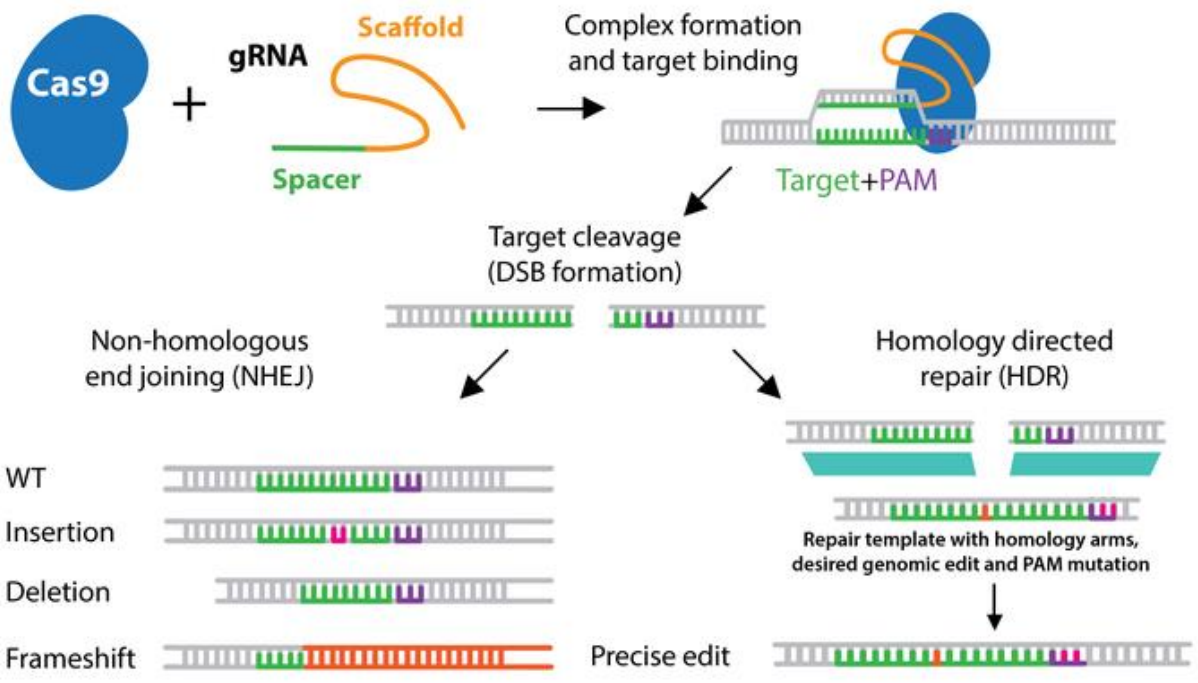

Figure 9 - **Repair mechanisms from double stranded DNA break.** Schematic figure of the CRISPR-Cas9 mechanism and the two possible pathways for double stranded DNA repair. HDR on the right side of the image and NHEJ on the left side of the image. NHEJ gives rise to indel formation and HDR generating a precise edit in the presence of a template with homology harms. Adapted from https://www.addgene.org/crispr/history/

These mechanisms allow scientists to employ the organoid technology in order to achieve better and more accurate results when studying genetically complex diseases.[22]

1.4.2 WNT Pathway

Cells in general are controlled by several pathways that lead them into different fates. These pathways start with chemical or physical signals that are then transduced into a response that will trigger a specific outcome. These signals pass from a cascade of molecular events mostly related to post-translational modifications, such as protein phosphorylation.

One of these pathways, the Wnt pathway has been widely studied and related to the stem cell field. Wnt signals can be transduced through their canonical pathway for cell fate determination and differentiation or through the noncanonical pathway for control of cell movement, axonal guidance and tissue polarity.[30;31]

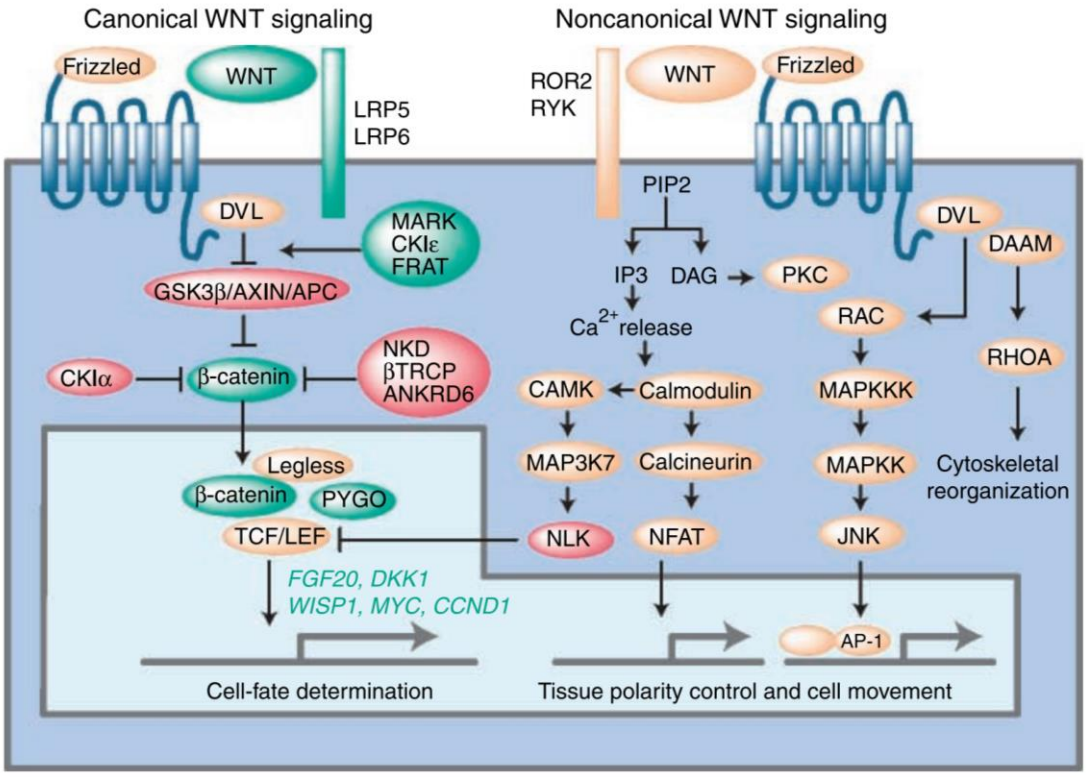

Figure 10 - **Wnt signaling pathway.** Schematic figure of the canonical(left), and non-canonical, (right), Wnt signalling cascades. Adapted from Katoh, et al., (2007)

In the canonical pathway, signals are transduced through Frizzled (FZD) and LRP5/LRP6 receptors for the β-catenin signalling cascade. In the absence of canonical Wnt signalling, the β-catenin, complexed with APC and AXIN, is phosphorylated leading to its degradation.[30]

Wnt canonical signaling plays a role in both embryonic development and adult homeostasis for maintenance of the stem cell pools. (**Figure 10**) In embryonic stem cells, overexpression of Wnt, stabilized β-catenin or lack of the APC complex results in the inhibition of neural differentiation. In the same manner, treatment of stem cells with a synthetic drug that activates the canonical Wnt pathway sustained pluripotency and self-renewal.[31]

This activity is also controlled negatively at several stages by other molecules, like Notch, transforming growth factor β (TGF-β) – BMP, fibroblast growth factors (FGF) and sonic hedgehog (Shh).[30] These can block the Wnt signal or antagonize it and lead to a different or opposite cell fate or behaviour.[34;45] (**Figure 11**)

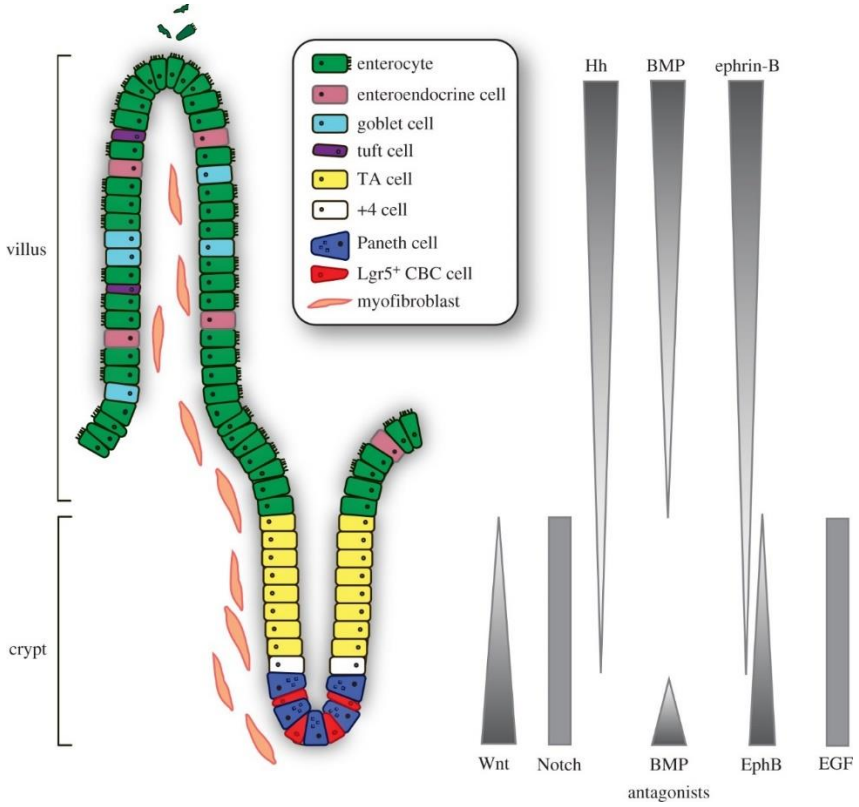

Figure 11 - **Differentiation vs stemness signals.** Schematic figure of the different factor and their gradients throughout the small intestinal villus and crypts. Adapted from Spit, et al., (2018)

In the case of small intestine and gastric epithelium, Wnt displays a short-range signalling and gradient throughout the glands[32] which maintains the stem cell pool and overall homeostasis

of the cell population of the tissue. An imbalance in the signalling pathway may have severe implications such as developmental abnormalities and cancer.

These pathways can then be used as the required niche factors to grow and maintain stem cells *in vitro* and to select resistant cells that survive and are able to sustain themselves without their niche factors just like some types of cancer cells. [33]

1.5 Cell cycle

Eukaryotic cells are governed by a cycle that is divided by 2 main stages, interphase and mitosis (cell division). Each of them can be further divided into several phases. The Interphase is the longest one and comprises G_1, S and G_2 phases, while in mitosis, there is prophase, metaphase, anaphase, telophase and cytokinesis. Cells can even exit this cell cycle and enter a resting phase called G_0. (**Figure 12**) All these phases are organized and regulated by the interaction and cooperation of certain proteins and enzymes. [24]

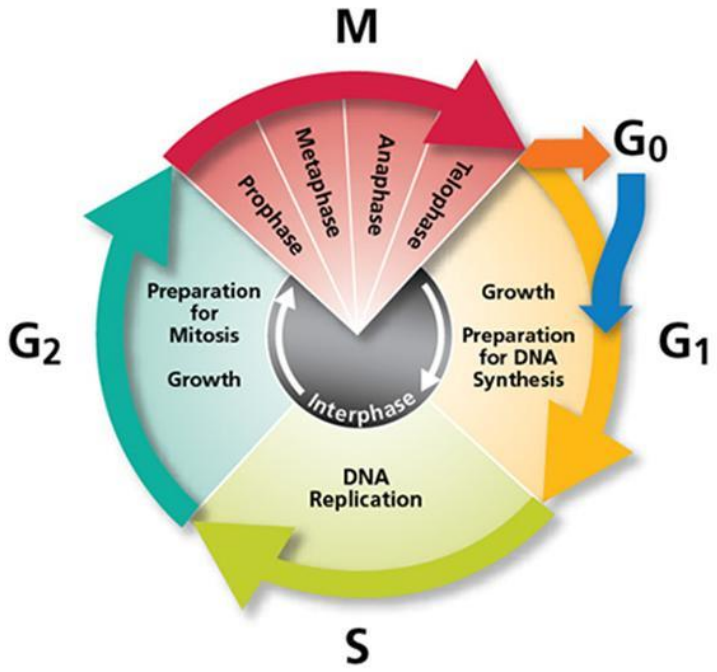

Figure 12 - **Cell cycle.** Schematic figure representing cell cycle major stages: interphase and mitosis, together with the different phases within them, such as G_1, S, G_2, G_0 during interphase and prophase, metaphase, anaphase and telophase during mitosis. Adapted from https://bjmbiology.weebly.com/

There is a step during the G1 phase during which the cell can turn to pause, exit or persist on the cell cycle depending on extrinsic factors. This step is denominated checkpoint. There are other checkpoints throughout the cell cycle, these being located in G1, S and M, and they are crucial for a good functioning of the cell and overall organism. Passing the G1 checkpoint and onto the S phase, the DNA gets replicated and the cell grows. In the G2 phase the cell prepares for mitosis. Within the M phase which stands for Mitosis, there are five main stages of chromosomal condensation and cell separation, Prophase, Metaphase, Anaphase, Telophase and lastly Cytokinesis.[25] In prophase the chromosomes start to condense and get spindles attached to them. Metaphase gets the chromosomes aligned and these then divide equally having their sister chromatids being pulled into opposite directions during Anaphase. In Telophase the nuclear membrane reshapes and reforms around each set of sister chromatids, these loosen the condensation and the spindle fibers disappear. Cytokinesis is the last one and here the cytoplasm divides and 2 identical cells are formed with identical genetic information.[73] (**Figure 13**)

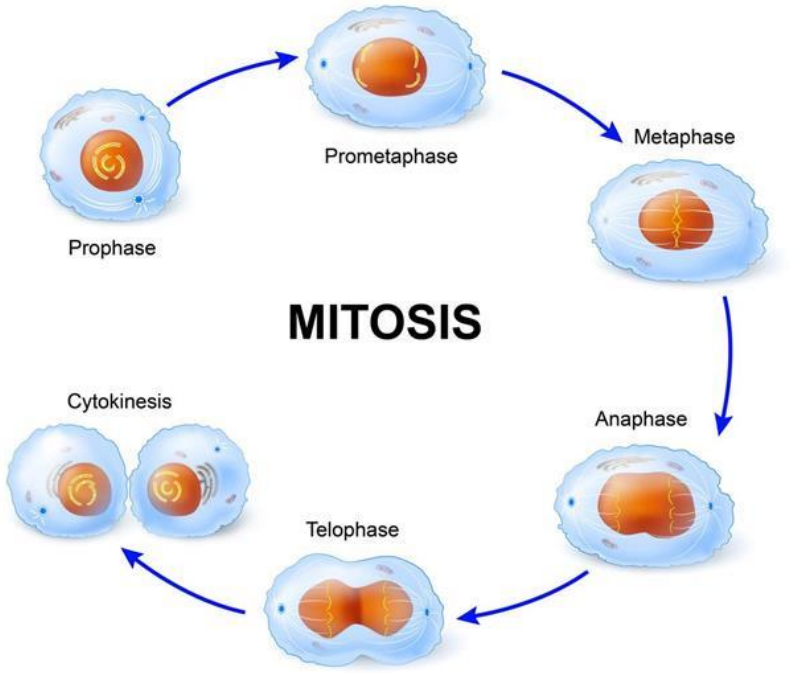

Figure 13 – **Mitosis.** Schematic drawing representing all the different stages comprising mitosis, prophase, prometaphase, metaphase, anaphase, telophase and cytokinesis (cell division). Adapted from https://biologywise.com/plant-mitosis-vs-animal-mitosis

This is the basic cycle of life and it has an intrinsic and important mechanism of regulation underlying it.[73]

1.6 P57, Cip/Kip family and cyclins.

As previously stated, the cell cycle is well regulated. Thus, each event is controlled through signalling transduction pathways as well as feedback loops to assure the correct sequence of them. Specific pathways connect the machinery. Mitogenic signals bind to the receptors and release a cascade of events that leads to expression of enzymes, more specifically kinases that also contain a regulatory subunit of which they are depend for function and regulation named cyclins. Such enzymes are so called cyclin dependent kinases, usually and more commonly referred as CDKs.[26] Having stated this, progression of the cell cycle through the different stages and phases previously stated, is regulated by these CDKs. An analogy that describes this cooperation between cyclins and CDKs is that CDKs are seen as the engine that leads to cell cycle progression and cyclins are considered as the gears that are changed to assist the transition between cycle phases.[27]

These cyclins and CDKs build pairs. CDK 4/6 go together with cyclins D; CDK 2 goes with cyclin E and A and CDK 1 associates with cyclins A and B. Cyclins get their designation from their cyclical nature as their concentration varies in a cyclical pattern during the cell cycle.[28] For progression through G_1 phase, cyclin D together with CDK4/6 is required. For a G_1 to S transition, cyclin E goes into place along with CDK2 and activates the replication machinery. Then, cyclins A and B associated with CDK1 work for the transition through G_2 and M phases.[29] (**Figure 14**)

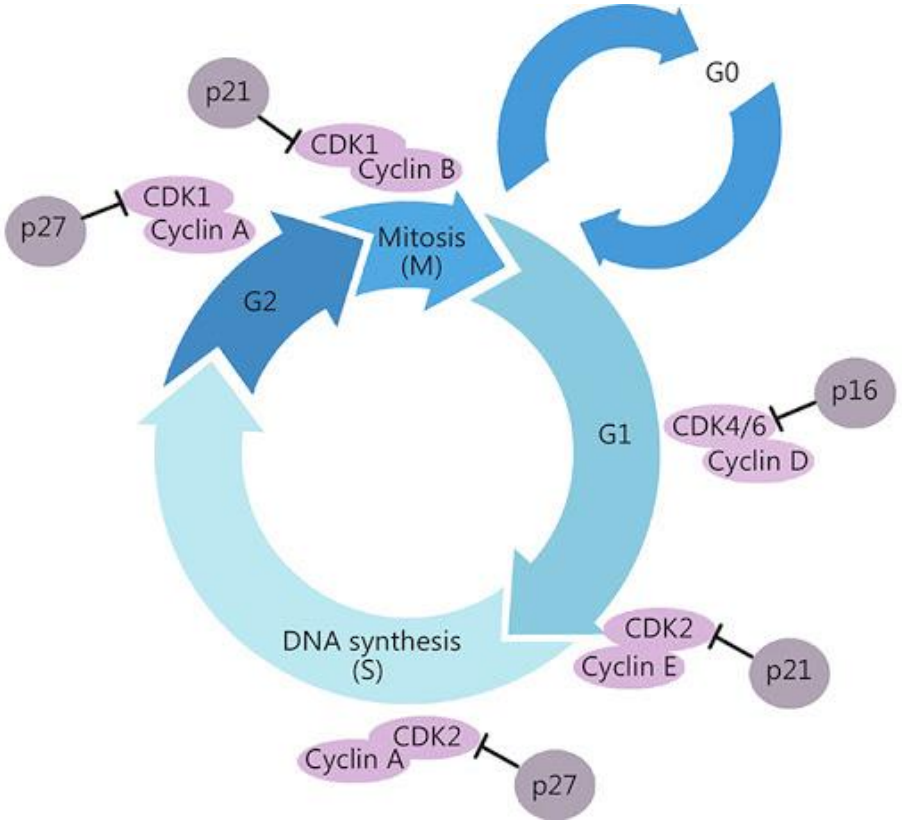

Figure 14 – **Cyclins, CDKs, CKIs and cell cycle.** Schematic figure representing each cyclin and CDK pair at each time point of the cell cycle and some of their inhibitor proteins. Adapted from Bai, et.al., (2017)

In the same manner that these proteins and enzymes help the cell cycle to take place and progress, other proteins also help this regulation in a negative way. CDKs can be inhibited by so called CDK inhibitors (CKIs). These belong to two different known families, Ink4 or Cip/Kip. Among the Ink4 families are the $p16^{Ink4a}$, $p15^{Ink4b}$, $p18^{Ink4c}$ and $p19^{Ink4d}$. These specifically inhibit CDKs 4 or 6 whereas the Cip/Kip family proteins, such as $p21^{Cip1}$, $p27^{Kip1}$and $p57^{Kip2}$, mostly inhibit CDKs 2 and 4 (sometimes 1). The G_1 phase is also the phase, in which cells can exit the cell cycle and enter the previously mentioned G_0 phase. As these Cip/Kip family proteins can interfere with and block the progression in the G_1 phase, they can also have an influence on sending the cells into this G_0 phase. $p21^{Cip1}$, $p27^{Kip1}$and $p57^{Kip2}$ have been implicated before in directing cells into G0 where they constitute a population of stem-cell-like cells in a quiescent state. $p57^{Kip2}$ has been found to be the main influencer, having a dominant role among their family pears into these subjects.[29]

1.7 Quiescence

Quiescence, by definition, is a state of quietness or inactivity. Concerning cells, the definition translates to a state of the cell where the same is not dividing. In a cellular prism, quiescence does not always translate or refer to inactivity. Some cells may be simply being put on hold on to sustain a maintenance pool for a specific tissue, yet they reversibly enter and exit the cell cycle depending on the environmental stimuli During their quiescence phase they enter G_0. Some stem cells can also avoid this phase depending on tissue requirements. Examples of these are the small intestinal stem cells, which demand a continuously cycling population to keep a steady supply of newly generated cells, either stem like or more differentiated ones to maintain a well-balanced tissue.

These stem-like cells serve as progenitors for repair and replacement in case of injury that may lead to damage of the tissue itself. Adult multipotent or unipotent progenitor stem cells with a slower turnover rate may usually experience vast periods of time in the quiescent state throughout the organism's life.[23]

Other cells in the adult body can also be found in a G_0 phase, such as terminally differentiated or senescent cells, but these ones are irreversible in this state.

This paused, out of the cycle state is of major importance for an overall balance of the organism itself. Certain reserved pools of stem cells are dependent of an appropriate balance to maintain itself, a simple mis- regulation or an imbalance of signals can critically damage the pool and extinguish the reserved cells leaving the organism unfit for repair or regulation. So, it is of great importance to have and preserve these pools of quiescent cells to maintain a healthy organism during its life span.[23]

Quiescent stem cells populations have a common set of characteristics: They all present a metabolism different from cells in the active state, where they opt for glycolysis and fatty acids instead of the phosphorylation pathway. This leads to a consequent reduction in the synthesis of proteins and reduced mRNA levels.[23]

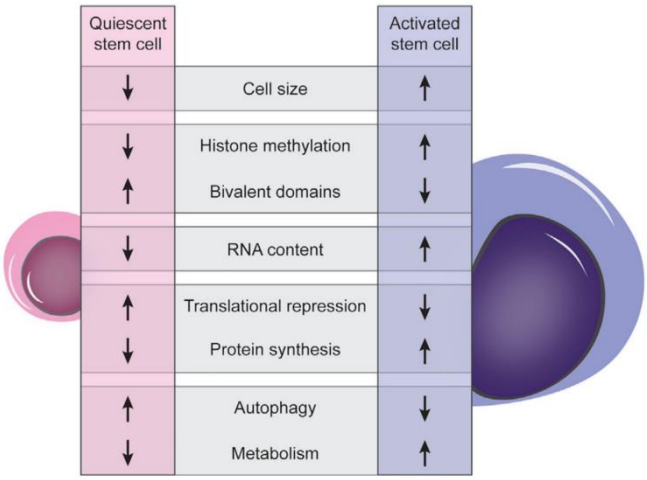

Figure 15 – **Differences between activated and quiescent stem cells.** Schematic figure comparing intrinsic and morphological stem cell characteristics between active (purple) and quiescent (pink) state. Adapted from Van Velthoven, et al., (2019)

As stated before, these cells are usually on hold and depend on stimuli to either enter a quiescent state or leave from it to iniciate proliferation. These cells might require a rapid response to overcome damage in tissues and for that matter they are primed and ready for a quick reentry in the cycle when needed. This can be acomplished by epigenetics or a production of transcripts without the consequent protein production.[23] (**Figure 15**)

Cells in a quiescent state reveal an individual profile regarding epigenetics. Several adult stem cells present both repressive and permissive histone metilation marks for promotors which indicates high plascticity in the cells. In the same manner, a range of these quiescent stem cells showed presence of severeal lineage restricted transcripts without any of the protein itself. A great number of post-translational mechanisms have been identified to have a role in maintanence and exit of this quiescent state, such as miRNA regulation for mRNA stability and translational repression. The regulation by these miRNAs is of great importance, since overexpression or knockdown of the same ones has been implicated in quiescence and increase of cell proliferation.[23]

This description of quiescence in general might lead to the idea that this concept exists as a binary state. But that is not the case, cells may exhibit several levels of it, from a deep quiescent state to light and shallow. Even though there might but several levels on the state, two are in particular distinction, the already mentioned canonical G_0 and a primed G_{Alert} state. Certain cells need to be ready for a more eminent response to tissue damage and those are the ones that can usually be found in a G_{Alert} state. These cells are reported to be sometimes bigger in size, transcriptional activity, mitochondrial activity and increased levels of ATP compared to those in a G_0 state. It must be kept in mind that these still show decreased levels of these activities compared to a fully active proliferating cell.[23]

The difference in cell states have also been compared with levels of certain proteins that provide an easier way out of the quiescent state, like the cell cycle's CDK6.[23] (**Figure 16**)

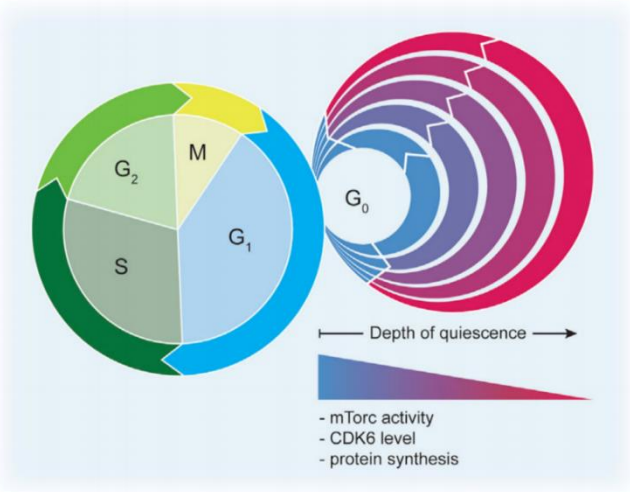

Figure 16 – **Different quiescent depts.** Schematic figure representing the different quiescent depts and comparison with protein and pathway activities. Adapted from Van Velthoven, et al., (2019)

Short-term stem cells have presented more abundance in CDK6 compared to their long-term counterparts. The abundance of this specific CDK allows the cells to move more quickly into the G1 phase of the cell cycle. This however does not comply with a G_{Alert}. CDK6 high or low levels have been reported with similar levels of mTORC activity, which means that these cannot be directly related.[23] Therefore, numerous quiescence level states are possible, and this concept cannot be treated with binary depth. Further studies might come to unveil these not yet understood processes that bridge between the several existing levels of complexity.[23]

1.8 Hypothesis/ Study objective

With the above statements, gastric pathologies are a major issue to the general population. To study and understand the homeostatic behaviour and signalling within the gastric tissue can bring important knowledge to overcome many of these roadblocks in treatments and diagnosis.

Here the new organoid technology was used to study previous data that demonstrated that upon injury stem cells, would change their behaviour and get activated to replenish the damaged tissue. It was proposed that these stem cells were under the control of a reversible switch that would make them change their performance according to certain stimuli. Based on extensive injury-response data CKI $p57^{Kip2}$ was identified as the most promising candidate to constitute such a switch

To characterise the candidate protein, electroporations were carried out to generate overexpressing organoids. We then investigated the long- and short-term effects of the protein in the stomach cells. After having confirmation of the candidate's performance as a switch for quiescence in the stomach epithelium we set out to investigate the possible effects in an ectopic manner with the use of small intestinal organoids. Gastric organoids with $p57^{Kip2}$ overexpression were set in different growth factor conditions to investigate possible niche requirements alterations or pathway regulations. From previous RNA sequencing data, a p57 pathway candidate was selected and its ligand and inhibitor treated to p57 OE organoids to assess its effects. Other Cip/Kip family members were also studied and compared to the p57 *in vitro* data. *In vivo* overexpression (OE) and conditional knock-out (cKO) mice already generated were used to investigate phenotype alterations and compare to the *in vitro* data.

Lastly one new construct was generated to overcome some of the problems found during the experiments *in vitro*.

2 Materials and methods

2.1 Ethical / animal facility statement

All animal experiments were approved by the Austrian Animal Care and Use Committee.

The in-house animal facility provided husbandry for the animals and services of all the different research groups within the institute. Also, it recognizes and takes responsibility regarding the care and use of animals, taking into account the highest ethical standards. Finally, the facility is also in compliance with the Austrian laboratory animal act 2012 as well as all possible relevant regulations and rules regarding laboratory animal husbandries. All the necessary certified exams and training, such as the laboratory animal science training certification by TransMIT GmbH, were taken before handling any animal.

2.2 Organoid technology establishment

As mentioned before, organoids are a novel technology that allows the study of cell interaction and signalling more accurately. For that reason, to study the effects of our candidate protein p57 in both gastric and small intestinal stem cells, we established both of these types of organoids in the lab and used them throughout the experiments.

2.2.1 Stomach corpus organoids

Our stem cells of interest are located, in abundance, in the corpus region of the stomach. Here we used mouse corpus glands to generate the organoids.

The organoids were then established from adult 9 to 12 weeks WT Black 6 (C57BL/6J) female mice from the mouse facilities of IMBA – Austria academy of science. The mouse was sacrificed with CO_2, the stomach was harvested, cut along the greater curvature and washed in cold 1x PBS on a petri dish.

The corpus part was then dissected and cut into small pieces with the help of a scalpel and scissors. The little pieces were placed on a 15 mL Falcon tube containing 10 mL of cell dissociation

mix (Stemcell Technologies SARL / 7174) and incubated for about 25 minutes (min) at room temperature (RT) on a roller.

After incubation, the tube was shaken vigorously and spun down at 300g for 5 (min). The pellet was removed from the tube with the help of a p1000 pipette and placed on a small (3 cm) petri dish under a bright field microscope to check the density of isolated glands (crypts). A cover slip was then placed above the pieces of tissue and squeezed to further separate the glands from the tissue. The content was collected using 1x PBS (5+5 mL) and passed through a 100µm filter.

The flow through was further spun down at 300g for 5 min and the supernatant discarded. The pellet was resuspended using 1mL of 1x PBS. 50µL were taken from the suspension and the number of glands was estimated. 50 to 100 glands were transferred to a 1.5mL Eppendorf (Epi) tube and spun down at 500g for 5 min.

The pellet was resuspended in 20µL of Matrigel and seeded in a previously warmed 48 well plate. The plate was incubated at 37°C for about 5 to 10 min. 250µL of gastric culture media were finally added to each seeded well. The media had ROCK (Rho-associated, coiled containing protein kinase) inhibitor for the first week to help the establishment of the organoids.

2.2.2 Small Intestine organoids

For the small intestinal organoids, the stem cells can only be found at the bottom of the crypts. Mouse small intestine was used and the crypts isolated.[65]

For that, organoids were established from adult (see the aforementioned ones) female mice. The intestine was harvested and placed onto a 10cm dish with pre-chilled PBS, remaining fat was removed from the intestine and the insides flushed by using a 10mL syringe. The intestine was then cut longitudinally and spread using tweezers.

The villi were scraped from the tissue with the help of a coverslip, until the intestine became lighter, leaving only the crypts behind. The tissue was then cut into 2-4mm pieces and transferred onto a 50mL tube containing pre-chilled PBS. The remaining villi were washed off by shaking vigorously. The pieces were, after well washed, transferred to another 50mL tube with pre-chilled PBS and the previous PBS tube was trashed. This process was repeated 6 times until the supernatant became almost clear. The pieces were then placed onto a 15mL Falcon with 25mL of dissociation reagent (STEM CELL) and incubated for 15 min at RT on a rocking tube platform. After this step the tube was shaken vigorously and 50-100uL were placed onto a small petri dish and looked at under the microscope to check if there were more crypts or villi into the suspension. If there were a lot of crypts, the protocol was proceeded, if there were many villi then a few more washed would be carried out. The solution was continued to be passed through a 100µm filter followed by a 70µm filter with a continuous flow. The suspension was spun down at 1200 rpm for 3 min, the supernatant discarded, and the pellet resuspended in 1 or 2mL of PBS. The number of crypts in a 50µL drop was estimated so that 50 to 100 crypts could be diluted in of Matrigel 20µL. The right amount of suspension was then transferred to a 1.5mL Eppi and spun down at 500g for 5 min. The supernatant was discarded and 20µL of Matrigel was added to resuspend the pellet, seeded to a pre-warmed 24 well plate and incubated at 37°C for about 5 to 10 min. 250µL of gastric culture media were finally added to each seeded well. The media had ROCK inhibitor (Selleckchem / S1049) for the first week to help the establishment of the organoids.

2.3 Organoid culture media

To be able to maintain the organoids in culture healthy, preserve their stemness and proliferative potential, stem cells need certain niche factors and pathways activated, such as the Wnt pathway. Here we made a cocktail of the required factors to sustain the specific gastric and small intestinal 3D cells cultures above mentioned.

2.3.1 Gastric

Table 1 – Growth factors and respective amounts used for organoid media.

Growth factors	Final concentration/ratio
Advanced DMEM +++ (HEPES, Glutamax, Penicillin/Streptomycin)	36%
B27 (50x)	2%
N-Acetyl-L-cysteine (Nac) (500mM)	1,25mM
Epidermal Growth Factor (EGF) (100µg/mL)	50ng/mL
Noggin (100µg/mL)	100ng/mL
Rspondin CM	10%
Human FGF10 (100µg/mL)	100ng/mL
Gastrin (100µg/mL)	10nM
Wnt CM	50%

2.3.2 Intestinal

Table 2 - Growth factors and respective amounts used for organoid media

Growth factors	Final concentration/ratio
Advanced DMEM +++ (HEPES, Glutamax, Penicillin/Streptomycin)	36%
B27 (50x)	2%
N-Acetyl-L-cysteine (Nac) (500mM)	1,25mM
Epidermal Growth Factor (EGF) (100µg/mL)	50ng/mL
Noggin (100µg/mL)	100ng/mL
Rspondin CM	10%
Wnt CM	50%
Nicotinamide (1M)	10mM

2.4 Splitting and maintenance of the organoids

Due to the growth and proliferative rate of the organoids, these need to be divided to be able to keep growing without reaching over-confluency and perish from it.

For that, organoids were split once a week on average, depending on the density or status and the media changed every two days. The ratio for the splitting of the stomach organoids was kept to an average of 1:3 and the small intestine 1:5.

To split the organoids, a 1mL tip was used to break the Matrigel domes. The gel was removed with the help of the media present in the wells and put into a 1.5mL Eppi. The organoids were dissociated by pipetting 50 to 100 times using a p1000 with a bent tip followed by another 100 times pipetting with a p200. The Epi was then spun down at 900g for 5 min. The supernatant was removed, and the pellet was resuspended using the required amount of Matrigel for the number of wells needed. (20µL per well). The Matrigel is then placed to each well and incubated at 37°C for about 5 to 10 min and 250µL of culture media were added to each seeded well.

2.5 Plasmids

In order to genetically modify wild-type organoids to be able to study our proteins of interest, we used plasmids. Plasmids are circular, extrachromosomal, double stranded DNA molecules more commonly known to come from bacteria. These can be easily modified to harbour DNA that expresses resistance for selection, promotors that can be read in our organism of interest and the proteins of relevance for the studies.[56]

The plasmids used here, were all previously made and given to us by Seungmin Han who was a previous member from the Koo lab in Cambridge University. All the plasmids containing the cDNA's use for this study were PiggyBacs. As mentioned above, PiggyBacs have a transposon recognition site element which can then be moved between vector and chromosomal DNA via a cut and paste like system with a transposase presence.

All the constructs contained IRES which separates the cDNA from the marker or selection cassette. Some constructs contained hygromycin and others ampicillin resistance genes for selection from bacterial culture and cell in cell culture, respectively. (**Figure 17**) A transposase was also used together with the cDNA containing plasmids. A GFP containing construct was used as a control to check for the electroporation efficiencies.

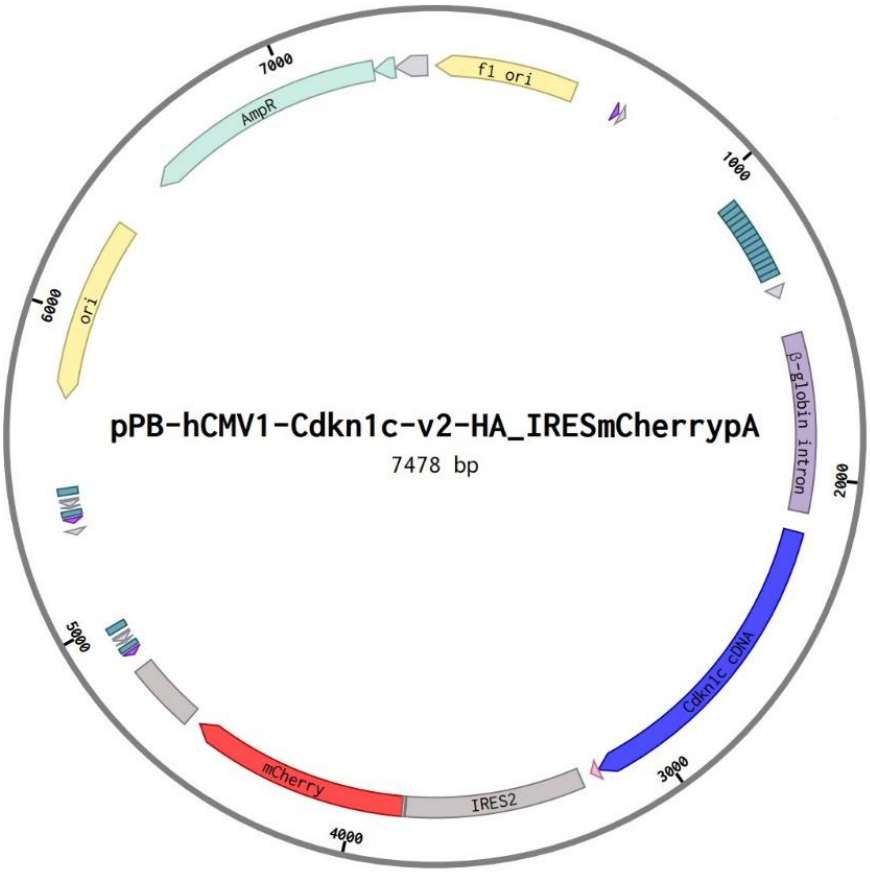

Figure 17 – The figure shows the Map of the p57 plasmid used for this study. The backbone was the same for p27 and p21. All plasmids contained a Amp (ampicillin) resistance (AmpR – light blue), replication origin (yellow); a tetracycline response element (teal), a CMV (cytomegalovirus) promotor (grey arrow), β-globin intron (light purple), the cDNA of the protein in question (dark navy blue), an IRES (internal ribosome entry site) sequence (dark grey) together with an mCherry sequence (red) and finally a bGH poly(A) (dark grey) in front of the mCherry.

2.6 Bacterial transformation

Transformation is a genetic alteration of a given cell by incorporation of an exogenous material. In this case, the transformation was made into competent bacteria, which means that these had a cell membrane ready to uptake the given exogenous material.[51]

This process was used every time we desired to have an expansion of the DNA constructs. To do so, the addgene Bacterial Transformation protocol was used as reference (**annex 8.1**).

Stbl3 competent cells stored in -80°C were thawed on ice for 20 to 30 min and agar plates containing ampicillin supplied by the institution were removed from 4°C to warm up at RT. 1 to 5µL of DNA (around 100ng) was added into the competent cells on an Eppi and gently mixed by flicking the bottom of the tube a few times. The Eppi was incubated on ice for 20 to 30 min. A heat shock was then carried out by placing the tube into a 42°C water bath for 45 seconds and put back on ice for 10 minutes. 50µL of the content were added to one of the ampicillin-containing plates, well distributed and the plate was then incubated overnight at 37°C. As a negative control, one plate was incubated with non-transformed bacteria that are unable to grow on ampicillin-containing agar plates due to the lack of an antibiotic-resistance cassette.

2.7 Plasmid preparation

After the bacteria expansion, the wanted DNA needed to be extracted and purified, for that a plasmid preparation method was used. This method consists in three main steps: Growth of the bacteria, harvest and lysis of the bacteria and finally purification of the plasmid.[52] For this study, a concentration of DNA above 1µg/µL was needed and to do so a midi size prep was chosen.

For the Midiprep, the Quiagen's® Plasmid Plus Midi Kit was used according to the manufacturer's instructions (**annex 8.2**). This involves three main steps: growth of bacteria, usually overnight and with an amount of 100mL LB (lysogeny broth) containing the right antibiotic for the plasmid's resistance; harvesting of the bacterial and subsequent lysis; extraction of the DNA. The Midiprep usually gave a DNA concentration of around 1000-3500 ng/µL, measured with nanodrop.

Two or more colonies were always harvested to check for any DNA damage or construct mis-assembly.

2.8 DNA ethanol precipitation

This process was used to have a more concentrated and purified DNA after the Midiprep extraction. For this purpose, the protocol MRC-Holland's Ethanol precipitation protocol was used as reference (**annex 8.3**).

To the final product of the Midiprep, a 1/10 volume of sodium acetate (3M) was added as well as 3x volume of 100% ethanol, calculated after the addition of the sodium acetate. The Eppi was then incubated at room temperature for 15 to 20 minutes. After the incubation time, the tube was centrifuged at 13000g for 30 min at -4°C. The supernatant was removed carefully with a p1000; 100µL of 70% ethanol was added and another centrifugation was made at -4°C for 15min with the same g force. The supernatant was again discarded, and the pellet dissolved in 200µL MilliQ H_2O. The concentration was measured with nanodrop.

2.9 Sanger sequencing

This method was used to check the existence of mutations on the construct as well as the correct placement of the cDNA into the vector backbone. The sequencing was performed by IMBA MBS (Molecular Biology service) facilities and prepared from us before submitting for the analysis.

For the preparation, the DNA concentration was measured and diluted to be in a range between 150 to 200 ng/µL. A master mix was made with the DNA and H_2O in the amounts described in table 3 and 6µL was pipetted onto each well. The primers listed in table 4 were added individually to each well with an amount of 1µL and a concentration of 5mM to have a total volume of 7µL in each well. The sequencing was always done for the DNA of two different colonies to check for any mutations related to the bacteria (recombination) or intrinsic to the construct. The pipetting of the content was always done vertically as required from the facility. (**Figure 18**)

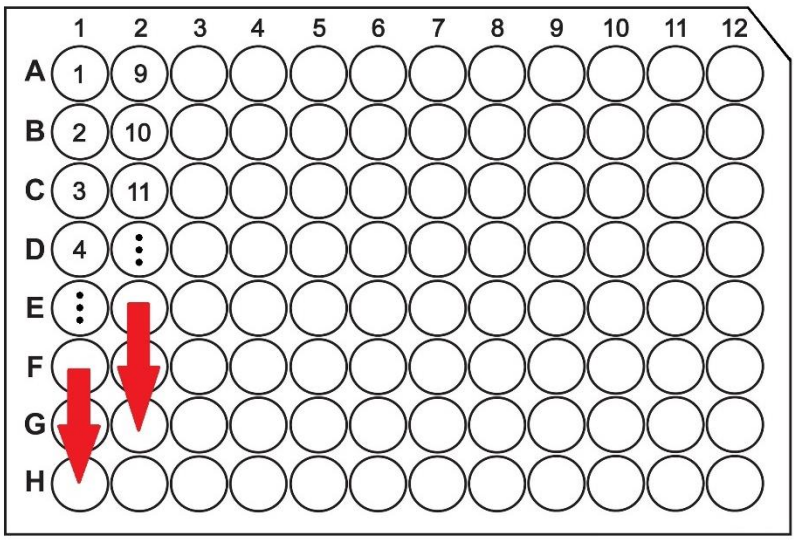

Figure 18 – 96 well Sequencing plate pipetting order. Red arrows point towards the pipetting order used. (From top to bottom)

Table 3 - Amounts in µL used per well for the sanger sequencing.

Components	Amount µL
DNA	1
MilliQ H_2O	5
Primer	1

Table 4 - List of primers used with p57, p27 and p21 for the sequencing analysis.

Name	Sequence
F1	GCCCACTACGTGAACCATCA
R1	CATTGACAAGCACGCCTCAC
F2	GCTGGCGTGGAAATATTCTT
R2	TTGATTCTCGTCCTGCTCCT
F3	CTGACCTCAGACCCAATTCC
R3	AGACCCCTAGGAATGCTCGT
F4	GTCTTTCCCCTCTCGCCAAA
R4	CCATGTTATCCTCCTCGCCC
F5	GCAGAAGAAGACCATGGGCT
R5	CCGCCTCAGAAGCCATAGAG

F6	CAGCTCACTCAAAGGCGGTA
R6	ATCCTGTTACCAGTGGCTGC
F7	CAGTGCTGCAATGATACCGC
R7	TCCTTGAGAGTTTTCGCCCC
M13 F	GTAAAACGACGGCCAGT
M13 R	CAGGAAACAGCTATGAC

All the sequences were aligned using Benchling software with the templates provided by the company the vector was previously ordered from.

2.10 Organoid electroporation

Electroporation is a method that uses electricity in order to permeabilize the cell membrane for introduction of DNA or chemicals into the cell of interest. In this study, this method was used every time a construct needed to be inserted onto the organoid cells.[53]

A minimum of 6 densely grown organoid wells was usually used per reaction. 1.25% DMSO and ROCK inhibitor (Selleckchem / S1049) 10 μM final concentration was added 1 or 2 days before the electroporation.

The DNA concentration of the constructs and transposase was measured, the absolute amount per construct used was 10 ug. To that, 100μL of BTXpress (BTX, Harvard Bioscience / catalogue number: 45-0805) was added, the content was pipetted 3 to 4 times to mix and was immediately put on ice. With the help of a pipette, the media was removed and stored into a Falcon, followed by the pooling of the Matrigel containing the organoids onto a different Falcon. A portion of the media stored on the Falcon was added to the second containing the organoids to help dissociating them with bended p1000 tip.

After mechanical dissociation, the organoids were aliquoted into different Eppis for the right amount of reactions. With the p200, the content of each Eppi was pipetted around 200x to make sure the organoids are disrupted as much as possible. The tubes were then centrifuged for 5min at 600g. After the centrifugation the supernatant was removed leaving only the cell pellet and 500μL

of TriplE was added to resuspend the pellet and desegregate the cells from each other. The tubes were incubated at 37°C for 7-15 min and pipetted every 5 minutes until clusters of 10-15 cells occurred. 10µL were put into a small dish to evaluate the clusters under the microscope. When ready, the Eppis were again centrifuged for 5min at 600g. While the centrifugation was taking place, a Falcon with the right amount OptiMeM (Gibco™ / 51985-034) with ROCK for the total amount of reactions was prepared.

The supernatant was removed from the tube and the 100µL of BTXpress plus the DNA was added to the tube and mixed well. The content was added to the electroporation cuvette, which was gently tapped before placing it into the electroporation chamber. Electroporation was performed according to the following settings (**Figure 19**).

	Voltage	Pulse length	Pulse interval	Number of pulses	Decay rate	Polarity
Poring pulse	175 V	5,0 ms	50,0 ms	2	10%	+
Transfer pulse	20 V	50,0 ms	50,0 ms	5	40%	+/-

Figure 19 - Electroporation settings used for completion of the protocol.

After the pulse, 500µL of the OptiMeM with ROCK was added to the cuvette and with the kit pipette, the suspension was removed and placed onto a new Eppi and the cells were left to recover at RT for 30 to 40 min. After waiting, one last centrifugation was made for 5 min at 600g. The supernatant was removed and 20µL of Matrigel were added to each Eppi to seed the cells. Finally, the added media contained ROCK and it was kept for at least two weeks.

2.10.1 Drug selection

Drug selection is a method of positive selection used when the construct being used expresses a gene for resistance to a specific drug and so only the cells carrying the construct can express the resistance and survive the treatment.[54]

In this case, the organoids containing the construct were resistant to hygromycin. For the selection, the drug was added to the media one week to two weeks after the cells were recovered enough from the electroporation and were resistant enough to survive the drug treatment. ROCK was kept until the end of the selection to help the cells resist the treatment and stay healthy. The selection was kept until resistant clones were clearly growing out with 100μg/mL of hygromycin. (invivoGen / ant-hg-1) The wells were only split if they looked healthy and dense. The hygromycin was always kept for the organoids that contained the rtTA cassette construct to avoid any escapers from CMV promoter silencing.

A control without hygromycin after splitting was kept.

2.11 Doxycycline treatments with Tet-ON system

Since stem cells are usually proliferative when kept *in vitro* and to be able to study p57 effects, an inducible Tet-ON system containing the protein was used.

The Tet-ON system consists of a controlled gene expression where the transcription is turned either on or off on the tetracycline response element containing construct depending on the presence of a tetracycline antibiotic or their derivates.[47]

The constructs carried an inducible rtTA that activates upon doxycycline addition to the media. (**Figure 20**) Only when the drug is present does the p57 protein get expressed. This protein is also accompanied to an mCherry fluorescent protein which enables the visualization of the protein being expressed. To that matter, any of the *in vitro* tests with the overexpression of the exogenous proteins were carried out by the addition of doxycycline (Sigma / D9891) to the media with an initial concentration of 1μg/mL for the p57 and p21 and 0,1μg/mL for the p27.

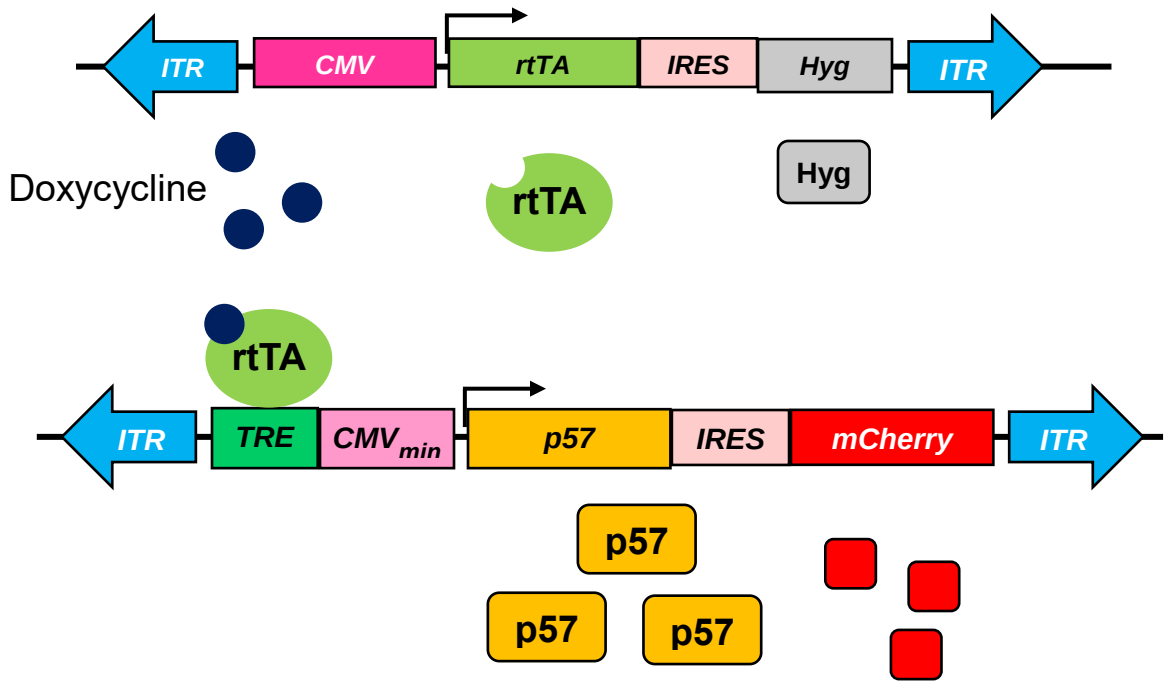

Figure 20 – The figure represents the constructs used with the organoids throughout the experiments. The top construct contains two ITR (inverted terminal repeat) regions recognizable by the transposase to integrate the cells genome; it also contains a CMV (cytomegalovirus); an rtTA which is expressed and activated upon doxycycline addition; an IRES (internal ribosome entry site) and finally a hygromycin resistance gene. The bottom construct also contained two ITR regions, a TRE (tetracycline response element) sequence that is activated upon active rtTA binding, connected to a CMV promotor; the p57 gene; an IRES sequence and an mCherry fluorescence sequence to express simultaneously to the p57 protein. Adapted from Ji-Hyun Lee.

After the selection, in order to assure monoclonality to have consistent results, the organoids were picked as single units to new wells.

To pick the clone, one single well, after the hygromycin selection, was disrupted and all the Matrigel together with the media was transferred with the use of a p1000 pipette to a small petri dish. The petri dish was then place under the microscope to be able to see the organoids. With a p20 single organoids were picked from the petri dish and placed into a 96 well plate. Around 20 were picked from one well. After picking all the single organoids into individual wells, 10µL of Matrigel and around 50µL of media were added and the organoids were left in the incubator to recover.

When the organoids start to show growth, these are pipetted up and down with a p200 in the well to break them as much as possible and seeded on a 48 well plate in 10µL Matrigel.

2.13 7 days/ 3 months quiescence induction

For the 7 days and 3 months quiescence experiments of the p57 OE gastric organoids, p57 small intestine or gastric p21 and p27, the organoids were split and doxycycline, in a ratio of was added to the media on the day of the splitting and counted as day zero of the treatment. Between 3 to 6 replicas were maintained in order to avoid losses, Matrigel breaking and possible organoids silencing the CMV promotor region on the mCherry and p57 containing construct, here denominated as escapers.

Two other wells were maintained, splitted on the same day but with no doxycycline treatment as a control. The media was changed every two days and splitting took place whenever necessary.

The retrieval from the treatment was made by splitting the organoids after the time established and no doxycycline was added to the media.

2.14 Generation of a new p57 Dox inducible Tet-ON system

2.14.1 Digestion

For the digestion, the DNA concentration from the constructs pUC57-IRES-Bla-P2A-mCherry (4.5kb) and pPB-hCMV1-p57-IRES-mCherry (7.5kb) was measured and the amount needed calculated.

To cut the pUC57-IRES-Bla-P2A-mCherry construct and extract the insert fragment (1.8Kb), and the vector (6.2Kb) from pPB-hCMV1-p57-IRES-mCherry XbaI and NotI-HF enzymes from NEB were used. After adding all the components mentioned in table 5, to a total of 25µL, the digestion mix was placed at 37°C for 4 hours.

After 4 hours of incubation, the mixture was placed at room temperature and 5µL of 6x loading dye were added to the total 25µL of the reaction and mixed to be loaded into the gel. Together with the reaction, the same amount of DNA was loaded uncut into the gel as a control.

The reaction and control were loaded into a 1% agarose gel. The gel ran for 30min at 135V.

Table 5 – Components used for the digestion protocol, respective amounts in µL and brands/reference.

Components	Amount (µL)	Brand
DNA (400-500 ng/µL)	2	-
Buffer	2,5	CutSmart - NEB
Enzyme	0,5	NEB
H_2O	20	In house Sterile Mono Q

2.14.2 Gel extraction

For the gel extraction, the expected band size from the digestion was estimated and the piece of gel containing the band of interest was cut with the help of a UV light and a scalpel. The gel pieces were placed in a sterile 1,5mL Eppi previously weighted.

For this protocol, the in-house Molecular Biology Service MiniPEx protocol was used accordingly. The gel weight was measured, and 3 volumes of the kit's buffer G, to 1 volume Gel, were added to the Eppi and placed at 55°C for 10 min, vortexing every 2 to 3 minutes to help dissolve the gel. After making sure that the gel slice was dissolved completely, 1X gel volume of isopropanol was added to the vector Eppi to increase the yield, since the fragment was bigger than 4Kb. The content of the Eppis was then placed into a column to bind the DNA and the column was centrifuged at 13000g for 1 min and the flow-through discarded. To wash, 750µL of buffer W were added to the column and centrifuged at 13000g for 1 min. The flow-through was discarded. Another centrifugation, at the same conditions, was made to remove any residual wash buffer. The column was then placed in a clean 1,5mL Eppi and 30µL of sterile H_2O were added to the centre of the column to elute the DNA. The DNA concentration and purity were checked using nanodrop.

2.14.3 Ligation

To ligate the two linear fragments of the DNA, the Ligation Protocol with T4 DNA Ligase (M0202) from NEB was followed. The reaction was made in a 0,7mL tube on ice.

The T4 DNA Ligase was added last and the molar ratio of 1:3 vector to insert was kept as instructed. (**Table 6**)

Table 6 – Reagents used for the DNA ligation process as well as the respective amounts and brands used.

Components	Amounts	Brand/Reference
T4 DNA Ligase Buffer (10x)	2 µL	NEB / B0202S
Vector DNA (4Kb)	50 ng (0.020 pmol)	-
Insert DNA (1Kb)	37.5 ng (0.060 pmol)	-
Nuclease free H_2O	Up to 20 µL	In house Sterile Mono Q
T4 DNA Ligase	1 µL	NEB / M0202S

After adding all the components, the reaction was pipetted up and down to mix and briefly spun down. Considering the enzyme cut left the DNA with sticky ends, the mixture was incubated at room temperature for around 10 min, as instructed. After the 10 min, the tubes were placed at 65°C for 10 minutes in order to inactivate the reaction. The tubes were then placed on ice to chill.

After the ligation the DNA was transformed into 50 µL of Stbl3 competent bacteria, midipreped, the DNA was precipitated with ethanol and sequenced as previously described in the materials and methods sections 2.6, 2.7, 2.8 and 2.9 respectively.

2.15 p57 influence on niche factor requirements

For the pathway regulation, different medias with growth factor removal or inhibitors were tested. (**Table 7**) Three replicate wells were used as controls as well as backup for any loses of Matrigel or occurrence of escapers. The same number of wells and conditions were made for a non-doxycycline treatment control. (**Figure 21; Figure 22**)

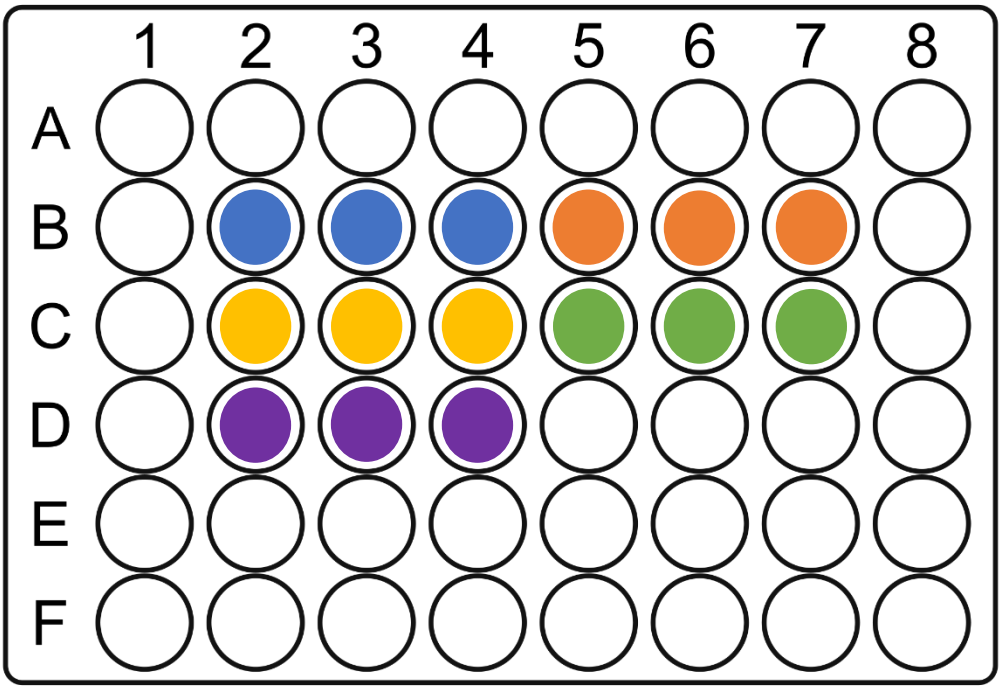

Figure 21 – Schematic drawing of the plate setup for the growth factor withdrawal test. The blue colour represents the complete media containing Wnt, Rspo, Noggin, Fgf10, Egf and Gastrin; Orange is depleted of Noggin and contains additional BMP4; Yellow is depleted of Egf and Fga10; Green is depleted of Egf and contains additional PD03 which is the designation used for Mirdametinib, a MEK inhibitor; Purple is depleted of both Wnt and Rspo.

Table 7 – Different medias used for the experiment. The concentrations and amounts of the growth factors used were the same as in the normal, complete gastric media. (Wnt (W); Egf (E); Noggin (N); Fgf10 (F); Rspondin (R); Gastrin (G)).

Colour	Description	Media composition
Blue	WENFRG	Wnt; EGF; Noggin; Fgf10; Rspondin; Gastrin
Orange	WEFRG + BMP4	Wnt; EGF; Fgf10; Rspondin; Gastrin; BMP4
Yellow	WNRG	Wnt; Noggin; Rspondin; Gastrin
Green	WNFRG + PD03	Wnt; Noggin; Fgf10; Rspondin; Gastrin; PD03
Purple	ENFG	EGF; Noggin; Fgf10; Gastrin

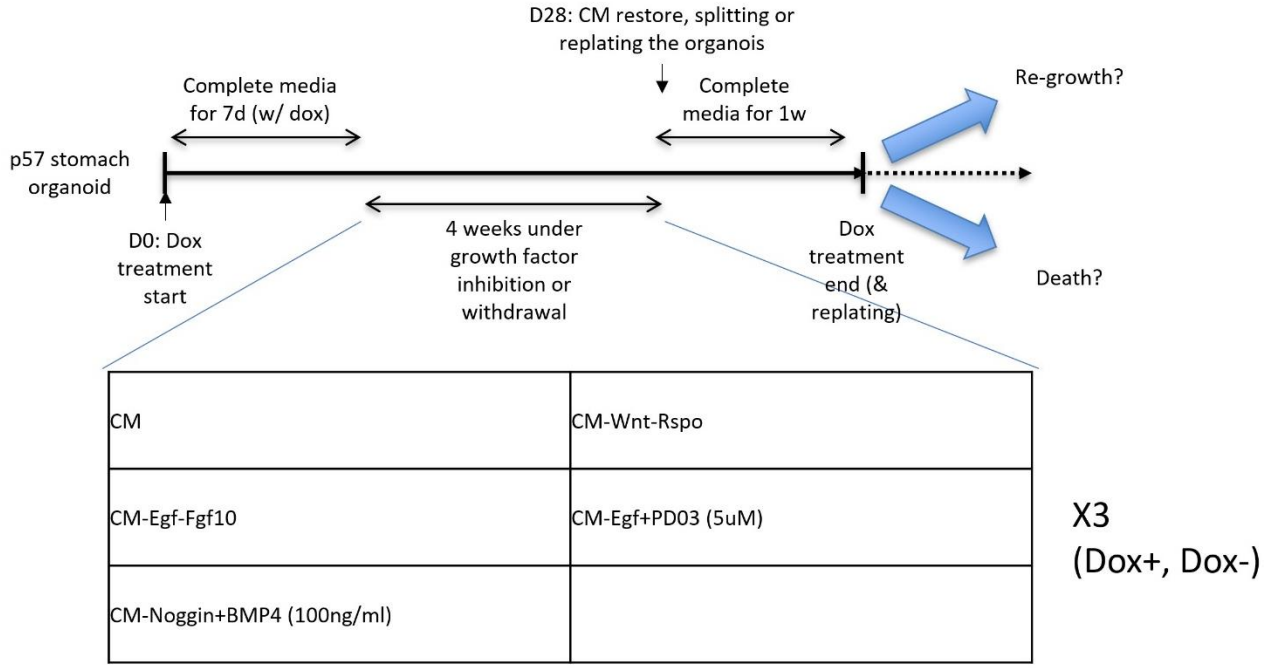

Figure 22 – Schematic figure representing the experimental setup and conditions used for the withdrawal test. CM stands for complete media; Rspo stands for Rspondin; PD03 is the designation used for Mirdametinib, a MEK inhibitor; D/d stands for day/days; w stands for weeks. Adapted from Ji-Hyun Lee.

2.16 Gene candidates interlocking with p57

Based on the data from RNA seq analysis *in vivo* and *in vitro* by Prof. Jong Kyoung Kim's lab in DGIST, we got 86 final genes as candidates of p57 signalling. Through extensive literature review, we selected genes that could potentially directly influence p57 as upstream effectors or constitute downstream targets of the pathway. For this we selected one of the genes in the list that had the most commonly used and well-known ligands and inhibitors, in this case it was the IGF1R gene.

For the experiment process, the ligand Recombinant Murine IGF-1 and inhibitor PPP were used. Both ligand and inhibitor were treated to Dox induced p57 OE gastric organoids for 10 days. Different concentrations were used considering previous literature with 2D cell cultures for optimization on the 3D organoid culture. (**Table 8**) On day 10, both dox and drug treatments were stopped and the organoids replated. A well without doxycycline was used as control.

Table 8 – Inhibitor and ligand used for the study with the respective concentrations and brand/reference.

Inhibitor	**Concentration 1 (µM)**	**Concentration 2 (µM)**	**Concentration 3 (µM)**	**Brand/Reference**
PPP	0,5	5	50	Selleckchem / S7668
Ligand	**Concentration 1 (ng/mL)**	**Concentration 2 (ng/mL)**	**Concentration 3 (ng/mL)**	**Brand/Reference**
RM IGF-1	10	50	100	Peprotech / 250-19

2.17 Organoids fixation and staining

2.17.1 Fixation

To be able to image the organoids with and without the inserted system activated, the cells were fixed.

For this process, the organoids had to be seeded on a plate specific for fitting onto the microscope sample holder. Due to that, the plates used for this purpose were from ibidi®. Gastric p57 OE organoids were seeded and treated with +/- Dox for 4 days. (**Figure 23**)

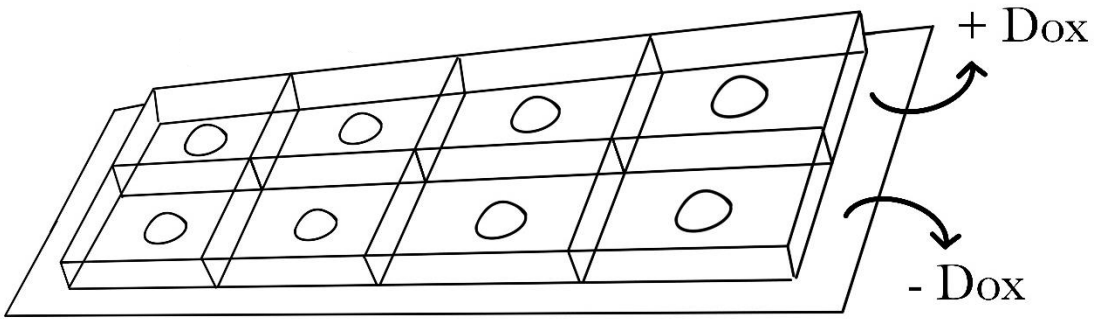

Figure 23 – schematic figure of the organoid placement for fixation and staining in both – and + Dox conditions.

On the fourth day, the media was removed, and the organoids were washed 2 times for 5 min with 1x PBS. After the washes, 4% PFA was placed onto the wells and left for 35 min to fix the

organoids. 2 more washes at RT for 10 min with 1x PBS were followed to remove the remaining PFA as much as possible before storage in the fridge.

2.17.2 Staining

The PBS was removed and a blocking and permeabilization solution containing 0.5% Triton-X, 2% NDS, 5% DMSO was added to the wells for 45 min. Once blocked, 3 washes for 5-10 min were made with 1x PBS. The AB's incubation was done with p57 a rabbit AB and Ki67 rat. Both were placed onto the wells containing 1X PBS with 0.5% Triton-X, 2% NDS, 1% DMSO with a ratio of 1:200, and were incubated overnight at 4°C.

The wells were again washed 5 times for 5 min with 1x PBS before incubation with 2nd AB with a ratio of 1:500. The second antibodies added were Alexa488: Dnk anti-rabbit for p57 and DyLight 651: Dnk anti-rat for Ki67; incubated overnight at 4°C. The wells were washed once more 2 times for 5 min with 1x PBS and a last incubation was made using Dapi in a 1:500 ratio for 30 min at RT. The Dapi containing solution was removed and the wells washed 3 times for 5 min with 1x PBS.

After this last step the organoids were placed onto the fridge at 4°C and imaged within a week of time.

Table 9 -List of antibodies and chemical compounds used for staining.

Antibodies	**Concentration**	**Brand/Reference**
1st p57 rabbit	3,7 mg/mL	Abcam / ab75974
1st Ki67 rat	0,5 mg/mL	Invitrogen™ / 14-5698-82
2nd Alexa488: Dnk anti-rabbit	2 mg/mL	Abcam / ab150073
2nd DyLight 650: Dnk anti-rat	0,5 mg/mL	Invitrogen / SA5-10029
Chemical	**Concentration**	**Brand/Reference**
Dapi	5 mg/mL	Invitrogen™ / D1306

2.18 Organoids imaging

The confocal microscope is an imaging technic that allows for increased optical resolution and contrast. The principal of this microscope is the use of a pinhole that blocks out-of-focus light, enabling for a much better resolution.[63]

The fixed organoids were imaged with the Leica confocal microscope, using a 25x water lens, 1 N.A and using the SP8 software. The lasers used were, 405 nm laser for DAPI; 488 nm laser for p57; 561 nm for mCherry and the 633 nm laser for Ki67.

The organoids in culture were imaged with the EVOS® FL system microscope and EVOS® light cube in bright field and with a TexasRed and GFP channels.

2.19 Mouse lines

The mouse lines were either obtain from other labs or made in house by our group. Anxa10-Cre line mice used for this study was obtained from Daniel Stange[57], p57 OE, denominated as R26loxpTA-p57k[58] was obtained from the Jackson Laboratory.[59] ES cell clones and mice of p57 cKO allele were produced by Bon-Kyoung Koo at the WT-MRC Cambridge Stem Cell Institute to generate a Cre inducible knock out allele.

Table 10 - Mouse strains used for the study.

Allele 1	Allele 2
Anxa10-Cre (het)	P57cKO (hom)
Anxa10-Cre (het/hom)	P57OE (hom)

2.19.1 Mouse constructs

The Cre-LoxP system derives from a natural mechanism present in bacteriophages P1. This technology recombines site specific and this recombination is achieved by a Cre recombinase enzyme that can target short specific sequences called the *Lox* and recombine them.[48]

In order to have a controllable system, a CreERT2 was used. This is a fusion between an estrogen ligand binding domain carrying a mutation and the Cre recombinase enzyme. This way, whenever the tamoxifen drug is present it binds to the ER and Cre is activated and able to perform its function.[49] In this case, a version of the CreERT was use. CreERT2 was developed to to minimize recombination independent of tamoxifen induction by leaking of activated Cre and maximize the sensitivity to tamoxifen.[50]

Here we used this technology in order to either over express the protein of interest or disrupt its endogenous expression specifically in the stomach. (**Figure 24; Figure 25**) These mice were previously created in house by our group and were ready to use by the time of this study.

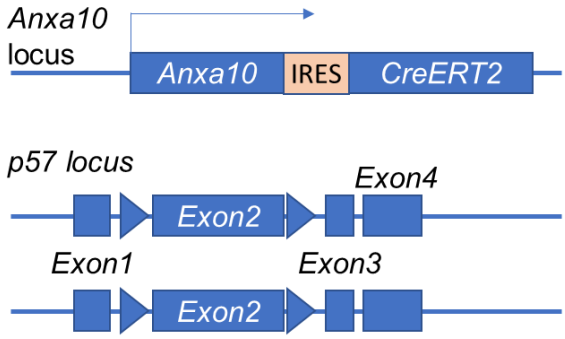

Figure 24 - **p57cKO construct.** This schematic figure shows the p57 conditional knockout construct designed to activate specifically at the stomach in Anxa10 locus and loxP sites flanking Exon 2 of the endogenous protein. Adapted from Ji-Hyun Lee.

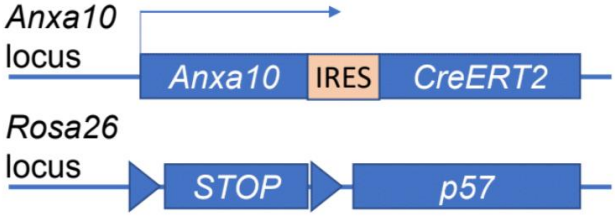

Figure 25 - **p57 OE construct.** This schematic figure shows the p57 OE construct designed to be present in the Rosa locus with lox p sites flanking a stop codon to be inducible upon Cre activation, specifically in the stomach with Anxa10 locus. Adapted from Ji-Hyun Lee.

2.19.2 Mice genotyping

To be able to confirm the existence of a modified or wildtype allele in the mice genomes, we used the PCR technique. This technique amplifies the strands of DNA with the use of specific primers that recognize either the wildtype allele of the modified version of it, allowing then to get an amount large enough to be visible and detected with the use of an intercalant dye.[66]

The DNA was extract from a 2 mm diameter ear notch from the mice used for the study. The ear notches were collected to 1,5mL Eppis and 29,7µL of Earclip DNA isolation mix was added together with 0,3µL of proteinase K for each of the tubes in order to isolate the DNA. The Eppis were incubated in the oven at 55°C for at least 6 hours or overnight. After the incubation, the samples were vortexed and 270µL of MilliQ H_2O were added to dilute the enzyme and stop any further digestion. A master mix was prepared (**Table 11; Table 12; Table 13**) for each specific genotype, 18µL of it loaded to a 96 well plate, together with the 2µL of the DNA and put onto the PCR machine and run with the program described in **Figure 26**. A 2% agarose gel was made, containing SYBR Safe run dye in a 1:1000 ratio, to run the gel. The gel ran for 30min at 135V and was finally imaged under a UV light.

Table 11 - PCR mix, amounts used for 3 primers

3 primers mix	1 reaction in µL
Buffer 5x	4
Primer F (10µM)	0,4
Primer R (10µM)	0,4
Primer F mut (10µM)	0,4
dNTPs (10mM)	0,4
MgCl2 (1,5 mM)	1,2
GO Taq (5U/µL)	0,1
H2O	11,1

Table 12 - PCR mix, amounts used for 2 primers

2 primers mix	1 reaction in µL
Buffer 5x	4
Primer F (10µM)	0,4
Primer R (10µM)	0,4
dNTPs (10mM)	0,4
MgCl2 (1,5 mM)	1,2
GO Taq (5U/µL)	0,1
H2O	11,5

Table 13 - List of the primers used for the PCR (OE stands for overexpressing, cKO for conditional knockout and bla for blasticidin).

Construct	Name	Sequence
p57cKO (bla)	Wildtype Reverse	CACTTAACCCCCTCCATGC
p57cKO	Knock-in Forward	TACCCGCTTCCATTGCTCAG
p57cKO (bla)	Wildtype Forward	GCACCCCTTTCCTACTGGT
Anxa10-Cre	Wildtype Forward	AGCTGACCTTTAGAAACAGGGA
Anxa10-Cre	Wildtype Reverse	TGAATACAGCACGCGTTCAG
Anxa10-Cre	Knock-in Reverse	TTGCATTCCTTTGGCGAGAG
R26loxpTA-p57	OE Mutant	GCGAAGAGTTTGTCCTCAACC
R26loxpTA-p57	OE Common	AAAGTCGCTCTGAGTTGTTAT
R26loxpTA-p57	OE Wildtype	GGAGCGGGAGAAATGGATATG

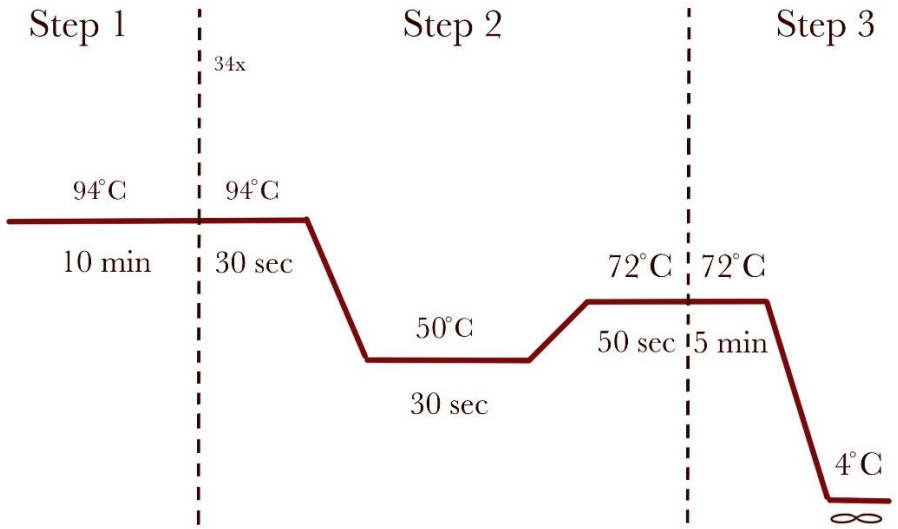

Figure 26 – Schematic figure of the PCR programme used for the study.

2.20 Tamoxifen treatments in mice

Tamoxifen is a drug that recognizes and binds to the estrogen receptor (ER) triggering a response. As stated above, in this case, the constructs present in the mice genome have a CreER element which is a Cre recombinase mutated and bound to an estrogen receptor ER which is then activated upon the administration of tamoxifen.[64] This was used in this study to have a controlled activation, through LoxP sites, of the over expressing or conditional knockouts of the proteins of interest and study their effects in determined timepoints and age of the mice.

Tamoxifen (Sigma / T5648-1G) was dissolved with 10% ethanol of the total volume, and 90% corn oil, the mixture was sonicated for easy homogenization. The drug was administered through Intravenous (I.V.) injections and these injections were administered by the lab technician.

2.21 Histology and tissue preparations

For this procedure, Anxa10-Cre/p57OE and Anxa10-Cre/p57cKO experimental mice (tamoxifen treatment) as well as control mice (no tamoxifen treatment) were sacrificed with CO_2, the stomach was harvested, cut along the greater curvature and washed in cold 1x PBS on a petri dish. The corpus part was then dissected, placed on a plate in cold 1x PBS and given to the histopathology department for paraffin embedding, sectioning and antibody incubation. Aliquots of the antibodies of interest for the study were also provided to the facility.

Table 14 – Antibodies given to the facility for tissue staining, concentration and brands/reference.

Antibodies	Concentration	Brand/Reference
p57 rabbit monoclonal	3,7 mg/mL	Abcam / ab75974
Ki67 rabbit monoclonal	0,03 mg/mL	Abcam / ab1666
Gif rabbit	0,10 mg/mL	Sigma / HPA040774

3 Results

3.1 Quality control

In order to have the technology suitable for the study and experiments, the organoids were electroporated with the construct of interest to express the desired protein. Several quality control steps were needed to assure that the cells populating the organoids in fact contained the construct and to see if the system was working properly and as expected.

3.1.1 Electroporation

This method was used every time a specific organoid line was needed for a given experiment.

3.1.1.1 Small intestine p57

The p57 constructs were electroporated into small intestinal organoids in order to study the effects in an ectopic manner. The construct was electroporated on the same day, together with the GFP control. These wells are representative of 2 replicates.

Table 15 – p57 small intestinal organoids 3, 5 and 7 days after electroporation. The images are shown in bright field (top row), green (middle row) and a merge (bottom row) of the two channels. BF and green had a light intensity of 9% and 50% respectively. Scale in each image: 2000µm, 2x objective.

Electroporation	Day 1	Day 3	Day 7
BF	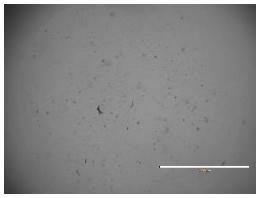	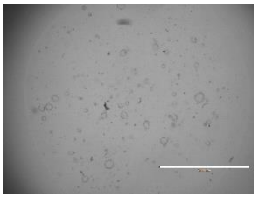	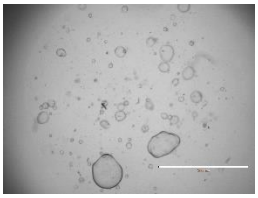
Green	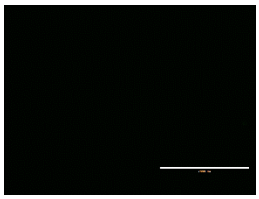	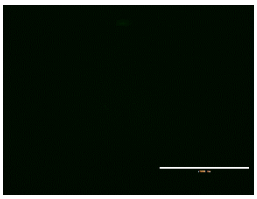	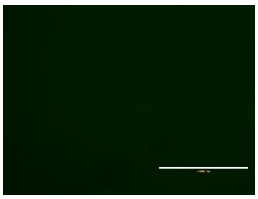
Merge	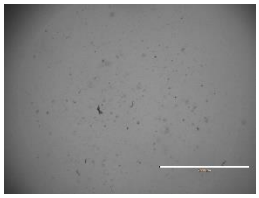	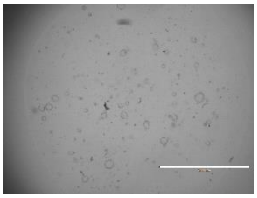	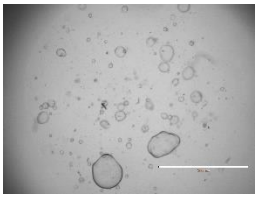

Table 16 - GFP control 3, 5 and 7 days after electroporation. The images are shown in bright field (top row), green (middle row) and a merge (bottom row) of the two channels. BF and green had a light intensity of 9% and 50% respectively; Day 7 the green channel had 60% light. The control shows the efficiency of the method. Scale in each image: 2000µm, 2x objective.

GFP Control	**Day 1**	**Day 3**	**Day 7**
BF	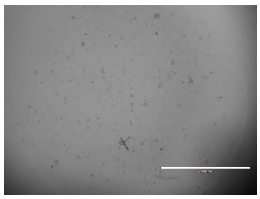	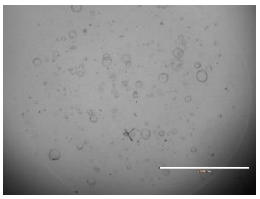	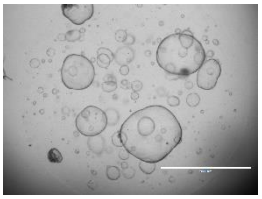
Green	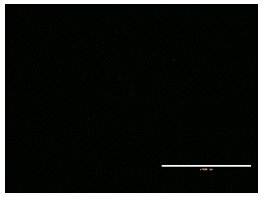	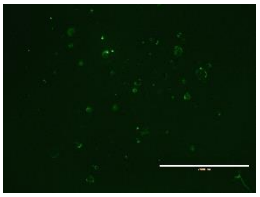	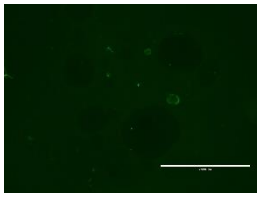
Merge	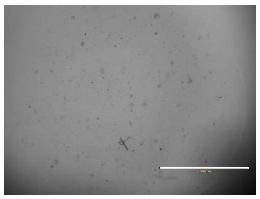	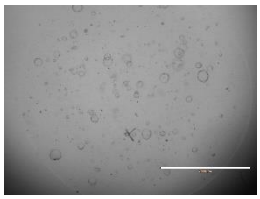	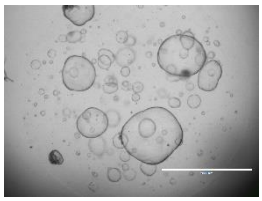

In these **Tables** (**15** and **16**) it can see that the seeding density after the electroporation was similar both on the control and experimental set. From **Table 16** we can see that the GFP on the green channel appears on a very small subset of cells. This demonstrates a transfection efficiency of the electroporation at less than 10%.

On day 3, we can already see organoids forming at a similar rate on the control and experimental sets. The GFP signal on the control can also be seen to start being expressed all over some of the organoids.

On day 7 the organoids had already recovered and reached a considerable size to split and start the drug selection. On this day, the green channel on the control had a light with 60% to help observing the GFP signal surrounding some of the organoids formed.

3.1.1.2 Hygromycin selection

Table 17 – Small intestine p57 OE organoids 3, 15 and 19 days after selection with 100 µg/mL of hygromycin. The images are in the bright field channel with 9% light source intensity. The organoids between day 3, 15 and 19 were split in between and so, these do not represent the same well. Scale in each image: 2000µm, 2x objective.

Selection	Day 3	Day 15	Day 19
BF	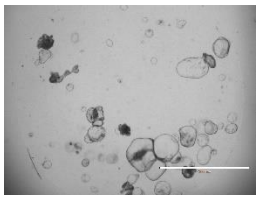	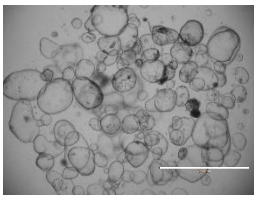	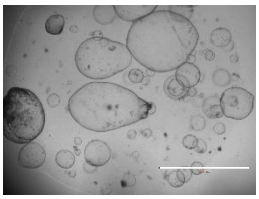

Table 18 - GFP control 3, 15 and 19 days after selection with 100 µg/mL of hygromycin. The images are in the brightfield channel with 9% light source intensity and 10% on day 3. The organoids between day 3, 15 and 19 were split in between and so, these do not represent the same well. Scale in each image: 2000µm, 2x objective.

GFP Control	Day 3	Day 15	Day 19
BF	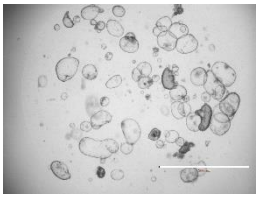	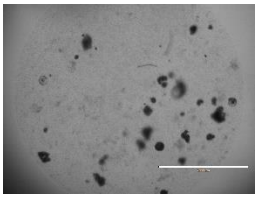	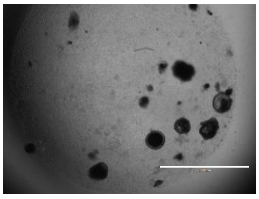

With the images of **Table 17**, we can see that on day 3 some black spots representative of organoids that have started dying and so selecting for the ones with the construct. On day 15 there is a clear overgrowth compared to the same day of the GFP control on **Table 18** where almost all organoids have fully died, representing a successful integration of the vector and selection of the organoids.

3.1.1.3 Clone picking

Several clones were picked after the selection and their expression of mCherry confirmed.

Table 19 – mCherry expression in p57 OE small intestine clones B7, C3, C5 and C9. The images are shown in bright field (top row), red (middle row) and a merge (bottom row) of the two channels. BF and red had a light intensity of 9% and 50% respectively. Scale in each image: 2000µm, 2x objective.

Clones	B7	C3	C5	C9
BF	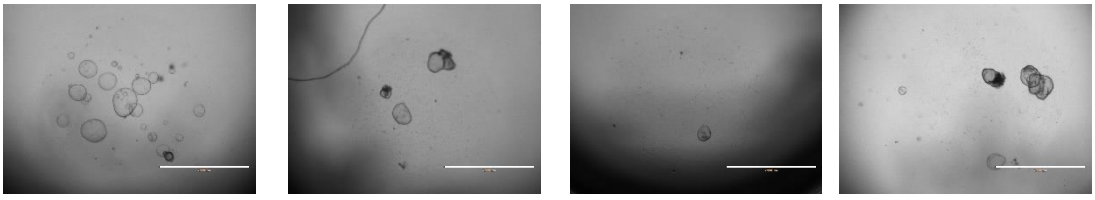			
Red				
Merge	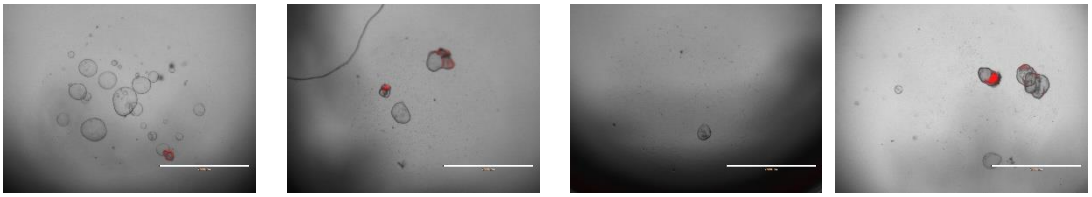			

It is possible to see, on the red channel row (middle) from **Table 19**, that clones B7 and C5 had very low signal compared to the others, although still having almost all the organoids with a uniform signal of mCherry, excluding the B7 clone. Clone C9 was then the one selected for further studies over the others since it was the one with a stronger signal that grew better over time.

3.1.1.4 Gastric p21 and p27

p21 and p27 constructs were electroporated into the organoids in order to study the effects of these two proteins and compare them to the p57 phenotype. All the constructs were electroporated on the same day, at the same time, together with the GFP control. These wells are representative of 2 replicates.

Table 20 - p21 gastric organoids 3, 5 and 7 days after electroporation. The images are shown in bright field (top row), green (middle row) and a merge (bottom row) of the two channels. BF and green had a light intensity of 9% and 50% respectively. Scale in each image: 2000µm, 2x objective.

Electroporation	Day 3	Day 5	Day 7
BF	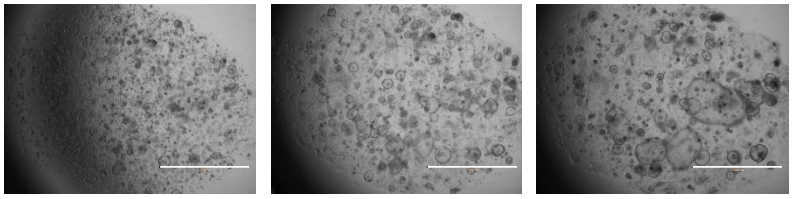		
Green	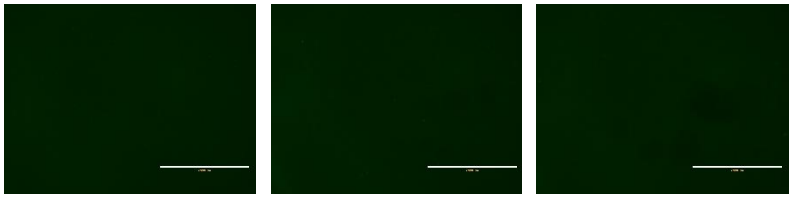		
Merge	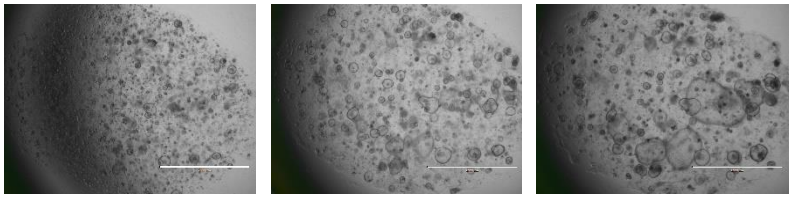		

Table 21 - p27 gastric organoids 3, 5 and 7 days after electroporation. The images are shown in bright field (top row), green (middle row) and a merge (bottom row) of the two channels. BF and green had a light intensity of 9% and 50% respectively. Scale in each image: 2000µm, 2x objective.

Electroporation	Day 3	Day 5	Day 7
BF	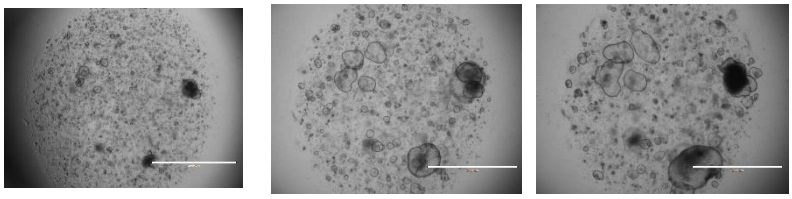		
Green	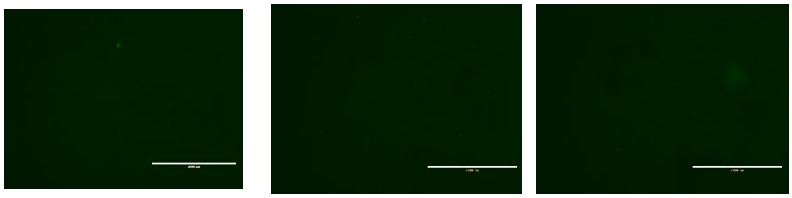		
Merge	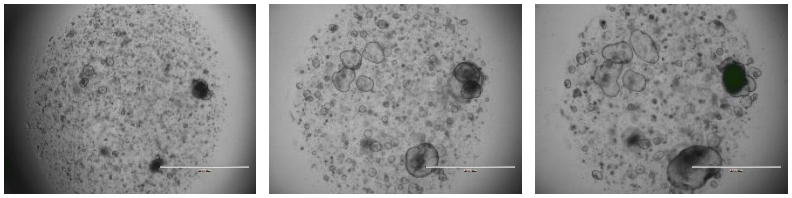		

Table 22 - GFP control 3, 5 and 7 days after electroporation. The images are shown in bright field (top row), green (middle row) and a merge (bottom row) of the two channels. BF and green had a light intensity of 9% and 70% respectively. The control shows the efficiency of the method. Scale in each image: 2000µm, 2x objective.

GFP Control	**Day 3**	**Day 5**	**Day 7**
BF	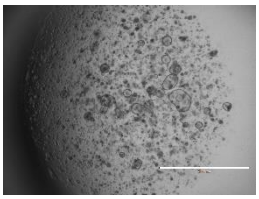	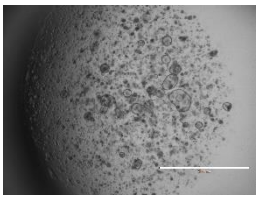	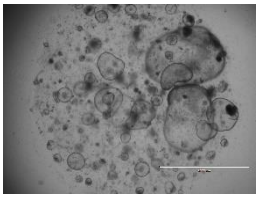
Green	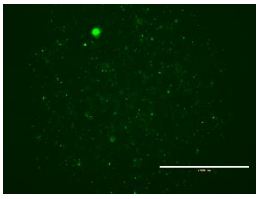	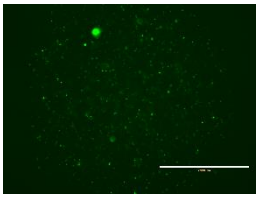	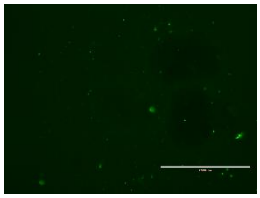
Merge	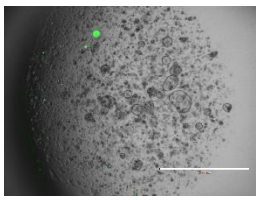	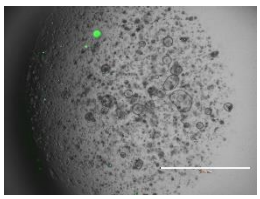	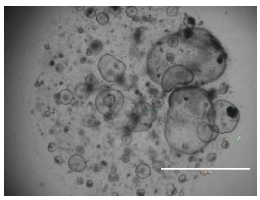

In **Tables 20** and **21** we can see that the seeding density after the electroporation was similar in all the conditions with a high number of cells. From the control **Table 22** we can see that the GFP signal, on the green channel(middle), appears on a high number of cells. This represents an efficiency rate of the electroporation of around 30%.

On day 3, we can already see organoids forming the control but less on both experimental **Tables 20** and **21**. On day 5 the experimental well from p21 appears to have organoids growing uniformly and faster than p27 or the GFP control.

On day 7 the organoids had already recovered and reached a considerable size to split and start the drug for all the reactions.

3.1.1.5 Hygromycin selection

After a week of recovery from the electroporation, the cells were selected for hygromycin resistance.

Table 23 - p21 gastric OE organoids 3, 15 and 26 days after selection with 100 µg/mL of hygromycin. The images are in the bright field channel with 9% light intensity. The organoids between day 3, 15 and 26 were split in between and so, these do not represent the same well. Scale in each image: 2000µm, 2x objective.

Selection	Day 3	Day 15	Day 26
BF	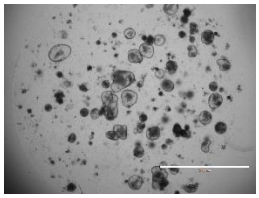	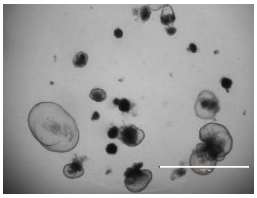	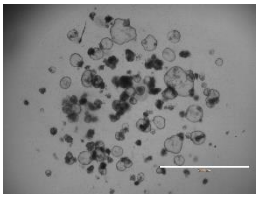

Table 24 - p27 gastric OE organoids 3, 15 and 26 days after selection with 100 µg/mL of hygromycin. The images are in the bright field channel with 9% light intensity. The organoids between day 3, 15 and 26 were split in between and so, these do not represent the same well. Scale in each image: 2000µm, 2x objective.

Selection	Day 3	Day 15	Day 26
BF	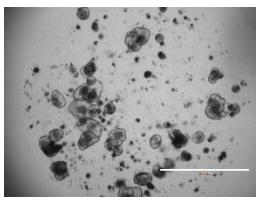	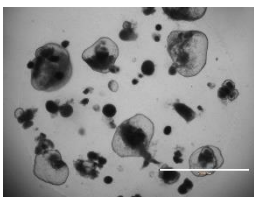	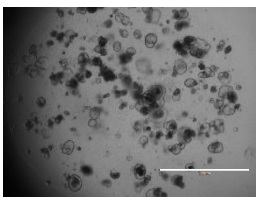

Table 25 - GFP control 3, 15 and 26 days after selection with 100 µg/mL of hygromycin. The images are in the brightfield channel with 9% light intensity. The organoids between day 3, 15 and 26 were split in between and so, these do not represent the same well. Scale in each image: 2000µm, 2x objective.

GFP Control	**Day 3**	**Day 15**	**Day 26**
BF	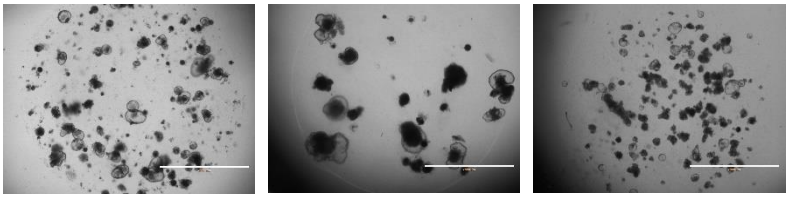		

On day 3 (**Tables 23** and **24**), some black spots started to appear. These spots were organoids that had started dying, representing a successful start of selection for the ones that contained the construct. On day 15 there was an outgrowth of the organoids compared to the same day of the GFP control in **Table 25**, where fewer and smaller organoids appeared.

On day 26 some of the GFP control organoids were still surviving, nonetheless, a clear difference could be seen, compared to the number of survivors in the experimental sets, representing a successful integration of the vector and selection of the organoids.

3.1.1.6 Clone picking

Several clones were picked after the selection and their expression of mCherry confirmed by Doxycycline treatment.

Table 26 – mCherry expression of p21 OE A2, A5, A6 and A8 clones. The images are shown in bright field (top row), red (middle row) and a merge (bottom row) of the two channels. BF and red had an intensity of 9% and 50% respectively. Scale in each image: 2000µm, 2x objective.

Clones	A2	A5	A6	A8
BF	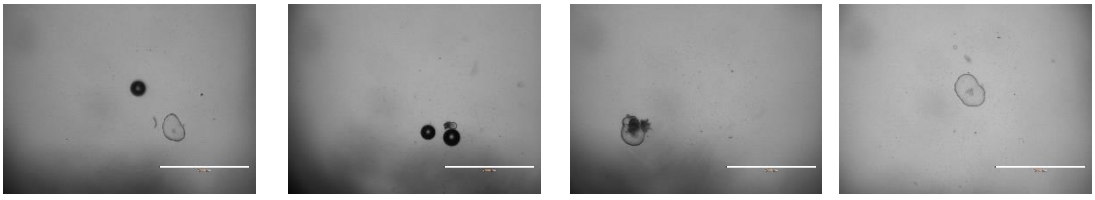			
Red	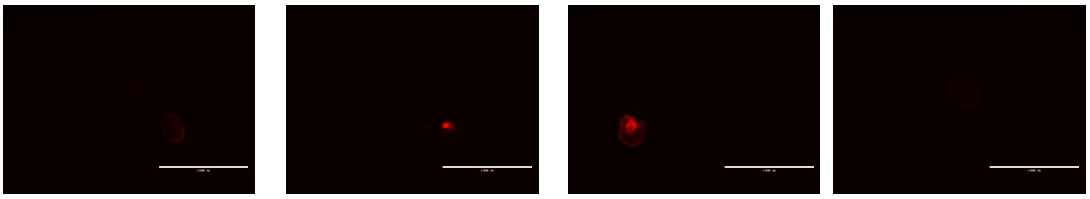			
Merge	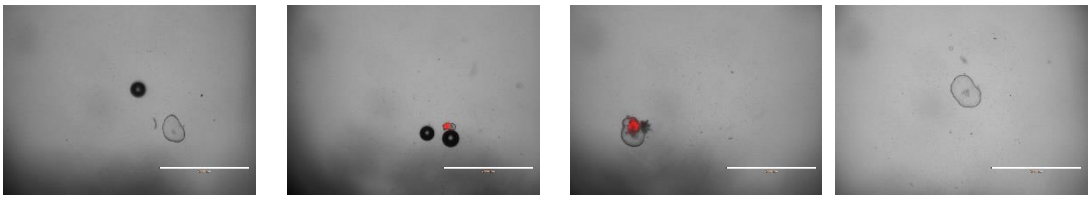			

All p21 clones showed a low signal of mCherry but consistent throughout the organoids. On the red channel row (middle) from **Table 26** it was possible to see that clones A2 and A8 had very low signal. On the other hand, clone A5 showed a stronger signal but had a smaller size of the organoid. These were continuously split every week and the ones that grew better and had the highest signal were used for the rest of the studies. With this criteria, clone A6 was chosen among the others.

Table 27 - mCherry expression of p27 OE A8, A11, B2 and B9 clones. The images are shown in bright field (top row), red (middle row) and a merge (bottom row) of the two channels. BF and red had an intensity of 9% and 50% respectively. Scale in each image: 2000µm, 2x objective.

Clones	**A8**	**A11**	**B2**	**B9**
BF	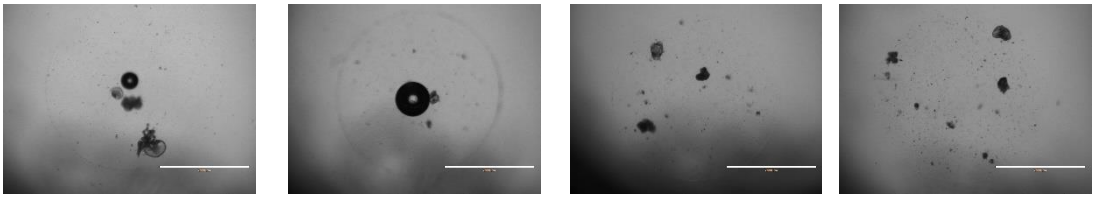			
Red	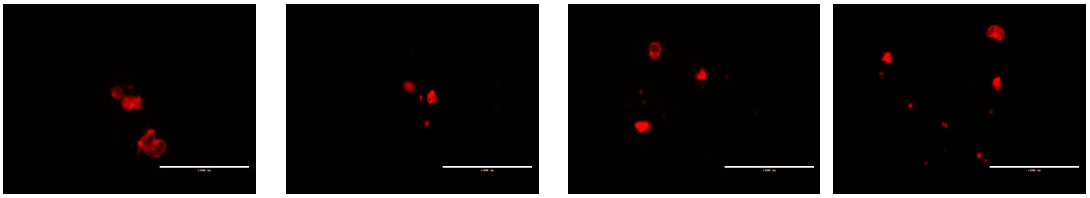			
Merge	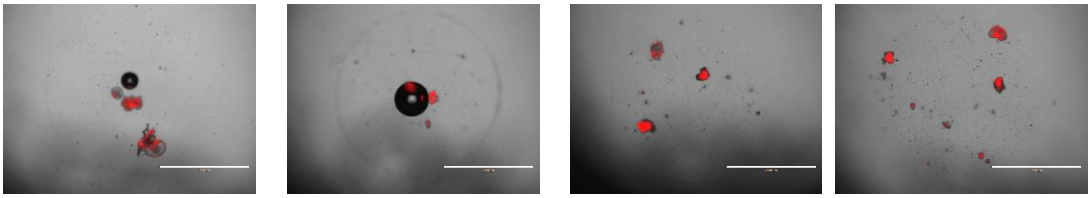			

With the p27 organoids, on the red channel row (middle) from **Table 27**, it was possible to see that all the clones had a strong and homogeneous mCherry signal. Due to this, the clones that grew better were chosen for further studies, such as A8, A11 and B9.

3.1.2 p57 OE *in vitro* system confirmation

The p57 organoids were stained with anti-rat Ki67 antibody and anti-rabbit p57 antibody for protein expression confirmation and overall system function assessment.

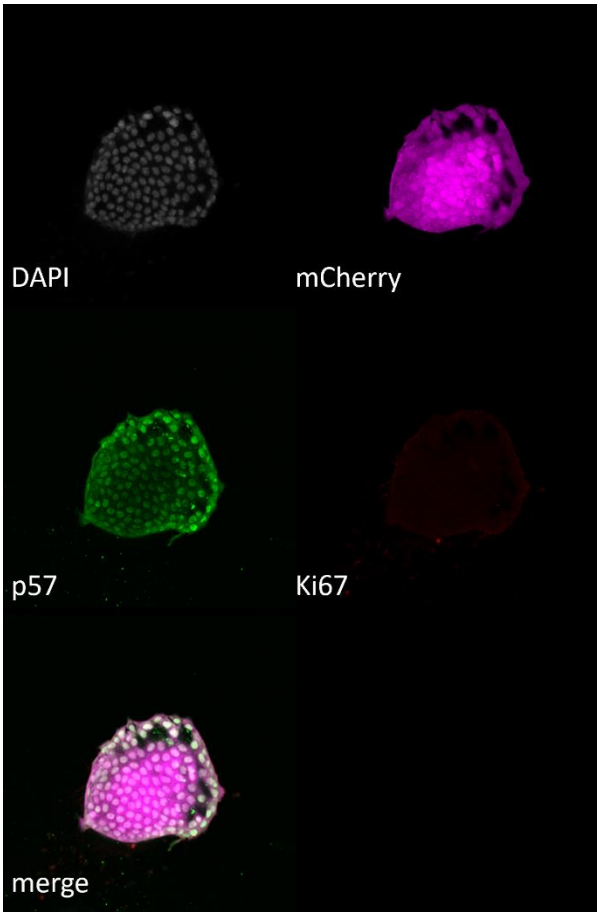

Figure 27 – p57 organoid confocal image under doxycycline. Grey shows dapi stainig for cells nuclei; Magenta shows mCherry expression ; Green channel shows p57 overexpression; Red shows Ki67 expression. The fifth image shows a merge of all the channels.

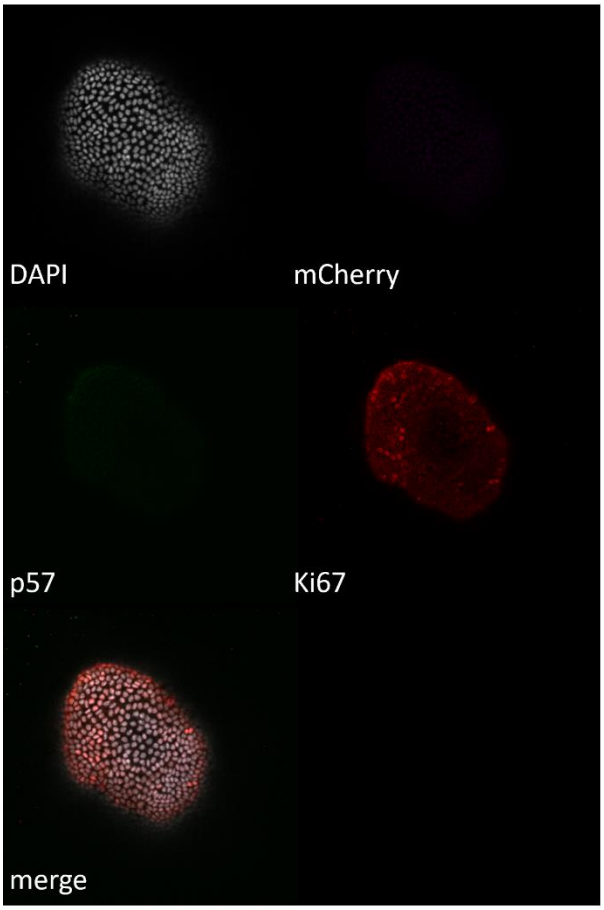

Figure 28 - p57 organoid confocal image without doxyccycline induction. Grey shows dapi stainig for cells nuclei; Magenta shows mCherry expression ; Green channel shows p57 overexpression; Red shows Ki67 expression. The fifth image shows a merge of all the channels.

Upon doxycycline induction (**Figure 27**) it was possible to see that the green channel showed a clear signal for p57 expression and that it was consistent with a strong signal shown here in magenta, representing the mCherry expression. Ki67 signal was almost non-existent compared to **Figure 28** where no Doxycycline had been added to the media and where Ki67 showed a more active state. It was also clear that on **Figure 28** with no Dox, the expression of p57 was almost non-existent together with the mCherry.

3.2 p57 gastric cells quiescence induction *in vitro*

The quiescence induction was studied by inducing the overexpression of p57 in gastric organoids with the use of doxycycline over either 7 days or 3 months, recovering the cells right after, by removing the drug, to assess if they could go back to a proliferative state.

3.2.1 Short term (7 days)

The well selected for the results on **Table 28** is representative of 5 other replicate wells. All the wells showed the same results. Only the merged channel is shown due to the clear red signal of the mCherry.

Table 28 - p57 OE organoids on days 1, 3, and 7 under doxycycline treatment for quiescence induction. The images show a merge of the bright field and Texas red channels 9% and 50% light intensity, respectively. Top row shows the experimental well and the bottom one the control well on days 0, 3, 5 and 7. Scale in each image: 2000µm, 2x objective.

+Dox	Day 1	Day 3	Day 7
Well 1	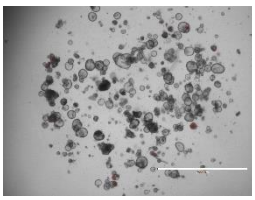	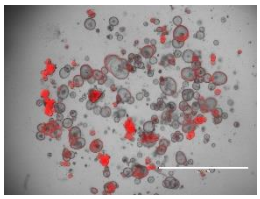	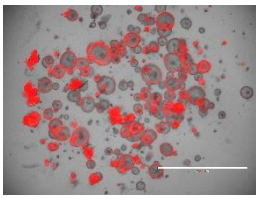
Control -Dox	**Day 1**	**Day 3**	**Day 7**
Well 1	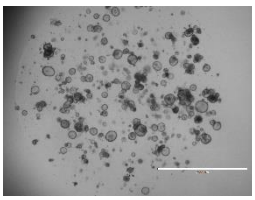	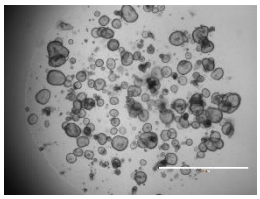	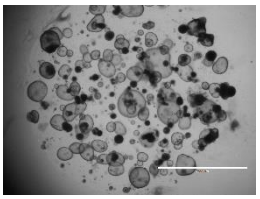

By day 3, on dox treatment, all the organoids showed a strong expression of mCherry and growth rate looked similar to the control. On day 7, the organoids only grew slightly bigger compared to day 3 and appeared to be smaller compared to the no dox control.

Table 29 - p57 OE gastric organoids on days 0, 3, 5 and 7 after stopping doxycycline treatment. The images show a merge of the bright field and Texas red channels 9% and 50% light, respectively. Top row shows the experimental well and the bottom one the control well. Scale in each image: 2000µm, 2x objective.

-Dox	Day 0 (Replating)	Day 3	Day 5	Day 7
Well 1	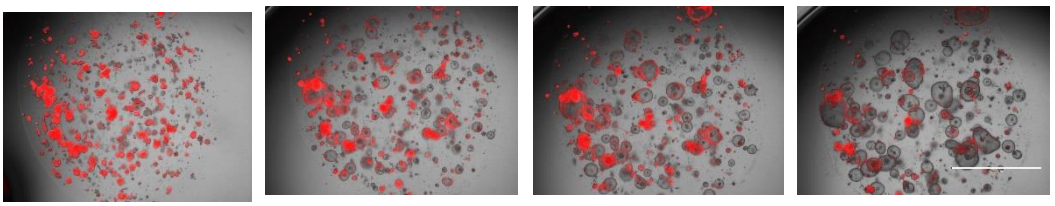			
Control -Dox	**Day 0**	**Day 3**	**Day 5**	**Day 7**
Well 1	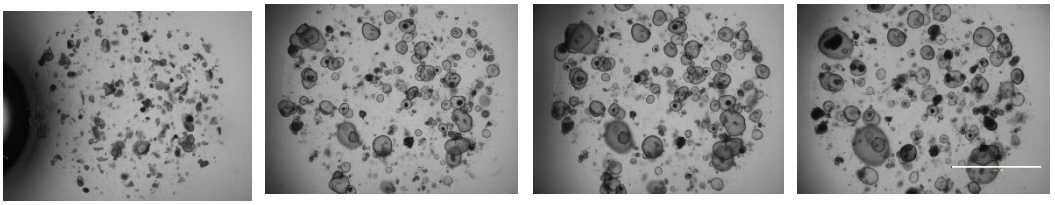			

After replating the wells and discontinuation of doxycycline treatment, it could be observed that the fluorescent signal had started to become darker and less frequent. (**Table 29**) The organoids also appeared to be getting bigger by day 5, on day 7 looked similar to the no dox control and were ready to be splitted.

3.2.2 Long term (3 months)

The well selected for the results on **Table 30** is representative of 5 other replicate wells. All the wells showed the same results. Only the merged channel is shown due to the clear red signal of the mCherry.

The Matrigel from the last image from day 95 add was detached and only half of the organoids remained in the well.

Table 30 – p57 OE organoids on days 0, 3, 14 and 24 under doxycycline treatment for quiescence induction. The images show a merge of the bright field and Texas red channels 9% and 50% light, respectively. Top row shows the experimental well and the bottom one the control well on days 0, 3, 5 and 7. Scale in each image: 2000µm, 2x objective.

+Dox	Day 0	Day 3	Day 14	Day 95
Well 1	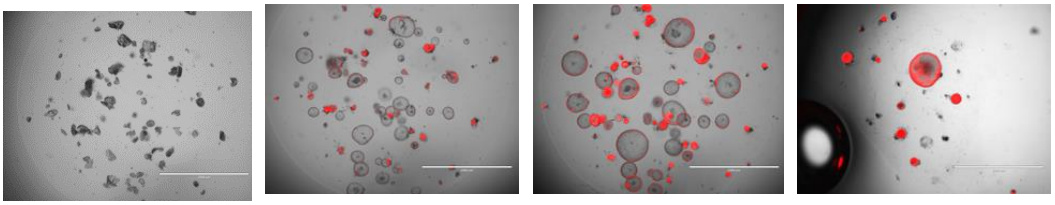			
Control -Dox	**Day 0**	**Day 3**	**Day 5**	**Day 7**
Well 1	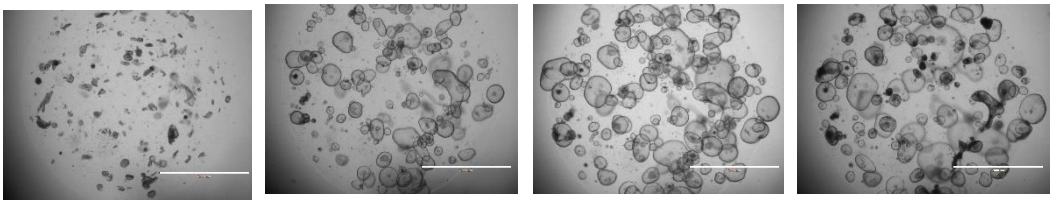			

On **Table 30**, under Dox condition, the organoids showed a similar growth rate until day 3. After day 3 the control organoids were already much bigger than the experimental wells on day 14. On day 7 of the control they were ready to be split while the organoids on the experimental set didn't change their size significantly from day 14 to day 95.

Table 31 – p57 OE gastric organoids on days 0, 3, 5 and 7 after stopping doxycycline treatment. The images show a merge of the bright field and Texas red channels 9% and 50% light, respectively. Top row shows the experimental well and the bottom one the control well. Scale in each image: 2000µm, 2x objective.

-Dox	Day 0 (Replating)	Day 3	Day 5	Day 7
Well 1	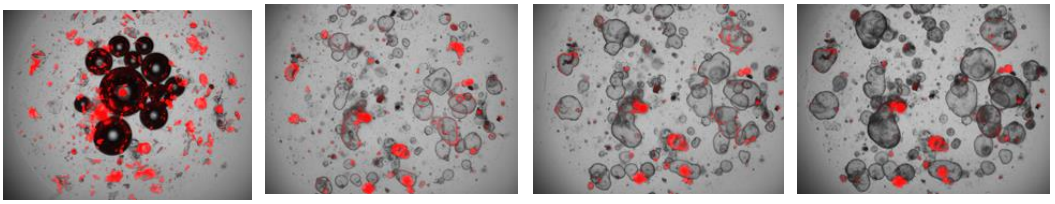			
Control -Dox	**Day 0**	**Day 3**	**Day 5**	**Day 7**
Well 1	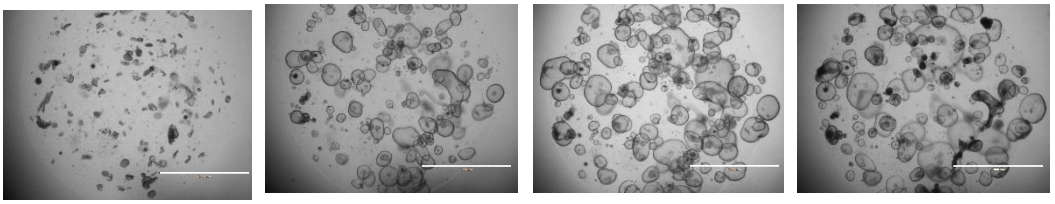			

After replating the wells and discontinuation of doxycycline treatment, we could perceive that the fluorescent signal started to become patchier and the organoids started to acquire a more proliferative state, resembling the controls. (**Table 31**) After 7 days without the treatment, the organoids were again ready to be split due to high confluence in the well.

3.3 P57 OE and cKO *in vivo* effects

p57 OE and cKO effects were assessed in a *in vivo* scenario, to compare with the results from the *in vitro* experiments. The results came from Cre only (*Anxa10-CreER$^{T2/+}$*) for the control of p57OE or p57cKO mice before Cre induction (*Anxa10-CreER$^{T2/+}$; p57cKO$^{flox/flox}$*) as a control of p57cKO, p57OE (*Anxa10-CreER$^{T2/T2}$; R26loxpTA-p57k$^{KI/KI}$*) and p57cKO (*Anxa10-CreER$^{T2/+}$; p57cKO$^{\Delta/\Delta}$*) mice injected with tamoxifen and terminated after a determined period depending on the experiment.

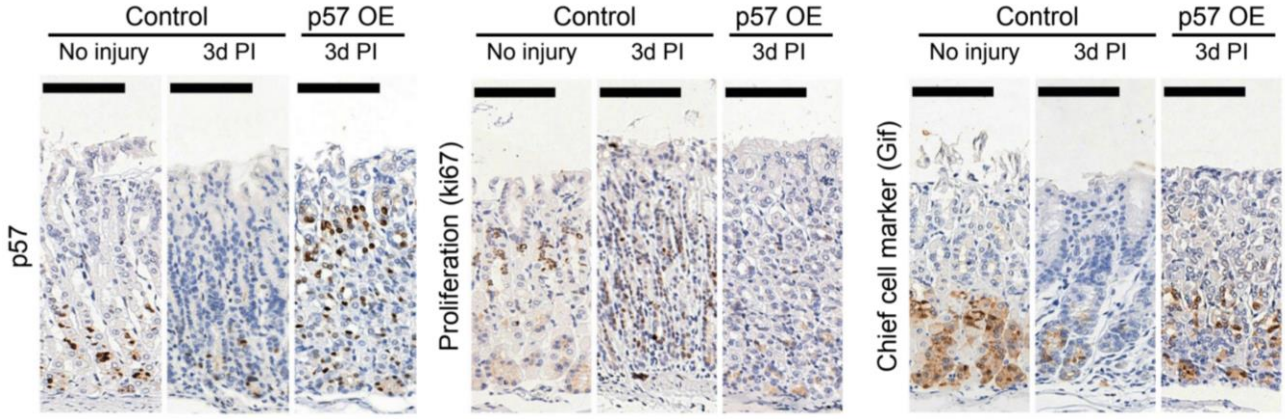

Figure 29 – **p57 OE 3 days after injury.** The 3 different images show 3 different stainings for the same conditions. The brown colour represents the immunostaining where the antibody has recognized the presence of the protein. The **first panel** on the left side shows immunostaining for the p57 protein on a tissue with no injury and 3 days after injury on a control mouse as a control as well the same injury time on a p57 OE mutant mouse. The **middle panel** shows an immunostaining for ki67, a proliferation marker on a tissue with no injury and 3 days after injury on a WT mouse as a control as well the same injury on a p57 OE mutant mouse. In the **last panel**, at the right side, the immunostaining was made against the chief cell marker Gif on a tissue with no injury and 3 days after injury of a control mouse, used as a control, as well the same injury on a p57 OE mutant mouse. Scale bar: 100µm.

With **Figure 29** it was possible to see that p57 was only being expressed in homeostasis, with no injury, at the bottom of the glands, where the reserved stem cells are usually located. The proliferation marker was also, in homeostasis, only being expressed at the top/middle section of the glands where the isthmus stem cell population is normally present. In the last image, with the chief cell marker we could also see the staining being present only at the bottom of the glands. 3 days after injury it was possible to see that the p57 in the control mouse was decrease, the ki67 had increased at the bottom of the glands and the chief cell marker had been depleted. With the p57OE it was possible to observe that after injury, the p57 protein showed presence throughout the gland, ki67 was almost non-existent and the chief cell marker had not decreased and could be mostly found at the bottom of the gland.

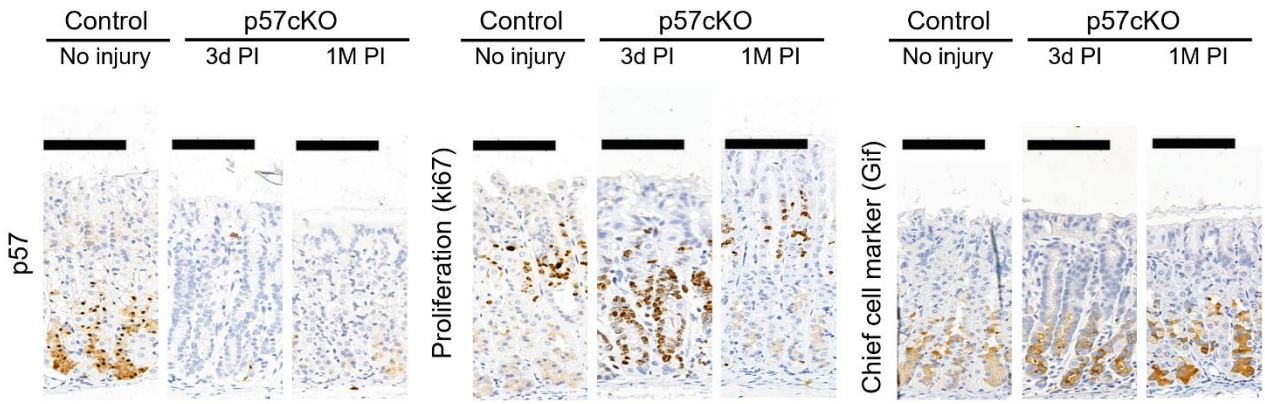

Figure 30 - **p57cKO 3 days and 1 month after injury.** The 3 different images show 3 different stainings for the same conditions. The brown colour represents the immunostaining where the antibody has recognized the presence of the protein. The **first panel** on the left side shows immunostaining for the p57 protein on a tissue with no injury, on an Anxa10-p57cKO homozygote mouse as a control as well the same genotype mouse with 3 days and 1 month after injury. The **middle panel** shows an immunostaining for ki67, a proliferation marker on a tissue with no injury, of a Anxa10-p57cKO homozygote mouse as a control as well the same genotype mouse with 3 days and 1 month after injury. On the **last panel**, at the right side, the immunostaining was made against the chief cell marker (Gif) on a tissue with no injury, on an Anxa10-p57cKO homozygote mouse as a control as well the same genotype mouse with 3 days and 1 month after injury. Scale bar: 100µm.

From **Figure 30** and similar with **Figure 29**, with no injury, in homeostasis, p57 was only being expressed at the bottom of the glands, where the troy and chief stem cells are usually located. The proliferation marker was also only being expressed at the top/middle section of the glands where the isthmus stem cell population is present and once again, in the last image, with the chief cell marker we could observe the staining being present mostly at the bottom of the glands. 3 days after injury, the Cre enzyme was activated and we could observe that there was no staining for p57 and again, after one month, almost no p57 expression could be detected. In terms of proliferation, we could see that 3 days after the injury many cells displayed expression of the marker but after one month most of the ki67 expression was situated at the isthmus region even if some staining can still be observed at the bottom of the glands. Regarding the chief cell marker, in this case the expression did not change significantly the expression upon 3 days after injury or even after a month of time.

3.4 p57 influence on niche factor requirements

P57 influence was studied by withdrawing niche factors already known to be required for stem cells to maintain their stemness. The study was carried out once more by inducing the overexpression of p57 with the use of doxycycline over one week, withdrawing different niche factors for four weeks and recovering the cells with complete media and no doxycycline afterwards.

3 wells were initially used for each condition to account for loosing wells either from handling or escapers from CMV promotor silencing. In the end some conditions ended with two replicates and others only with one possible to use. The experiments were also repeated 4 more times independently.

The experiment had two sets of controls. One with the complete media they are usually subjected to for growth and expansion *in vitro*, and a second one with all the different media conditions but no doxycycline induced expression of the protein.

Table 32 – **p57 OE organoids media withdrawal** on day 25 and 7 days after restoring. The images show a merge of the bright field and Texas red channels 9% and 50% light, respectively. On the left side of the table the letters show the components added or taken out of the normal CM media. -Dox, showed on the right side of the table, was used as a control. E – mouse EGF; F – human FGF; P – PD03; W – Wnt; R – Rspondin; N- noggin; CM – complete media. Scale in each image: 2000µm, 2x objective.

+Dox	Day 25 withdrawal	Day 7 After restoring	Control -Dox	Day 25 withdrawal	Day 7 After restoring
CM	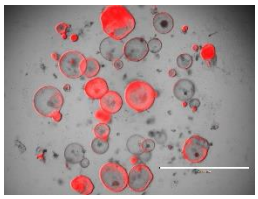	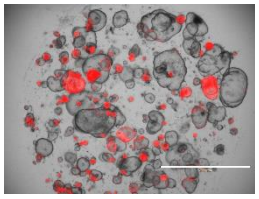	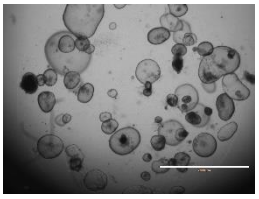	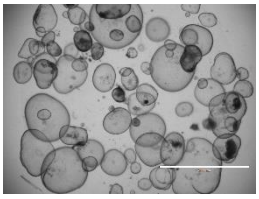	
-E -F	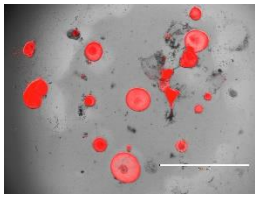	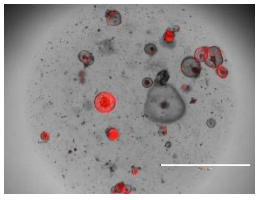	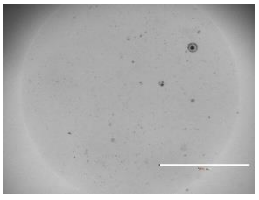	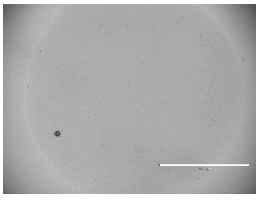	
-E +P	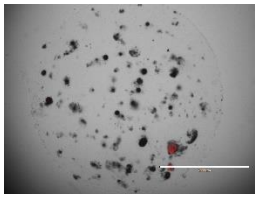	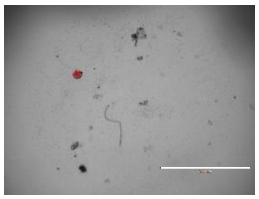	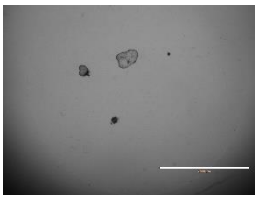	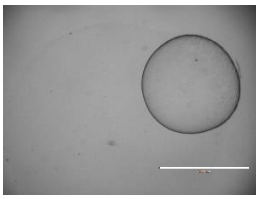	
-W -R	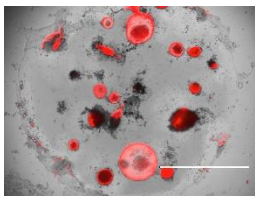	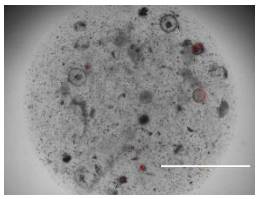	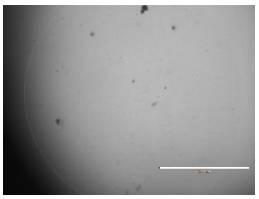	No Organoids left for restoring	
-N +BMP4	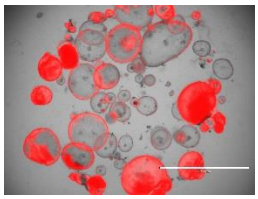	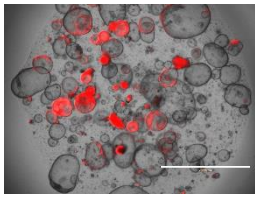	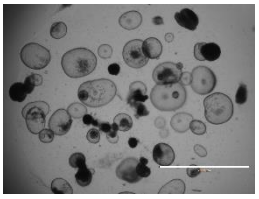	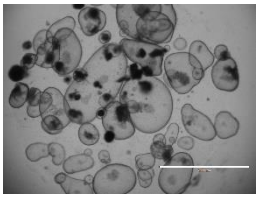	

From **Table 32** we could observe that the number of organoids on complete media (CM) remained fairly the same and they were able to recover from the doxycycline and regrow well after 7 days as the previous experiments.

On the second row from the top of the table, mouse EGF and human FGF were removed from the media. On the left side, where the wells were also under Dox treatment, the organoids seem to have had a low number of organoids, but the remaining ones kept a normal size and shape. After media restore and replating, the same organoids were able to grow again and at a good rate. Comparing this to the -Dox, under the same media condition, after 25 days almost no organoids were left in the well and none of them grew or survived after media restore and replating.

With the removal of mouse EGF and addition of PD03 to the media, on the third row from the top of the table, all the organoids seemed to have died under Dox and a few with no Dox managed to remain a regrow after the media restore and replating.

Removing Wnt and Rspondin from the media made the organoids survive under p57 OE, but as soon as these were replated, only few maintained with the ability to regrow, but with less effective growth rate, and form the organoids again. Under no Dox condition, on day 25 all the organoids were gone and so there were none to replate and put under complete media once more.

Without noggin and with the addition of BMP4, on final row of the table, the organoids seem to have been able to maintain their number under Dox for 25 days and to grow well after replating and with CM after 7 days. The control with no induction of the p57 showed similar results, only with a few more black spots representing cell death.

3.5 Gene candidates interlocking with p57

3.5.1 Candidate gene effects

As above stated, from the previous data, 86 final genes were selected and clustered together. IGF1r was the one selected to be tested for the p57 pathway effects since it had more information, known ligand and inhibitors already being use on other studies and also known to be involved in proliferation.[69]

Table 33 - **IGF-1 treatment on p57 OE organoids** on days 1, 5, 10 and 4 days after replating and stopping the treatment. The images show a merge of the bright field and Texas red channels 9% and 50% light, respectively. On the left side of the table the letters show the different drug concentrations (ng/mL) used for the treatment. -Dox with no drug treatment, showed on the bottom of the table, was used as a control. Scale in each image: 2000µm (representative bar is missing), 2x objective.

IGF-1 (ng/mL) +Dox	Day 1	Day 5	Day 10	Day 4 After replating
0	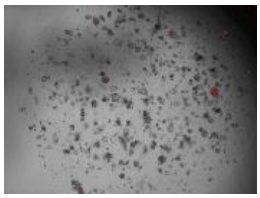	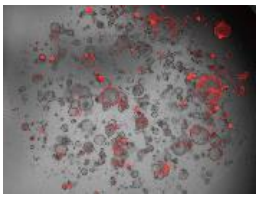	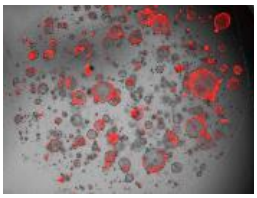	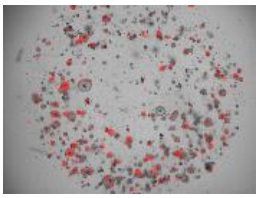
10	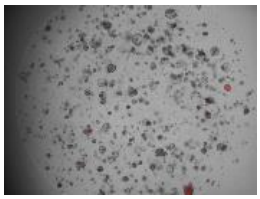	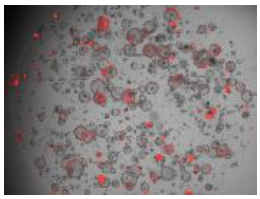	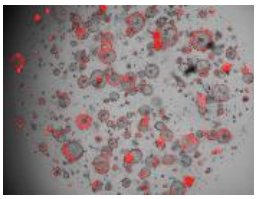	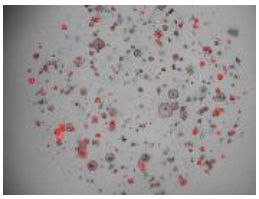
50	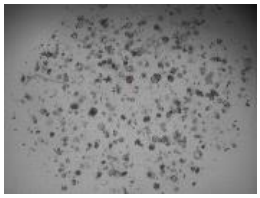	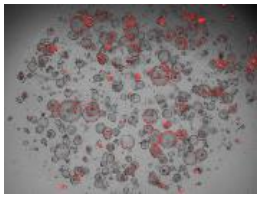	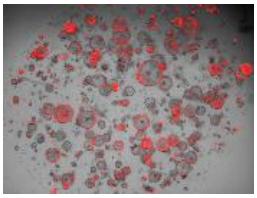	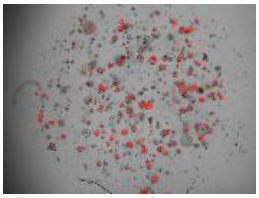
100	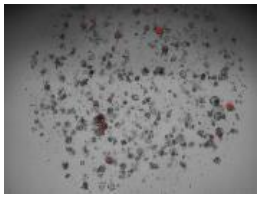	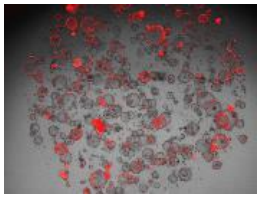	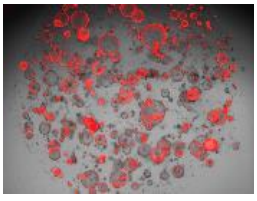	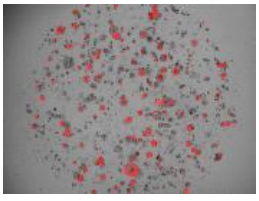

Control IGF-1 (ng/mL) - Dox	Day 1	Day 5	Day 10	Day 4 After replating
0	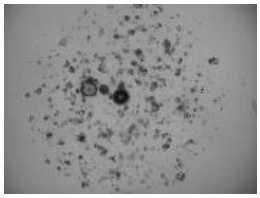	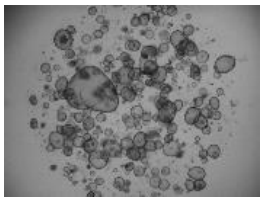	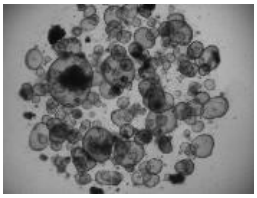	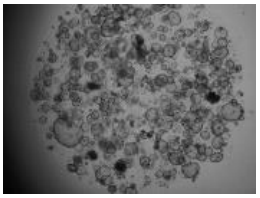

On **Table 33** p57 OE with no ligand treatment showed a similar growth compared to any of the treatments seeming also, independent from the dosage. Compared to the no Dox and no drug treatment, the quiescence seemed to have been kept and so, the growth rate appeared slower than the control by day 10. After replating and removing Dox, all the previously Dox treated conditions seemed to behave the same way and to have had a slower growth compared to the control.

Table 34 – **PPP treatment on p57 OE organoids** on days 1, 5, 10 and 4 days after replating and stopping the treatment. The images show a merge of the bright field and Texas red channels 9% and 50% light, respectively. On the left side of the table the letters show the different drug concentrations (ng/mL) used for the treatment. -Dox with no drug treatment, showed on the bottom of the table, was used as a control. Scale of each image: 2000µm (representative bar is missing) , 2x objective.

PPP (µM) +Dox	Day 1	Day 5	Day 10	Day 4 After replating
0	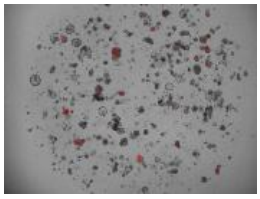	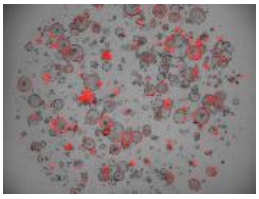	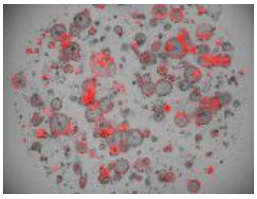	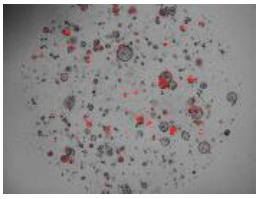
0,5	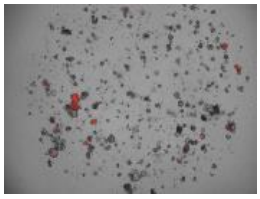	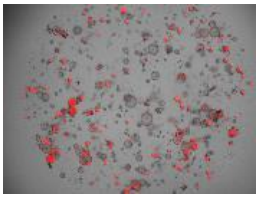	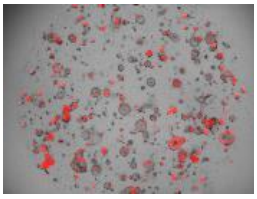	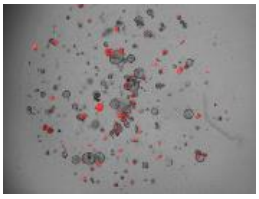
5	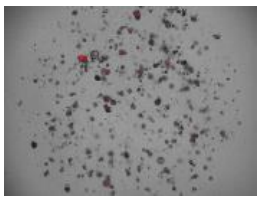	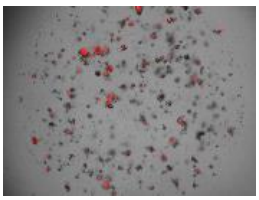	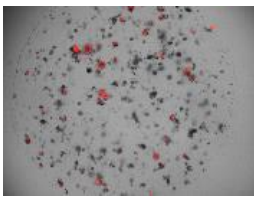	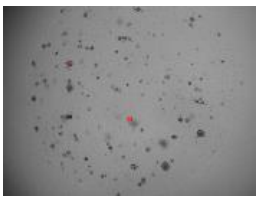
50	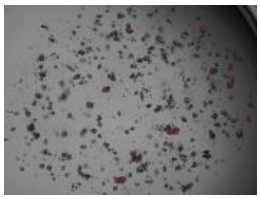	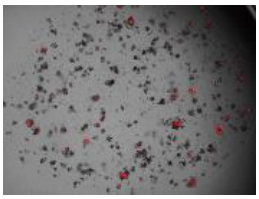	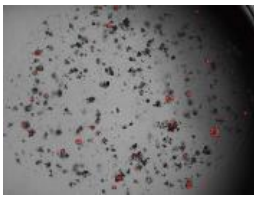	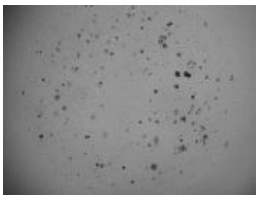

Control PPP (µM) - Dox	Day 1	Day 5	Day 10	Day 4 After replating
0	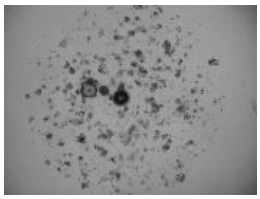	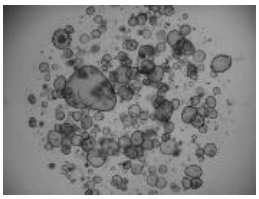	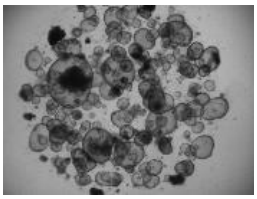	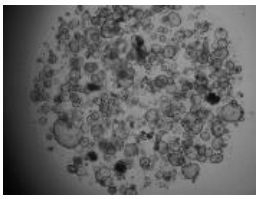

With **Table 34**, we could see that the organoids under Dox condition remained smaller than the no Dox treatment. It was also clear that with the increase of the drug concentration, there were less and less organoids being formed. By day 10 it was possible to see that with 0,5µM of PPP, the organoid number formation was similar to the no treatment under Dox. The major difference was the size of the organoids which under 0,5µM were much smaller than the others with no drug treatment. Under 5 or 50µM, almost no organoids could be spotted. After replating, the no treatment organoids or the 0,5 µM, both under Dox condition, were able to start growing again, although the higher concentrations didn't show any traces of organoids or cells regrowing or assembling into the 3D shape.

3.6 Other Kip/Cip family members *in vitro* effects

To see if any of the other Kip/Cip family members, such as p21 and p27 had the same ability of quiescence induction as the p57, both proteins were placed in the same construct backbone as the p57, electroporated into gastric cell organoids and the same short-term and long-term experiments conducted.

3.6.1 p21 short term (7 days)

In these tables the red channel is shown due to the weak signal of mCherry for a good analysis instead of the merged image. The Texas red signal here is at 70%. The – Dox control organoids had to be split every 3 days.

Table 35 – p21 A6 clones 7 days under doxycycline treatment. The control is the same line of organoids with no addition of doxycycline. Images are Texas red channel and merged images of Texas red and brightfield, 70% and 9% light source intensity, respectively. Scale in each image: 2000µm, 2x objective.

+Dox	Day 1	Day 3	Day 7
Red	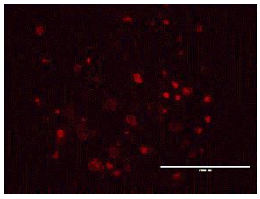	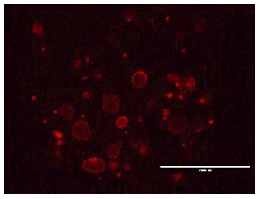	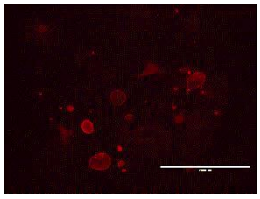
Merge	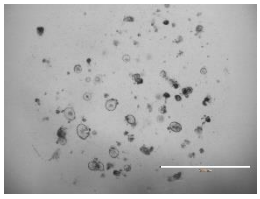	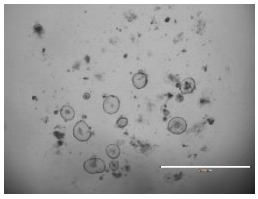	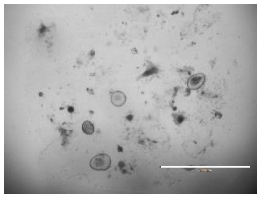
Control -Dox	Day 1	Day 3	1 day after split
Red	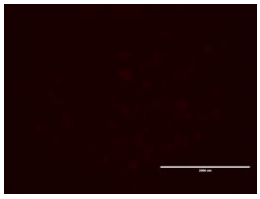	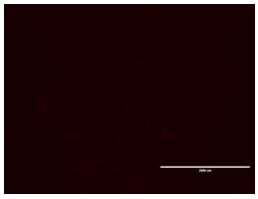	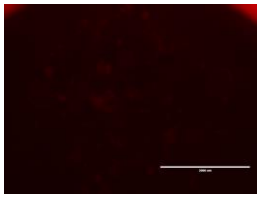
Merge	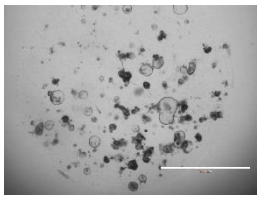	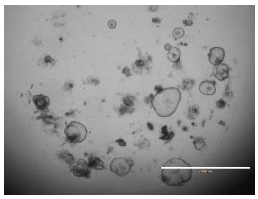	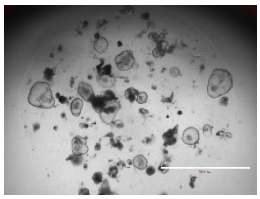

Table 36 - p21 A6 clones replating after Dox treatment. All the conditions are -Dox. Images are Texas red channel and merged images of Texas red and brightfield, 70% and 9% light source respectively. Scale in each image: 2000µm

(replating) -Dox	**Day 1**	**Day 3**	**Day 7**
Red	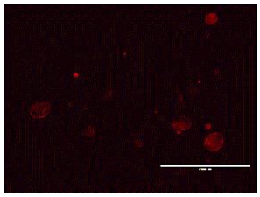	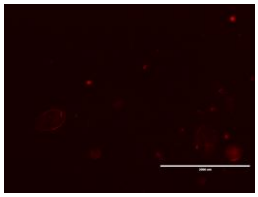	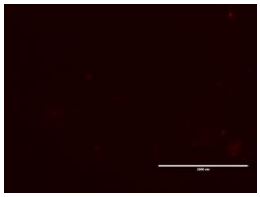
Merge	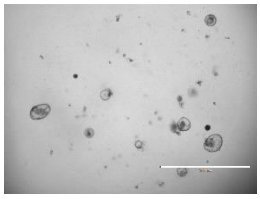	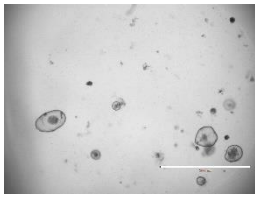	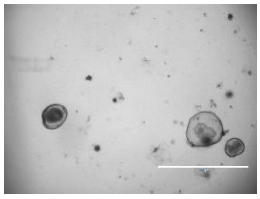
Control -Dox	Day 1	Day 3	1 day after split
Red	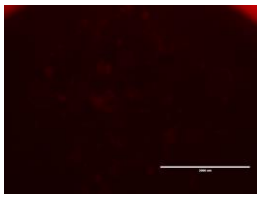	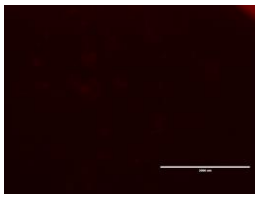	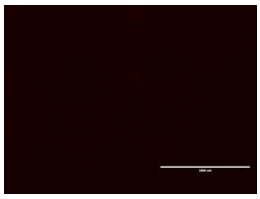
Merge	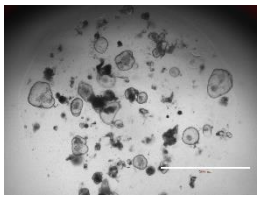	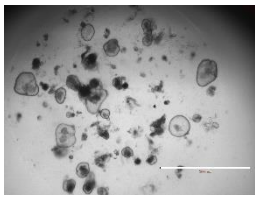	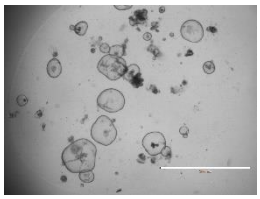

With p21 OE, (**Table 35**) the growth rate of the organoids looked slower than the no Dox control on day 3. By day 7, most of the organoids under Dox condition stopped growing compared to the control.

In **Table 36** it's possible to see that the few remaining organoids could regrow after stopping Dox treatment at a similar rate compared to the no Dox control.

3.6.2 p27 short term (7 days)

The 3 clones were picked to show the consistent outcome of p27 effect just after 3 days under Dox.

Table 37 - p27 clones 3 days under Dox induction.One well was kept without Dox as a control. The images are merged from Texas red and BF channels at 50% and 9% light respectively. Scale in each image: 2000µm, 2x objective.

3 days +Dox	A8	A11	B9
Merge	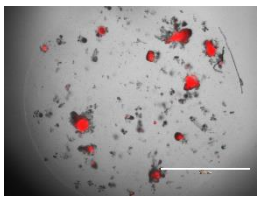	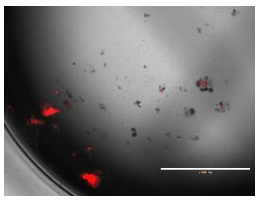	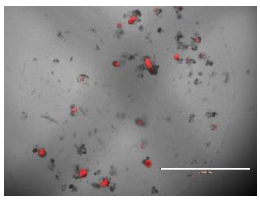
Control -Dox	A8	A11	B9
Merge	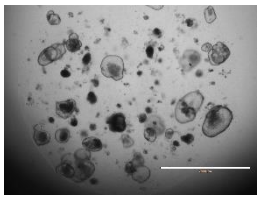	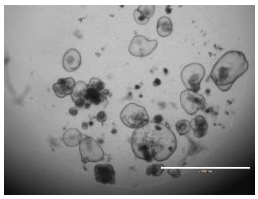	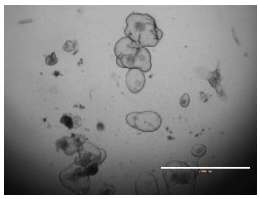

p27 OE organoids showed a very strong mCherry signal, stronger than the p57 and p21 and they all died just after 3 days under Dox effect. The results were consistent with all the clones picked.

3.7 p57 ectopic (small intestine) *in vitro* quiescence induction

To check the potential universality of the molecular switch, the p57 inducible construct was inserted into small intestinal cells and the same short-term and long-term experiments were planned.

3.7.1 Short term (7 days)

Clone 9 was used to carry out the experiment. The well shown is representative of a set of 6 replicas. On day 2 the signal of mCherry was still low so all the red channel images were taken at 60% light source. On day 4 and 7 the light was changed back to the normal used 50%.

Table 38 - **p57 OE small intestinal organoids** on days 2, 4 and 7 under doxycycline treatment for quiescence induction. The images show bright field (top row), red (middle row) and a merge (bottom row) of the two channels. BF and Texas red had a light 9% and 50% respectively. Scale in each image: 2000µm, 2x objective.

+ Dox	Day 2	Day 4	Day 7
BF	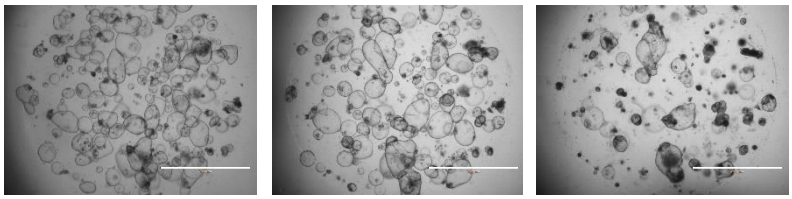		
Red	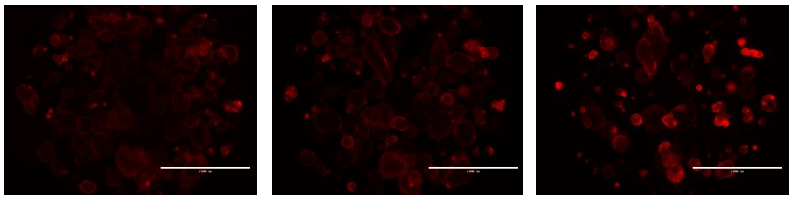		
Merge	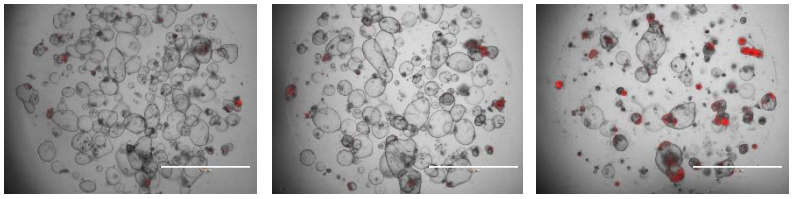		

Table 39 - p57 OE small intestinal organoids on days 2, 4 and 7 control, without doxycycline treatment. The images show bright field (top row), red (middle row) and a merge (bottom row) of the two channels. BF and Texas red had a light 9% and 50% respectively. Scale in each image: 2000µm, 2x objective.

Control -Dox	**Day 2**	**Day 4**	**Day 7**
BF	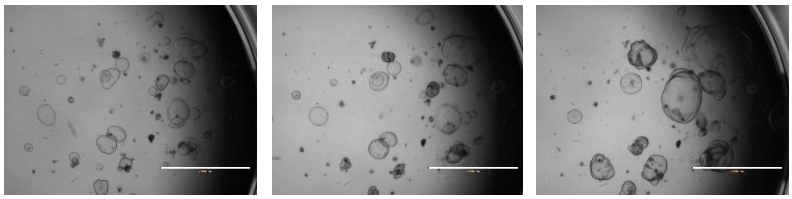		
Red			
Merge	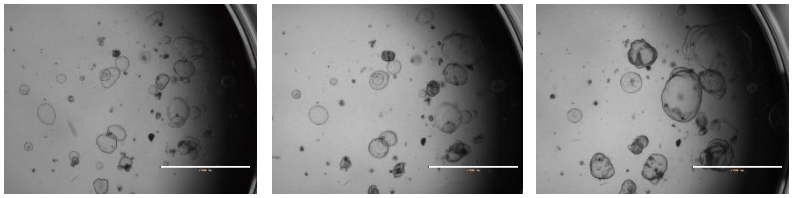		

No rescue experiment was done since many of the organoids started to show CMV promoter silencing.

Still, it was possible to see that the growth rate was reduced compared to the control organoids on **Table 39** and that the mCherry signal grew stronger with time. The original seeding density of the control was lower compared to the experimental wells, so the difference must be considered while analysing the results as well as the increase in mCherry signal/p57 overexpression.

It was also possible to see that on day 7, on **Table 38,** some organoids started to die after the fourth day under the doxycycline effect and a clear depletion in number could be noticed compared to the control at the same timepoint.

3.7.2 Long term (3 months)

As mentioned above, the small intestine organoids showed CMV silencing in every well after 7/9 days of quiescence induction. For that reason, the experiment was stopped shortly after the two weeks of time. These images are from clone A7 and representative of all the carried experiments. This clone was chosen to show a clear image of the CMV promotor silencing.

Table 40 - 15 days doxycycline treatment of p57 OE small intestinal organoids. The red arrows point at organoids that have their CMV promotor silenced and are for that reason outgrowing their neighbours. We can see the organoids in a bright field, Texas red channel and a merged image of both. Scale in each image: 2000µm, 2x objective.

+ Dox	Day 11	Day 15
BF	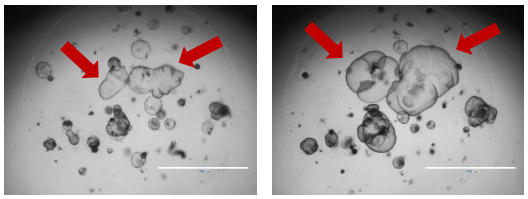	
Red	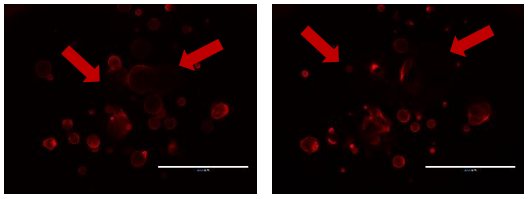	
Merge	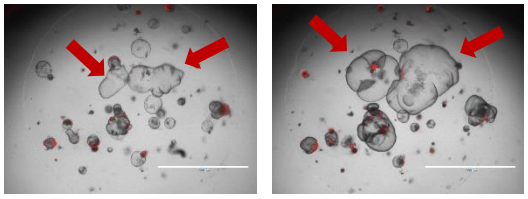	

With the images on **Table 40**, it was possible so see that on the 11th day of Dox treatment the escaper organoids had start to appear and quickly outgrew the others faster that still maintained a normal expression of the construct. It was also possible to see the lack of mCherry signal in the outgrown organoids.

3.8 Generation of a new p57 Dox inducible Tet-ON system

Due to the existence of the high number of escapers during the experiments, as mentioned before, we decided to make a different construct in order to have a more reliable system with no cells showing silencing the CMV promotor.

The gel on **Figure 31** shows cuts derived from the gel extraction. No image was taken before due to possible DNA damage from the UV light that the gel is exposed to take the image.

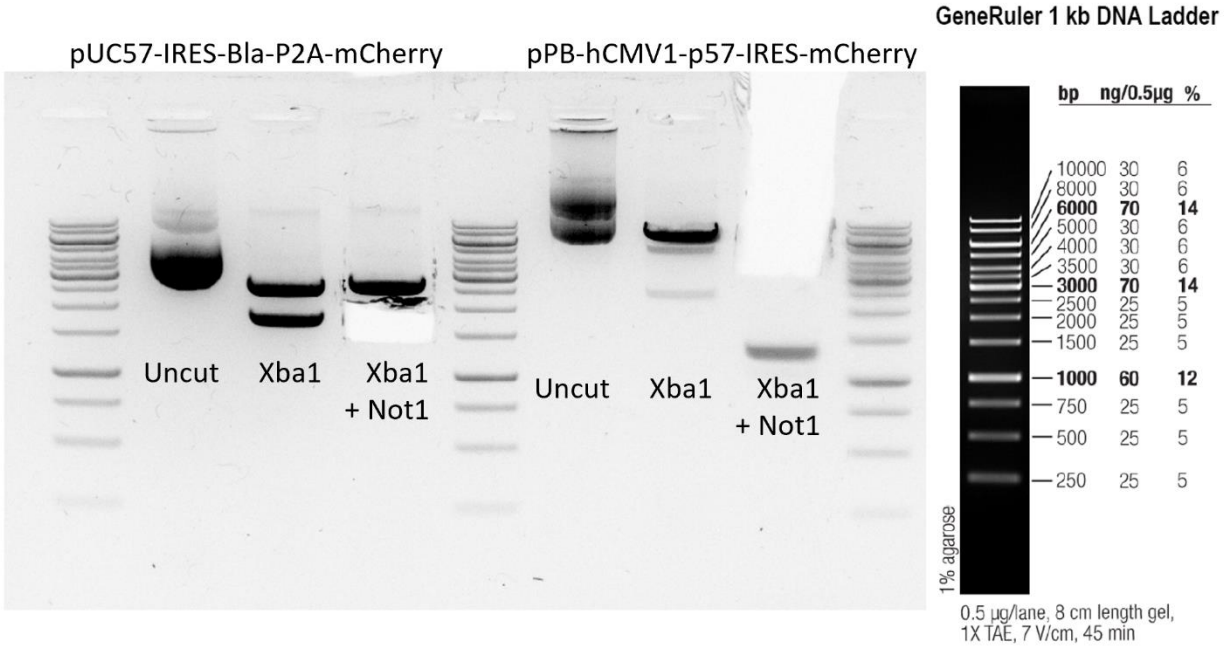

Figure 31 – **pUC57-IRES-Bla-P2A-mCherry and pPB-hCMV1-p57-IRES-mCherry enzymatic digestion.** The figure shows a 1% gel containing a 1Kb ladder for size comparison, a reaction with the uncut DNA, a single enzyme (XbaI) and double enzyme (XbaI and NotI) reaction for both original constructs.

Both constructs showed the expected band sizes with the different enzymes. pUC57-IRES-Bla-P2A-mCherry showed the uncut version around the 4.5 kb, with the XbaI cut, two bands around 1.8 kb and 2.7kb and similar with XbaI and NotI. With the pPB-hCMV1-p57-IRES-mCherry, the uncut construct was around 7.7kb and with XbaI single cut we could see a clear band between 6kb and 8 kb mark. The double enzyme cut, with XbaI and NotI, showed a band, that was cut off the gel, 6kb situated and a second one near the 1.5kb mark.

4 Discussion

4.1 p57 quiescence induction *in vitro* on gastric organoids

Cells, when maintained *in vitro*, tend to preserve a proliferative state. With the over expression of the p57 protein, these cells were induced to a quiescent state. Organoids that have been under the effect of p57 for a week were completely able to leave the activation state when p57 OE was withdrawn and immediately started changing the character to highly proliferative resembling their control, which means that the cells maintain their stemness in quiescence and remain able to divide and proliferate.

When put under the influence of an overexpression of the protein for three months, which mimics the situation *in vivo*, the organoids were able to maintain their shape and size without any major cell number loss and could once more proliferate and give rise to new cells and so, bigger organoids once the induction was stopped. This suggests that p57, can stop the cells from proliferating while maintaining them in a perhaps ‘paused’ state without sending them to a differentiated state, since these can still give rise to new and a high number of cells once the induction is stopped.

4.2 p57 overexpression and conditional knockout *in vivo*

In an *in vivo* scenario, it was previously observed that, after injury to the stomach, the base stem cells that are in a quiescent state in homeostasis, started proliferating and p57 was downregulated. These observations were confirmed by the immunostainings with control mice.

By overexpressing the p57 protein *in vivo*, the mice showed a great amount of p57 scattered along the glands and no expression of Ki67, which suggests that the overexpression completely stopped cells from proliferating and thus hamper their ability to repopulate the tissue after damage.

When knocking out the endogenous protein, no signs of p57 were visible 3 days after injury and Ki67 could be spotted along the entire gland, including the base of the glands, confirming the capacity of the protein to put these base stem cells into quiescence. After 1M, post injury, the

majority of the Ki67 was located at the isthmus region, but some positive cells could still be spotted at the base of the glands. Most of the p57 was still non-existent but no other effects, such as over growth of the tissue or loss of the stem cell pool could be detected, even in the Chief cell marker, possibly due to the compensating effect of other cip/kip family members such as p27 and p21. Other mice models with a double or even triple knockout together with different experimental set-ups and timepoints would have been necessary to test this hypothesis.

4.3 p57 influence on niche factor requirements of gastric stem cells

For stem cells to maintain their stemness, a group of specific growth factors are necessary and must be available in their niche. It was also already known that both Wnt and Egf/Fgf were required for maintaining organoids stemness *in vitro*.[6;70;71] Having that in mind, we sought to find if the protein in question had any influence on the cells and would change their requirements regarding growth factors, in order to maintain their stemness.

By inducing the organoid system to overexpress the p57 protein, surprisingly, we could see that the organoids only required Wnt signaling to keep their stemness. This showed to be different from the control where both Wnt/Rspo and Egf/Fgf signaling were required to maintain the stemness of the cells, confirming the previous results from Nick Baker, et.al., (2010), Stange, Daniel E., et al (2013) or Bartfeld, Sina, et al. (2015). This suggests that p57 is able to place the cells into a different state where the requirements to maintain certain properties intrinsic to the cell are changed.

Regarding the results from PD03, where most of the cells seem have died after 25 days, in any of the conditions, it was discussed that it might have been due to an incorrect dosage that lead to a rapid cell death and that it needs to be further optimized.

4.4 Gene candidates interlocking with p57

Certain genes are co-dependent, meaning that when one gene is being upregulated the others are as well and once that gene goes down, the others are also going to be downregulated. So, here we questioned which other genes would behave the same way as p57 and where in the pathway they would act with regards to p57.

Having Igf1r as the candidate gene, from a series of RNA analysis, both ligand and inhibitor treatments were used.

With the ligand, 3 different concentrations were used and in all three the results were similar to the p57 OE with no ligand added. This suggests that either Igf-1 shows no impact on p57 OE organoids by the fact that overexpressing p57 will make p57 independent of IGF-1or that the p57 effect is stronger than the Igf1r signalling. Another hypothesis is that because the cells are being manipulated *in vitro* and 'forced' into quiescence, Igf1r, which leads to proliferation, is being overexpressed to exit the induced state and that might explain the tandem expression with p57, despite Igf1r potentially being a negative regulator. To check any of the hypothesis in the future, the ligand needs to be treated to WT organoids.

With the Igf1r inhibitor, PPP, 3 different concentrations were also used, and the response was different from the control under Dox with no drug and appeared dose dependent. The results from this drug treatment showed that the organoids can still be formed but, with higher concentrations less and less cells can divide to give rise to bigger organoids. This suggests that the drug is in a way 'helping' the cells entering quiescence. PPP is known to be involved in inhibiting cell proliferation,[62] and so there is a need to know if PPP alone could achieve a similar phenotype as p57 OE. To check the latter hypothesis in the future, the inhibitor needs to be treated to WT organoids.

4.5 *In vitro* overexpression of other Cip/Kip family members

Other CKIs from the cip/kip family, are implicated in cell cycle arrest and have been reported to put certain stem cells in and out of the quiescent state.[61] Taking these observations into account, gastric organoids were electroporated with either p21 or p27 containing PiggyBac vectors and induced to overexpress the proteins to see if the results were similar to the p57 ones.

p21 had a dim mCherry signal compared to the rest and it was argued that it might have been from low copy number integration of the construct. Nevertheless, the signal was evenly distributed in all organoids which is why they were used for further experiments. The organoids were treated with doxycycline for a week and the results showed a high number of cell death and some size reduction compared to the control. After replating the organoids that had previously survived, they managed to grow again. This suggests that even though p21 didn't show the same clear and strong induction as p57 it had a certain degree of influence in putting the cells into quiescence for a short term.

p27, on the other hand, had a very strong mCherry signal even compared to the p57. The organoids were induced with doxycycline for overexpression of the protein, but shortly after 3 days all the organoids had died. It was reasoned that motive for the death of the organoids might have been due to the strong expression of the protein and that a lower dose of doxycycline might be necessary to reduce the expression. No short-term quiescence was able to be continued nor the replating and withdrawal of dox was made since there were no organoids left alive to see if they could grow back from the induction.

4.6 p57 ectopic quiescence induction *in vitro* with small intestinal organoids

Since p57 was able to put the gastric organoid stem cells into quiescence *in vitro*, the same was attempted with stem cells from the small intestine. These cells are usually proliferating, even *in vivo* in homeostatic conditions. After the electroporation with the construct, the cells were induced for a protein overexpression for 7 days.

The small intestinal organoids showed an arrest in their growth compared to the no Dox control. Shortly after the 7th day a high number of organoids started to show lack of mCherry expression. It was argued that this might have been due to a CMV promotor silencing only on the construct that wasn't expressing the hygromycin resistance. In order to overcome that, a new construct had to be design.

Even though no replating was done, it was possible to see that the organoids that were lacking the mCherry signal were clearly overgrown compared to their neighbours within the same well. This suggests that the p57 was in fact putting the small intestinal stem cells into quiescence and that they could grow out once more after the overexpression of the protein was stopped.

This suggests that the p57 protein is a master of quiescence induction even when ectopically expressed.

4.7 Generation of a new p57 Dox inducible PiggyBac construct

Regarding the possibility of certain cells in the organoids silencing the CMV promotor, as mentioned above, a new construct was made containing a blasticidin resistance in the construct that contains both the protein DNA and mCherry. This would make a double selection and only the cells containing and expressing both constructs would survive.

To generate the construct a bla containing insert was put into the already stablished p57 construct.

We could see from the results that the bands were having the expected sizes after the restriction enzyme cuts. They will be ligated, and the final generated construct will be in the future electroporated into new WT organoids and the functionality will be tested by double-selection with hygromycin and blasticidin.

5 Conclusion

This study emphasizes the importance of understanding the normal homeostatic behaviour and signalling within the gastric tissue since gastric pathologies are a major issue to the general population and understanding them can convey important information for treatment and diagnosis.

For that we used organoid models overexpressing p57 protein and tested for its capacity to put them into a quiescence state *in vitro*. *In vivo* effects were also assessed for both overexpression and knockout of the protein. All the results of the overexpression of the protein showed a clear reduction in proliferation and the capacity in the cells to regrow after stopping the overexpression induction. The *in vivo* knockout results didn't show a clear phenotype after a month without the protein and so we hypothesised that other kip/cip CKI family member could be compensating for this lack of effects. We also tested if the protein was capable of changes in the cells that would alter their niche requirements for stemness and if p57 was the only protein or major protein, within the kip/cip CKI family, to have this effect on the cells. In addition, we sought to find if p57 would have the same behaviour on cells that are usually proliferating and show no expression or low number of the protein. Due to CMV promotor silencing, no clear argument could be made, so a new construct that would circumvent this limitation was generated. Genes that could potentially influence the protein were also investigated and after narrowing down a candidate list to one gene, its inhibitor or ligand were treated in the p57 OE background.

With the above statements, it is possible to conclude that p57 has an ability to set the cells into a quiescent state, with the possibility of having the same performance even in an ectopic epithelium. Also, that p21 and p27, although having some effect on the organoids were still weaker than the p57. These findings reinforce p57 as a major molecular switch for quiescence in the gastric epithelium.

6 Future perspectives

In the future it would be of interest to investigate if p57 is capable of a long-term quiescence induction in the small intestinal stem cells, both *in vitro* and *in vivo*, and which would be the long-term consequences of this if expressed *in vivo* in this ectopic manner. It would also be curious to explore the effects of Igf1r inhibitor in WT organoids, to check the same drug can induce quiescence without p57 OE and if so, to check whether p57 is a downstream target of the Igf1r pathway.

Finally, it would be of great importance to study the p57 effects on gastric cancer line organoids, derived from patients and whether the p57 could also be implicated in drug resistance when overexpressed or lost.

7 References

1 - Gordon., Betts, J. Anatomy and physiology. DeSaix, Peter., Johnson, Eddie., Johnson, Jody E., Korol, Oksana., Kruse, Dean H., Poe, Brandon. Houston, Texas. p. 9. ISBN 9781947172043. OCLC 1001472383

2 - Cannon, Walter B. "Organization for physiological homeostasis." Physiological reviews 9.3 (1929): 399-431.

3 - Cox, Thomas R., and Janine T. Erler. "Remodeling and homeostasis of the extracellular matrix: implications for fibrotic diseases and cancer." Disease models & mechanisms 4.2 (2011): 165-178.

4 - Nguyen, Thi Loan Anh, et al. "How informative is the mouse for human gut microbiota research?" Disease models & mechanisms 8.1 (2015): 1-16.

5 - Willet, Spencer G., and Jason C. Mills. "Stomach organ and cell lineage differentiation: from embryogenesis to adult homeostasis." Cellular and molecular gastroenterology and hepatology 2.5 (2016): 546-559.

6 - Stange, Daniel E., et al. "Differentiated Troy+ chief cells act as reserve stem cells to generate all lineages of the stomach epithelium." Cell 155.2 (2013): 357-368.

7 - Han, Seungmin, et al. "Defining the identity and dynamics of adult gastric isthmus stem cells." Cell stem cell 25.3 (2019): 342-356.

8 - Reya, Tannishtha, et al. "Stem cells, cancer, and cancer stem cells." nature 414.6859 (2001): 105-111.

9 - Leitch, Harry G., et al. "Naive pluripotency is associated with global DNA hypomethylation." Nature structural & molecular biology 20.3 (2013): 311.

10 - Seydoux, Geraldine, and Robert E. Braun. "Pathway to totipotency: lessons from germ cells." Cell 127.5 (2006): 891-904.

11 - Hong, Kyung U., et al. "In vivo differentiation potential of tracheal basal cells: evidence for multipotent and unipotent subpopulations." American Journal of Physiology-Lung Cellular and Molecular Physiology 286.4 (2004): L643-L649.

12 - Berdasco, María, and Manel Esteller. "DNA methylation in stem cell renewal and multipotency." Stem cell research & therapy 2.5 (2011): 42.

13 - Nichols, Jennifer, and Austin Smith. "Naive and primed pluripotent states." Cell stem cell 4.6 (2009): 487-492.

14 - Weinberger, Leehee, Yair S. Manor, and Jacob H. Hanna. "Stem cell states: naive to primed pluripotency." Nat Rev Mol Cell Biol (2015).

15 - Takahashi, Kazutoshi, and Shinya Yamanaka. "Induction of pluripotent stem cells from mouse embryonic and adult fibroblast cultures by defined factors." cell 126.4 (2006): 663-676.

16 - Yamanaka, Shinya. "A fresh look at iPS cells." cell 137.1 (2009): 13-17.

17 - Boers, Sarah N., et al. "Organoid biobanking: identifying the ethics." EMBO reports 17.7 (2016): 938-941.

18 - Ben-David, Uri, et al. "Patient-derived xenografts undergo mouse-specific tumor evolution." Nature genetics 49.11 (2017): 1567.

19 - Kamb, Alexander. "What's wrong with our cancer models?" Nature reviews Drug discovery 4.2 (2005): 161-165.

20 - Kim, Hyun Jung, ed. Biomimetic Microengineering. Chapter 5: Wu et al. 'Organoid Technology For Basic Science And Biomedical Research' CRC Press, 2020.

21 - Kopper, Oded, et al. "An organoid platform for ovarian cancer captures intra-and interpatient heterogeneity." Nature medicine 25.5 (2019): 838-849.

22 - Teriyapirom et al. 'Genetic Engineering in Organoids' - Journal of Molecular Medicie, 2020. - Under review

23 - Van Velthoven, Cindy TJ, and Thomas A. Rando. "Stem cell quiescence: dynamism, restraint, and cellular idling." Cell Stem Cell 24.2 (2019): 213-225.

24 - Cooper GM. "Chapter 14: The Eukaryotic Cell Cycle". The cell: a molecular approach (2nd ed.). Washington, D.C: ASM Press 2000.

25 - Johnson, David G., and C. L. Walker. "Cyclins and cell cycle checkpoints." Annual review of pharmacology and toxicology 39.1 (1999): 295-312.

26 - Graña, Xavier, and E. Premkumar Reddy. "Cell cycle control in mammalian cells: role of cyclins, cyclin dependent kinases (CDKs), growth suppressor genes and cyclin-dependent kinase inhibitors (CKIs)." Oncogene 11.2 (1995): 211-220.

27 - Lim, Shuhui, and Philipp Kaldis. "Cdks, cyclins and CKIs: roles beyond cell cycle regulation." Development 140.15 (2013): 3079-3093.

28 - Morgan, D. O. "The Cell Cycle: Principles of Control New Science Press." (2006).

29 - Matsumoto, Akinobu, et al. "p57 is required for quiescence and maintenance of adult hematopoietic stem cells." Cell stem cell 9.3 (2011): 262-271.

30 - Katoh, Masuko, and Masaru Katoh. "WNT signaling pathway and stem cell signaling network." Clinical cancer research 13.14 (2007): 4042-4045.

31 - Kléber, Maurice, and Lukas Sommer. "Wnt signaling and the regulation of stem cell function." Current opinion in cell biology 16.6 (2004): 681-687.

32 - Farin, Henner F., et al. "Visualization of a short-range Wnt gradient in the intestinal stem-cell niche." Nature 530.7590 (2016): 340-343.

33 - Nusse, Roel, et al. "Wnt signaling and stem cell control." Cold Spring Harbor symposia on quantitative biology. Vol. 73. Cold Spring Harbor Laboratory Press, 2008.

34 - Scoville, David H., et al. "Current view: intestinal stem cells and signaling." Gastroenterology 134.3 (2008): 849-864.

35 - Rawla, Prashanth, and Adam Barsouk. "Epidemiology of gastric cancer: global trends, risk factors and prevention." Przeglad gastroenterologiczny 14.1 (2019): 26.

36 - Seidlitz, Therese, et al. "Human gastric cancer modelling using organoids." Gut 68.2 (2019): 207-217.

37 - Seo, Seyoung, et al. "Loss of HER2 positivity after anti-HER2 chemotherapy in HER2-positive gastric cancer patients: results of the GASTric cancer HER2 reassessment study 3 (GASTHER3)." Gastric Cancer 22.3 (2019): 527-535.

38 - Malfertheiner, Peter, Francis KL Chan, and Kenneth EL McColl. "Peptic ulcer disease." The lancet 374.9699 (2009): 1449-1461.

39 - Burkitt, Michael D., et al. "Helicobacter pylori-induced gastric pathology: insights from in vivo and ex vivo models." Disease models & mechanisms 10.2 (2017): 89-104.

40 - Tsai, Susan, et al. "Development of primary human pancreatic cancer organoids, matched stromal and immune cells and 3D tumor microenvironment models." BMC cancer 18.1 (2018): 1-13.

41 - Sidhaye, Jaydeep, and Jürgen A. Knoblich. "Brain organoids: an ensemble of bioassays to investigate human neurodevelopment and disease." Cell Death & Differentiation (2020): 1-16.

42 - Schwank, Gerald, et al. "Functional repair of CFTR by CRISPR/Cas9 in intestinal stem cell organoids of cystic fibrosis patients." Cell stem cell 13.6 (2013): 653-658.

43 - Bartfeld, Sina, and Hans Clevers. "Organoids as model for infectious diseases: culture of human and murine stomach organoids and microinjection of Helicobacter pylori." JoVE (Journal of Visualized Experiments) 105 (2015): e53359.

44 - Liang, Qi, et al. "Chromosomal mobilization and reintegration of Sleeping Beauty and PiggyBac transposons." Genesis 47.6 (2009): 404-408.

45 - Spit, Maureen, Bon-Kyoung Koo, and Madelon M. Maurice. "Tales from the crypt: intestinal niche signals in tissue renewal, plasticity and cancer." Open biology 8.9 (2018): 180120.

46 - Choi, Eunyoung, et al. "Cell lineage distribution atlas of the human stomach reveals heterogeneous gland populations in the gastric antrum." Gut 63.11 (2014): 1711-1720.

47 - Gossen, Manfred, et al. "Transcriptional activation by tetracyclines in mammalian cells." Science 268.5218 (1995): 1766-1769.

48 - Turan, Soeren, et al. "Recombinase-mediated cassette exchange (RMCE): traditional concepts and current challenges." Journal of molecular biology 407.2 (2011): 193-221.

49 – Nakamura, Eiichiro, Minh-Thanh Nguyen, and Susan Mackem. "Kinetics of tamoxifen-regulated Cre activity in mice using a cartilage-specific CreERT to assay temporal activity windows along the proximodistal limb skeleton." Developmental dynamics: an official publication of the American Association of Anatomists 235.9 (2006): 2603-2612.

50 - Kristianto, Jasmin, et al. "Spontaneous recombinase activity of Cre–ERT2 in vivo." Transgenic research 26.3 (2017): 411-417.

51 - Johnston, Calum, et al. "Bacterial transformation: distribution, shared mechanisms and divergent control." Nature Reviews Microbiology 12.3 (2014): 181-196.

52 - Humphreys, G. O., Geraldine A. Willshaw, and E. S. Anderson. "A simple method for the preparation of large quantities of pure plasmid DNA." Biochimica et Biophysica Acta (BBA)-Nucleic Acids and Protein Synthesis 383.4 (1975): 457-463.

53 - Weaver, James C., and Yu A. Chizmadzhev. "Theory of electroporation: a review." Bioelectrochemistry and bioenergetics 41.2 (1996): 135-160.

54 - Kleckner, Nancy, John Roth, and David Botstein. "Genetic engineering in vivo using translocatable drug-resistance elements: new methods in bacterial genetics." Journal of molecular biology 116.1 (1977): 125-159.

55 - Ma, Junli, et al. "Lauren classification and individualized chemotherapy in gastric cancer." Oncology letters 11.5 (2016): 2959-2964.

56 - Del Solar, Gloria, et al. "Replication and control of circular bacterial plasmids." Microbiology and molecular biology reviews 62.2 (1998): 434-464.

57 - Seidlitz, Therese, et al. "Mouse Models of Human Gastric Cancer Subtypes With Stomach-Specific CreERT2-Mediated Pathway Alterations." Gastroenterology 157.6 (2019): 1599-1614.

58 - Haley, Sheila A., et al. "Forced expression of the cell cycle inhibitor p57 Kip2 in cardiomyocytes attenuates ischemia-reperfusion injury in the mouse heart." BMC physiology 8.1 (2008): 4.

60 - Mouse Genome Database (MGD) at the Mouse Genome Informatics website, The Jackson Laboratory, Bar Harbor, Maine. World Wide Web (URL: http://www.informatics.jax.org). - 07.2020

61 - Andreu, Zoraida, et al. "The Cyclin-Dependent Kinase Inhibitor p27kip1 Regulates Radial Stem Cell Quiescence and Neurogenesis in the Adult Hippocampus." Stem Cells 33.1 (2015): 219-229.

62 - Doghman, Mabrouka, Magnus Axelson, and Enzo Lalli. "Potent inhibitory effect of the cyclolignan picropodophyllin (PPP) on human adrenocortical carcinoma cells proliferation." American journal of cancer research 1.3 (2011): 356.

63 - Fellers TJ, Davidson MW. "Introduction to Confocal Microscopy". Olympus Fluoview Resource Center. National High Magnetic Field Laboratory (2007). Retrieved 2007-07-25.

64 - Indra, Arup Kumar, et al. "Temporally-controlled site-specific mutagenesis in the basal layer of the epidermis: comparison of the recombinase activity of the tamoxifen-inducible Cre-ERT and Cre-ERT2 recombinases." Nucleic acids research 27.22 (1999): 4324-4327.

65 - Montgomery, Robert K., and David T. Breault. "Small intestinal stem cell markers." Journal of anatomy 213.1 (2008): 52-58.

66 - Cheng, Suzanne, et al. "Effective amplification of long targets from cloned inserts and human genomic DNA." Proceedings of the National Academy of Sciences 91.12 (1994): 5695-5699.

67 - Malfertheiner, Peter, Francis KL Chan, and Kenneth EL McColl. "Peptic ulcer disease." The lancet 374.9699 (2009): 1449-1461.

68 - Bai, Jingwen, Yaochen Li, and Guojun Zhang. "Cell cycle regulation and anticancer drug discovery." Cancer biology & medicine 14.4 (2017): 348.

69 - Okubo, Yumiko, et al. "Cell proliferation activities on skin fibroblasts from a short child with absence of one copy of the type 1 insulin-like growth factor receptor (IGF1R) gene and a tall child with three copies of the IGF1R gene." The Journal of Clinical Endocrinology & Metabolism 88.12 (2003): 5981-5988.

70- Barker, Nick, et al. "Lgr5+ ve stem cells drive self-renewal in the stomach and build long-lived gastric units in vitro." Cell stem cell 6.1 (2010): 25-36.

71 - Bartfeld, Sina, et al. "In vitro expansion of human gastric epithelial stem cells and their responses to bacterial infection." Gastroenterology 148.1 (2015): 126-136.

72 - Young, Madeleine, and Karen R. Reed. "Organoids as a model for colorectal cancer." Current colorectal cancer reports 12.5 (2016): 281-287.

7 References

73 - Noguchi, Eishi, and Mariana C. Gadaleta, eds. Cell Cycle Control: Mechanisms and Protocols. Springer New York, 2014.

74 - Miller, Justine D., et al. "Human iPSC-based modeling of late-onset disease via progerin-induced aging." Cell stem cell 13.6 (2013): 691-705.

75 - Sun, Ning, Michael T. Longaker, and Joseph C. Wu. "Human iPS cell-based therapy: considerations before clinical applications." Cell Cycle 9.5 (2010): 880-885.

76 - Mendelson, Avital, and Paul S. Frenette. "Hematopoietic stem cell niche maintenance during homeostasis and regeneration." Nature medicine 20.8 (2014): 833-846.

77 - Addgene website, Bacterial Transformation protocol - (URL: https://www.addgene.org/protocols/bacterial-transformation/) - 07.2020

78 – MRC-Holland's website, ethanol precipitation protocol – (URL: https://support.mrcholland.com/kb/articles/ethanol-precipitation-protocol) – 07.2020

8 Annexes

8.1 Addgene bacterial transformation protocol[77]

addgene

Bacterial Transformation

Introduction

Transformation is the process by which foreign DNA is introduced into a cell. Transformation of bacteria with plasmids is important not only for studies in bacteria but also because bacteria are used as the means for both storing and replicating plasmids. Because of this, nearly all plasmids (even those designed for mammalian cell expression) carry both a bacterial origin of replication and an antibiotic resistance gene for use as a selectable marker in bacteria.

Scientists have made many genetic modifications to create bacterial strains that can be more easily transformed and that will help to maintain the plasmid without rearrangement of the plasmid DNA. Additionally, specific treatments have been discovered that increase the transformation efficiency and make bacteria more susceptible to either chemical or electrical based transformation, generating what are commonly referred to as 'competent cells.'

You may also like...

Plasmid Cloning by Restriction Enzyme Digest

Restriction Digest of Plasmid DNA

DNA Ligation

Many companies sell competent cells, which come frozen and are prepared for optimal transformation efficiencies upon thawing. **For the highest transformation efficiency, we recommend that you follow the instructions that came with your competent cells.**

Pro-Tip Commercial competent cells range significantly in their transformation efficiency. The lowest efficiency cells (usually the least expensive) are fine for transforming plasmid DNA for the purposes of storage and amplification. Higher efficiency cells are more important if you will be transforming with very small amounts of DNA or if you're multiple plasmids at once.

Pro-Tip To save money, many labs also make their own competent cells. This is a relatively simple procedure and is useful for performing low efficiency transformations.

Last Update: Nov. 13, 2017

Equipment

- Shaking incubator at 37 °C
- Stationary incubator at 37 °C
- Water bath at 42 °C
- Ice bucket filled with ice
- Microcentrifuge tubes
- Sterile spreading device

8 Annexes

Reagents

- LB agar plate (with appropriate antibiotic)
- LB or SOC media
- Competent cells
- DNA you'd like to transform

Procedure

1. Take competent cells out of -80°C and thaw on ice (approximately 20-30 mins).
2. Remove agar plates (containing the appropriate antibiotic) from storage at 4°C and let warm up to room temperature and then (optional) incubate in 37°C incubator.
3. Mix 1 - 5 µl of DNA (usually 10 pg - 100 ng) into 20-50 µL of competent cells in a microcentrifuge or falcon tube. GEN Help Center bottom of the tube with your finger a few times.

Pro-Tip Transformation efficiencies will be approximately 10-fold lower for ligation of inserts to vectors than for an intact control plasmid.

4. Incubate the competent cell/DNA mixture on ice for 20-30 mins.
5. Heat shock each transformation tube by placing the bottom 1/2 to 2/3 of the tube into a 42°C water bath for 30-60 secs (45 secs is usually ideal, but this varies depending on the competent cells you are using).
6. Put the tubes back on ice for 2 min.
7. Add 250-1,000 µl LB or SOC media (without antibiotic) to the bacteria and grow in 37°C shaking incubator for 45 min.

Pro-Tip This outgrowth step allows the bacteria time to generate the antibiotic resistance proteins encoded in the plasmid backbone so that they will be able to grow once plated on the antibiotic containing agar plate. This step is not critical for Ampicillin resistance but is much more important for other antibiotic resistances.

8. Plate some or all of the transformation onto a 10 cm LB agar plate containing the appropriate antibiotic.

Pro-Tip We recommend that you plate 50 µL on one plate and the rest on a second plate. This gives the best chance of getting single colonies, while allowing you to recover all transformants.

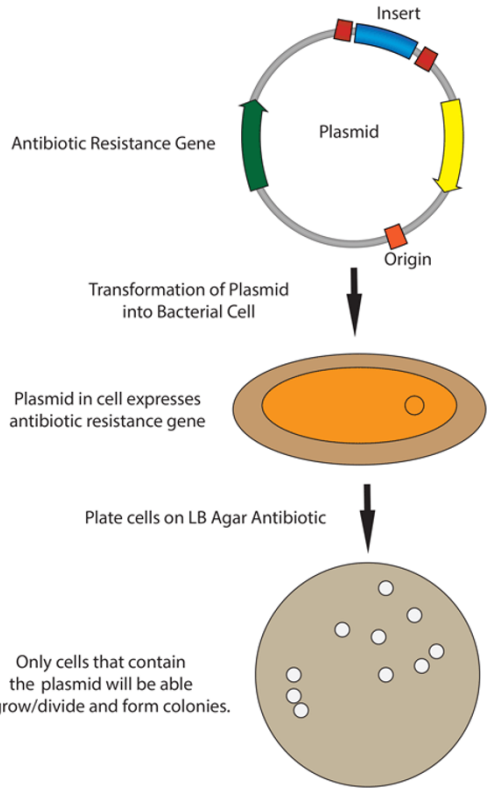

9. Incubate plates at 37°C overnight.

Pro-Tip If the culture volume is too big, gently collect the cells by centrifugation and resuspend in a smaller volume of LB so that there isn't too much liquid media on the agar plates. If the agar plate doesn't dry adequately before the cells begin dividing, the bacteria diffuse through the liquid and won't grow in colonies.

8.2 Quiagen's® Plasmid Plus Midi Kit

Quick-Start Protocol March 2016

QIAGEN® Plasmid *Plus* Midi Kit

The QIAGEN Plasmid *Plus* Midi Kit (cat. nos. 12943 and 12945) can be stored at room temperature (15–25°C) for up to 24 months if not otherwise stated on label.

Further information

- *QIAGEN Plasmid* Plus *Purification Handbook*: **www.qiagen.com/HB-0155**
- Safety Data Sheets: **www.qiagen.com/safety**
- Technical assistance: **support.qiagen.com**

Notes before starting

- Add RNase A solution to Buffer P1, mix and store at 2–8°C.
- **Optional**: Add LyseBlue® reagent to Buffer P1 at a ratio of 1:1000.
- Add ethanol (96–100%) to Buffer PE concentrate before use (see bottle label for volume).
- Harvest bacterial culture after 12–16 h incubation.
- Symbols: ● standard protocol; ▲ high-yield protocol.

Table 1. Maximum recommended LB culture volumes

Protocol	High-copy plasmid	Low-copy plasmid
Standard	20–25 ml	50 ml
High-yield	25–35 ml	Not recommended

1. Harvest bacterial culture by centrifuging at 6000 x *g* for 15 min at 4°C.
2. Completely resuspend pelleted bacteria in ● 2 ml or ▲ 4 ml Buffer P1.

3. Add ● 2 ml or ▲ 4 ml Buffer P2, gently mix by inverting until the lysate appears viscous and incubate at room temperature (15–25°C) for 3 min. If LyseBlue reagent has been added, the cell suspension will turn blue.
4. Place the QIAfilter Cartridge into a new and suitable tube, allowing space for the addition of Buffer BB.
5. Add ● 2 ml or ▲ 4 ml Buffer S3 to the lysate, and mix by inverting 4–6 times. If LyseBlue reagent has been added, mix the solution until it is completely colorless.
6. Transfer the lysate to the QIAfilter Cartridge and incubate at room temperature for 10 min.
7. During incubation, place QIAGEN Plasmid *Plus* spin columns into the QIAvac 24 Plus. Insert Tube Extenders into each column.
8. Gently insert the plunger into the QIAfilter Cartridge and filter the cell lysate into the tube.
9. Add 2 ml Buffer BB to the cleared lysate, and mix by inverting 4–6 times.
10. Transfer lysate to a QIAGEN Plasmid *Plus* spin column on the QIAvac 24 Plus.
11. Apply approximately –300 mbar vacuum until the liquid has been drawn through all columns.
12. To wash the DNA, add 0.7 ml Buffer ETR and apply vacuum until the liquid has been drawn through all columns.
13. To further wash the DNA, add 0.7 ml Buffer PE and apply vacuum until the liquid has been drawn through all columns.
14. To completely remove the residual wash buffer, centrifuge the column at 10,000 x *g* (9,700 rpm) for 1 min in a tabletop microcentrifuge.
15. Place the QIAGEN Plasmid *Plus* spin column into a clean 1.5 ml tube. To elute the DNA, add 200 µl Buffer EB or water to the center of the QIAGEN Plasmid *Plus* spin column, let it stand for ≥1 min and centrifuge for 1 min.

8.3 MRC-Holland's ethanol precipitation protocol[78]

8.3.1 Method

1. Add 1/10 volume of sodium acetate (NaOAc; 3 M, pH 5.2).
2. Add 2.5 volumes (calculated after addition of sodium acetate) of at least 95% ethanol.
3. Incubate at room temperature or on ice for at least 15 minutes. In case of small DNA fragments or high dilutions, overnight incubation gives better results.
4. Centrifuge at > 12,000 × g for 30 minutes at a temperature between 4°C and room temperature.
5. Discard the supernatant carefully, making sure the DNA pellet (which may not be visible) remains in the tube.
6. Rinse with 70% ethanol and centrifuge again (> 12,000 × g) for 15 minutes.
7. Centrifuge the tube to remove all the remaining ethanol.
8. The pellet may be air-dried (leave the tubes open for ~10 min until the pellet borders lose their milky-white colour). It is important not to over-dry the pellet as this may make resuspension harder. SpeedVac should not be used.
9. Dissolve the pellet in TE0.1 (10 mM Tris-HCl pH 8.0 + 0.1 mM EDTA). Make sure that the buffer comes into contact with the whole surface of the tube as a significant portion of DNA may be deposited on the walls instead of in the pellet.